

**Characterisation of Vasodilator-Stimulated
Phosphoprotein DdVASP, a third profilin isoform and
Ste-20 like kinases from *Dictyostelium discoideum***

**Dissertation
der Fakultät für Biologie der
Ludwig-Maximilians-Universität
München**

vorgelegt von

Rajesh Arasada

München, September 2006

Ehrenwörtliche Versicherung

Diese Dissertation wurde selbständig und ohne unerlaubte Hilfsmittel angefertigt.

München, September 2006

Arasada Rajesh

Erstgutachter: Prof. Dr. Michael Schleicher

Zweitgutachter: Prof. Dr. Dirk Eick

Tag der mündlichen Prüfung: 30.01.2007

Parts of this work have been already published:

Papers:

Schirenbeck, A., Bretschneider, T., Arasada, R., Schleicher, M. and Faix, J. (2005). The Diaphanous-related formin dDia2 is required for the formation and maintenance of filopodia. **Nature Cell Biology** 7, 619-625.

Schirenbeck, A., Arasada, R., Bretschneider, T., Schleicher, M. and Faix, J. (2005). Formins and VASPs may co-operate in the formation of filopodia. **Biochem. Soc. Trans.** 33, 1256-1259.

Schirenbeck, A*, Arasada, R*, Bretschneider T., Stradal, T.E.B., Schleicher, M. and Faix, J. (2006). The bundling activity of VASP is required for filopodium formation. **Proc. Natl. Acad. Sci. USA** 103, 7694-7699 (* authors contributed equally).

Arasada, R., Son, H., Ramalingam, N., Eichinger, L., Schleicher, M. and Rohlf, M. (2006). Characterisation of the Ste20-like kinase Krs1 of *Dictyostelium discoideum*. **Eur. J. Cell Biol.** 85, 1059-1068.

Arasada, R. and **Schleicher, M.** (2006). The actin cytoskeleton. **Encyclopedic Reference of Genomics and Proteomics in Molecular Medicine**, Springer Verlag, in press.

Meeting abstracts:

Arasada R., Son, H., Eichinger, L., Schleicher, M. (2002). STE20-like kinases and their role in the actin cytoskeleton in *Dictyostelium discoideum*. European Life Science Organisation (ELSO), Congress in Nice, France. **ELSO proceedings, Abstract:756.**

Faix, J., Arasada, R., Schleicher, M. (2003). Formins as regulators of microfilament dynamics and cell motility in *Dictyostelium*. The American Society of Cell Biology, **43th Annual Meeting Abstracts, Abstract: B03 (B15)**

Rohlf, M., Arasada, R., Son, H., Schleicher, M. (2003) STE20-like kinases and their role in the actin cytoskeleton in *Dictyostelium discoideum*. European Life Science Organisation (ELSO), Congress in Dresden, Germany. **ELSO proceedings, P. 289.**

Arasada, R., Rohlf, M., Son, H., Schleicher, M. (2004) *Dictyostelium* Ste20-like kinases in signalling pathways to the cytoskeleton. **Eur. J. Cell Biology** 83 **Abstract: MS1-2**

Rohlf, M., Arasada, R., Batsios, P., Schleicher, M. (2004) Ste20-like kinases in *Dictyostelium discoideum* are involved in chemotaxis, cytokinesis and development. The American Society of Cell Biology, **44th Annual Meeting Abstracts, Abstract: 1600.**

Schirenbeck, A., Bretschneider T., Arasada, R., Schleicher M., Faix, J. (2004) The Diaphanous-related formin dDia2 interacts with VASP and is required for the formation and maintenance of filopodia. The American Society of Cell Biology, **44th Annual Meeting Abstracts, Abstract: 1481.**

Arasada, R., Gloss, A., Faix, J., Noegel, A.A., Schleicher, M. (2005) Characterisation of a low abundant profilin isoform in *Dictyostelium discoideum*. The American Society of Cell Biology, **45th Annual Meeting Abstracts, Abstract: 154.**

Batsios, P., Arasada, R., Rohlfs, M., Schleicher, M. (2005). A *Dictyostelium discoideum* Ste20-like kinase is involved in phagocytosis. **Eur. J. Cell Biology 84 Abstract: S4-8**

Batsios, P., Arasada, R., Rohlfs, M., Schleicher, M. (2005). The Ste20-like kinase DST10 is involved in phagocytosis and late development of *Dictyostelium discoideum*. **Eur. J. Cell Biology 84 Abstract: O-23**

The experimental parts of the work presented here were carried out in the laboratory of Prof. Dr. Michael Schleicher from October 2001 to March 2006 at the Adolf-Butenandt-Institute / Cell Biology, Ludwig-Maximilians-Universität München.

TABLE OF CONTENTS

SUMMARY	8
ZUSAMMENFASSUNG	10
1 Introduction	12
1.1 The actin cytoskeleton	12
1.2 Vasodilator Stimulated Phosphoprotein	16
1.3 Formins	18
1.4 Profilins	21
1.5 Ste20 like kinases	23
1.6 <i>Dictyostelium discoideum</i> as a model organism	24
1.7 Goals of the project:	25
2 Materials and Methods	27
2.1 Materials	27
2.1.1 Computer programs	27
2.1.2 Reagents	27
2.1.3 Centrifuges and rotors	28
2.1.4 Media	28
2.1.5 Buffers	29
2.1.6 Instruments	30
2.1.7 Bacteria strains	30
2.1.8 Vectors	31
2.2 Molecular Biological Methods	31
2.2.1 Isolation of <i>D. discoideum</i> genomic DNA using a High Pure PCR Template Preparation Kit (Roche)	31
2.2.2 Isolation of total RNA by the Qiagen method	31
2.2.3 RT-PCR	32
2.2.4 Polymerase Chain Reaction (PCR)	32
2.2.5 Agarose gel electrophoresis (Sambrook and Russell, 2001)	33
2.2.6 Determination of DNA concentration	33
2.2.7 Isolation of DNA fragments from agarose gels	33
2.2.8 Purification of PCR products	33
2.2.9 DNA cleavage with restriction enzymes	34
2.2.10 Mini preparation of plasmid DNA using Qiagen Miniprep Kit	34

2.2.11	Mini preparation of plasmid DNA by the method of Holmes and Quigley	34
2.2.12	Phosphatase treatment (Sambrook and Russell, 2001).....	34
2.2.13	Ligation of DNA into a plasmid vector	35
2.2.14	Preparation of chemically competent cells.....	35
2.2.15	Transformation of <i>E. coli</i>	35
2.2.16	Transformation of <i>E. coli</i> by electroporation	35
2.2.17	Transformation of <i>E.coli</i> using the TOPO TA Cloning kit.....	35
2.2.18	<i>E. coli</i> permanent cultures	36
2.2.19	Maxi preparation of plasmid DNA.....	36
2.3	Biochemical Methods.....	37
2.3.1	SDS-Polyacrylamide Gel Electrophoresis (SDS-PAGE).....	37
2.3.2	Commassie Blue staining of proteins	37
2.3.3	Silver staining.....	37
2.3.4	Drying of SDS-PAGE gels.....	38
2.3.5	Western blotting	38
2.3.6	GST-tagged protein expression	38
2.3.7	Cleavage of the GST tag.....	39
2.3.8	Purification of histidine-tagged constructs.....	39
2.3.9	Preparation of actin from rabbit skeletal muscle.....	39
2.3.10	Pyrene-labelling of actin.....	40
2.3.11	Pyrene actin assays	40
2.3.12	Immunoprecipitation	41
2.3.13	F-actin bundling assays	41
2.3.14	Preparation of profilin III affinity resin.....	41
2.4	Cell Biological Methods.....	42
2.4.1	Growth in liquid medium and on agar plates	42
2.4.2	Preservation of spores.....	42
2.4.3	Storage of <i>D. discoideum</i> cells at -70°C.....	42
2.4.4	Transformation of <i>D. discoideum</i> cells.....	43
2.4.5	Cloning of transformants	43
2.4.6	Analysis of cell shape and cell migration.....	43
2.4.7	Phagocytosis assay	43
2.4.8	Expression of Cre and selection of Bsr minus clones	44
2.4.9	Phototaxis	44

2.4.10	Indirect immunofluorescence	44
2.4.11	Reflection Interference Contrast Microscopy.....	45
2.4.12	Yeast strains, maintenance, recovery from frozen stocks, and routine culturing	45
2.4.13	Yeast plasmids.....	45
2.4.14	Yeast transformation	45
2.4.15	YPAD medium (YPD plus adenine)	46
2.4.16	Synthetic Complete drop out (SC drop-out) Medium	46
2.4.17	Constructs used for the yeast two hybrid	47
3	Results	48
3.1	Characterisation of DdVASP	48
3.1.1	The VAsodilator Stimulated Phosphoprotein DdVASP from <i>Dictyostelium. discoideum</i>	48
3.1.2	Domain structure of DdVASP.....	48
3.1.3	Complementation of VASP null cells with GFP-DdVASP	50
3.1.4	Cell dynamics	51
3.1.5	Purification of capping proteins Cap32/34 and CapG.....	52
3.1.6	Purification of GST DdVASP	53
3.1.7	dDia2 interacts directly with DdVASP	54
3.1.8	Regulation of actin polymerization by dDia2 and DdVASP <i>in vitro</i>	56
3.1.9	DdVASP bundles F-actin filaments in high salt.....	61
3.1.10	F-actin bundling activity is required for filopodia formation <i>in vivo</i>	62
3.1.11	Human VASP (HsVASP) displays virtually identical properties as <i>Dictyostelium</i> VASP.....	64
3.2	Characterisation of <i>D. discoideum</i> profilin III.....	66
3.2.1	DdVASP interacts with the profilin III isoform through its polyproline domain	66
3.2.2	Isolation of a profilin III minus mutant	67
3.2.3	Estimation of profilin III concentrations in wild type AX2 and in pI/II minus cells	68
3.2.4	Cellular distribution of profilin III	69
3.2.5	Overexpression of profilin III rescues the cell morphology and cytokinesis defect of pI/II- cells	71

3.2.6	<i>Profilin III</i> -null cells exhibit motility defects.....	72
3.3	Characterisation of <i>D. discoideum</i> Ste20-like kinases	74
3.3.1	Sequence analysis of Krs1	74
3.3.2	<i>In vitro</i> kinase activity of Krs1	76
3.3.3	Subcellular localization of Krs1	77
3.3.4	Isolation and characterization of <i>krsA</i> -null mutants and GFP overexpressors	78
3.3.5	Development of <i>krsA</i> -null mutant on phosphate agar and in suspension....	79
3.3.6	Properties of severin kinase.....	80
3.3.7	Isolation of <i>svkA</i> -null mutants	81
3.3.8	<i>svkA</i> -null mutants exhibit growth defects.....	81
3.3.9	<i>svkA</i> -null mutants show a defect in phagocytosis	82
3.3.10	<i>svkA</i> -null cells are defective in cytokinesis	83
3.3.11	<i>svkA</i> -null cells exhibit developmental defects.....	85
3.3.12	<i>svkA</i> -null cells do not exhibit any motility defects.....	86
3.3.13	SvkA is necessary for correct phototaxis	86
4	Discussion.....	88
4.1	DdVASP	88
4.2	Profilin III	90
4.3	<i>Dictyostelium</i> Ste20-like kinases.....	92
4.3.1	Krs1	92
4.3.2	Severin kinase.....	95
5	References	97
6	Abbreviations	114
	Curriculum Vitae.....	116
	Acknowledgements.....	117

SUMMARY

The major goal of the project was the investigation of proteins that regulate dynamic rearrangements of the actin cytoskeleton in *Dictyostelium discoideum* amoebae. Among the proteins studied in detail were (i) *D. discoideum* vasodilator stimulated phosphoprotein DdVASP and a new profilin isoform as putative regulators of filopodia formation, and (ii) the Ste20-like kinases Krs1 and Severin-Kinase as members of signalling cascades towards the actin cytoskeleton.

Filopodia are bundles of actin filaments projecting from the cell surface. They are found on a variety of cell types and are needed among others, for cell adhesion, sensory and exploratory functions. Filopodia are frequently found associated with sheet-like arrays of actin filaments called lamellipodia and membrane ruffles. The function of the VASP homolog from *D. discoideum* in filopodia formation was studied using molecular, biochemical and cell biological approaches. The protein sequence of DdVASP shares a significant homology to the members from other species. The protein harbours two Ena/VASP homology domains EVH1 and EVH2 separated by a polyproline stretch. The EVH2 domain is characterised by a G-actin binding site (GAB), an F-actin binding site (FAB) and a tetramerisation domain. As a tetramer the DdVASP protein can nucleate actin polymerization and bundle actin filaments. The *in vitro* nucleating activity of DdVASP is salt dependent and its nucleating activity is completely abolished at 100 mM salt. However, the F-actin bundling activity as determined by the low speed sedimentation assay was not disturbed.

The ability of DdVASP to influence the binding of capping protein to the growing ends of the actin filaments was tested through elongation of capped F-actin seeds and by depolymerization of capped filaments upon dilution below the critical concentration of the barbed ends. Results from both sets of experiments showed that DdVASP cannot remove capping protein from the barbed ends. The *D. discoideum* formin dDia2, which was previously reported to be essential for filopodia formation could elongate the capped F-actin seeds. *In vitro* biochemical data led to the conclusion that the bundling activity of DdVASP is the essential *in vivo* function to stabilise actin filaments in emerging filopodia. To test this hypothesis, a DdVASP null mutant was isolated. As expected the mutant failed to produce any filopodia. Expression of wild type DdVASP, but not DdVASP Δ FAB, rescued the phenotype suggesting the importance of the bundling activity of DdVASP in filopodia formation. To confirm that the data obtained with DdVASP were not species

specific, key biochemical functions of HsVASP were also tested. The results indicated that VASPs are functionally well conserved throughout evolution.

During this study, a third profilin isoform, profilin III, was further characterised. Specific interaction between profilin III and DdVASP was discovered. Profilin III shares a limited homology at the amino acid level with the other two and well studied profilins. Polyclonal antibodies that recognise only the profilin III isoform showed that in wild type cells profilin III represents less than 1% of all profilins. This suggests a distinct role for profilin III, because a low protein concentration argues against an actin sequestering function. Immunolocalisation studies showed profilin III in filopodia and enriched at their tips. Cells lacking the profilin III protein show defects in cell motility during chemotaxis.

The second part of the project dealt with the characterisation of two *D. discoideum* Germinal Centre Kinases (GCK). The catalytic domain of Krs1 was found to be highly homologous to the catalytic region of human MST1 and MST2 from the GCK-II subfamily. The regulatory region harbours the putative inhibitory domain (aa 330-379) and a possible multimerization (SARAH) domain (aa 412-458) described for GCKs in higher organisms. This SARAH region spans about 50 amino acid residues, is located at the extreme carboxyl terminus and most likely forms an α - helical coiled-coil motif. GFP-Krs1 overexpressing wild type cells showed an enrichment of the kinase in the cell cortex, and motility of these cells during aggregation was reduced. Krs1 knockout strains exhibited only subtle differences to wild type cells. Severin kinase is encoded by the gene *svkA*, and phylogenetic analysis groups it into subfamily GCK-III, along with human MST3, MST4 and YSK/SOK-1. Immunoblot analysis with polyclonal antibodies showed a uniform expression level throughout development. Gene disruption of *svkA* resulted in cells that had problems to divide both in submerged or in shaking cultures. Though the motility and chemotaxis of these cells remain unaltered compared to the wild type cells, the movement of the multicellular slugs is disturbed. In addition, development was delayed and the mutant formed aberrant fruiting bodies.

ZUSAMMENFASSUNG

Das wichtigste Ziel der vorliegenden Arbeit war die Untersuchung von Proteinen, die den dynamischen Umbau des Aktin Zytoskeletts in *Dictyostelium discoideum* Amöben regulieren. Unter den im Detail untersuchten Proteinen waren einerseits, das *D. discoideum* Vasodilatator-stimulierte Phosphoprotein DdVASP und eine neue Profilin Isoform als mögliche Regulatoren der Ausbildung von Filopodien, und andererseits die STE20-ähnlichen Kinasen Krs1 und Severin-Kinase als Teile von Signalketten in Richtung Zytoskelett.

Filopodien bestehen hauptsächlich aus Bündeln von Aktin Filamenten und sind Strukturen der Zelloberfläche. Sie sind in vielen Zelltypen vorhanden und werden unter anderem für die Zelladhäsion und sensorische Aufgaben benötigt. Sie sind außerdem häufig mit großflächigen Lamellipodien und anderen Aktin-gefüllten Membranausstülpungen assoziiert. Die Funktion des *D. discoideum* VASP Homologs bei der Ausbildung von Filopodien wurde mit molekularen, biochemischen und zellbiologischen Versuchsansätzen untersucht. Die Proteinsequenz von DdVASP ist signifikant homolog zu den entsprechenden Proteinen in anderen Arten. Besonders charakteristisch sind die Ena/VASP Homologiedomänen EVH1 und EVH2, die durch eine Polyprolin-Region von einander getrennt sind. Typisch für die EVH2 Domäne sind eine G-Aktin- und eine F-Aktin-Bindungsdomäne, sowie eine Region, die für die Tetramerisierung von VASP wichtig ist. Als ein Tetramer kann DdVASP die Aktin Polymerisation nukleieren und Aktin Filamente bündeln. *In vitro* ist diese Nukleationsaktivität von DdVASP salzabhängig und bei 100 mM Salz bereits völlig verloren gegangen. Im Gegensatz dazu bleibt F-Aktin Bündelungsaktivität, wie sie in Sedimentationsversuchen getestet werden kann, erhalten.

Der Einfluss von DdVASP auf die Bindung von verkappenden Proteinen am schnell wachsenden Ende von Aktin Filamenten wurde anhand der Elongation von verkappten F-Aktin Nuklei und durch Depolymerisation von verkappten Filamenten nach Verdünnung unter die kritische Konzentration des schnell wachsenden Endes untersucht. In beiden Fällen konnte gezeigt werden, dass DdVASP verkappende Proteine nicht vom Filamentende ablösen kann. Das Formin dDia2 aus *D. discoideum*, das als essentiell für die Ausbildung von Filopodien eingestuft werden kann, ist im Gegensatz zu den DdVASP Ergebnissen in der Lage, verkappte Aktin Nuklei zu elongieren. Biochemische Daten legen nahe, dass die F-Aktin bündelnde Aktivität von DdVASP durch die Stabilisierung der

filopodialen Filamente entscheidend für die Ausbildung der Filopodien ist. Um diese Hypothese zu untermauern, wurden DdVASP Null-Mutanten isoliert. Wie zu erwarten war, konnten diese Mutanten keine Filopodien entwickeln. Eine Einschleusung von vollständigem DdVASP stellte den Wildtyp Phänotyp wieder her, die Expression einer VASP Mutation ohne die F-Aktin Bindungsdomäne (DdVASP Δ FAB) aber nicht. Schlüsselexperimente mit humanem VASP bestätigten, dass die Funktionen von DdVASP in der Evolution erhalten geblieben sind.

Im Verlaufe dieser Studien wurde auch die neue Profilin Isoform (Profilin III) weiter charakterisiert. Es stellte sich heraus, dass Profilin III spezifisch mit DdVASP interagiert. Profilin III zeigte keine ausgeprägte Ähnlichkeit zu den bereits gut untersuchten Profilin Isoformen I und II, und ist mit einem Konzentrationsanteil von weniger als 1% in der Zelle sehr niedrig konzentriert. Dieser Befund legt nahe, dass Profilin III für die Sequestrierung von Aktin keine Rolle spielt. Immunfluoreszenz-Experimente zeigten Profilin III in Filopodien und an ihren Spitzen, eine Minus-Mutante weist Veränderungen bei der gerichteten Zellbewegung auf.

Der zweite Teil des Projekts befasste sich mit zwei Kinasen aus der Germinal Centre Kinase (GCK) Gruppe. Die katalytische Domäne von Krs1 stellte sich als hoch homolog zu MST1 und MST2 aus dem Menschen heraus. Die regulatorische Region enthält eine vermutlich inhibitorische Domäne (As 330-379) und eine vermutlich multimerisierende Domäne ('SARAH', As 412-458), die auch für homologe Kinasen aus höheren Organismen beschrieben ist. Die SARAH Region umfasst circa 50 Aminosäuren, befindet sich am äußersten C-Terminus und bildet sehr wahrscheinlich ein 'coiled-coil' Motiv aus. GFP-Krs1 reichert sich bei Wildtyp Zellen im Kortex an und die Motilität dieser Zellen bei der Aggregation ist reduziert. Krs1-minus Zellen zeigten nur geringe Unterschiede zum Wildtyp. - Die Severin Kinase wird durch das Gen *svkA* kodiert und kann phylogenetisch zusammen mit den humanen Kinasen MST3, MST4 und YSK/SOK-1 in die GCK-III Untergruppe eingeordnet werden. Die Disruption von *svkA* führte zu Zellen mit aberranter Zytokinese sowohl in Petrischalen als auch in Schüttelkulturen. Obwohl die Motilität und Chemotaxis dieser Zellen weitgehend unverändert sind, ist die Bewegung der 'slugs' gestört, die Entwicklung ist verzögert und die Fruchtkörper zeigen eine aberrante Morphologie.

1 Introduction

1.1 The actin cytoskeleton

Actin is a major component of the cytoskeleton and was first isolated as part of the actomyosin complex from muscle cells (Halliburton, 1887; Szent-Gyorgyi, 1945; Zallar and Szabo, 1989). Actin was subsequently identified in all eukaryotic cells. Its most characteristic feature is the reversible polymerization of globular actin monomers (G-actin) into filaments (F-actin) that build either a relatively permanent structure in sarcomeres of fully differentiated muscle cells or, in nearly all other cell types a continuously restructured filamentous meshwork. Remodelling of the actin cytoskeleton is required in many cellular processes like cell migration, wound healing, immune responses, phagocytosis, cytoplasmic streaming and organelle transport (Engqvist-Goldstein and Drubin, 2003; Pollard and Borisy, 2003); without cytoskeletal dynamics axonal growth cones would not be available for wiring the human brain with about 1 million miles of neurites. Given its role in many important cellular processes the amino acid sequence of actin is highly conserved throughout evolution. Deletion of the single actin gene in yeast is lethal. In many other organisms more than one gene codes for this protein. In humans for example are at least six isoforms of actin which differ only slightly in their protein sequence and cell type specific expression.

Characteristics of actin:

Actin in vitro

Actin has a molecular mass of about 42,000 Da and can be stored in its monomeric form. Addition of simple salts like KCl or MgCl₂ induces the monomers to form filaments which lead to solutions with extremely high viscosities.

The polymerization of G-actin into F-actin can be subdivided into at least three phases (Figure 1):

Lag Phase: The polymerization of actin requires trimeric intermediates ('actin nuclei') which are highly unstable and, therefore delay rapid elongation.

Elongation: The elongation of actin filaments is very rapid and continues until it reaches an equilibrium at which nearly all of the actin molecules are part of filaments.

Steady State: At the steady state a continuous exchange of actin monomers occurs at both ends of filaments but the net polymerization of actin is zero. This constant concentration of G-actin which remains in equilibrium with filament ends is termed 'critical concentration'. If a cellular factor binds to actin monomers and thus lowers the critical concentration of free monomers at steady state, then depolymerization of filaments occurs and continues until the critical concentration is reached again, thus reducing number and length of filaments and consequently the viscosity of the solution.

Actin filaments are polar with two ends being different from each other. The polarity can be observed by decorating the filaments with myosin which gives the filament an appearance of an arrow head, hence the names 'pointed' and 'barbed' ends. The dissociation constants differ at both ends with actin monomers being added at the barbed end about 10-times faster than at the pointed end. This explains why the critical concentration at the barbed ends is about 0.1 μM in contrast to that of the pointed end with approximately 0.6 μM G-actin (Pollard and Cooper, 1986).

ATP-actin has a higher affinity for the barbed end than ADP-actin. However, ATP hydrolysis is not immediately required for polymerization. The very end of an actin filament at the fast growing side consists of a small stack of ATP-actin units, followed by a stretch of hydrolysed ADP/ P_i -actin complexes. After the release of P_i , actin filaments consist almost entirely of ADP-actin which leads to a remarkably decreased stability if distinct cellular proteins, e.g. actin-depolymerization factor/cofilin attack the filament. Thus ATP might also serve as a timer for depolymerization and filament turnover.

Regulatory mechanisms:

The average eukaryotic cell contains a large number of actin-binding proteins of different functions, locations and concentrations (Pollard and Cooper, 1986; Schleicher et al., 1995; Stossel et al., 1985). These proteins themselves are regulated, in most cases by phosphorylation, changes in free Ca^{2+} or interaction with lipids (dos Remedios et al., 2003). The physiological concentrations of Mg^{2+} or K^+ are such that all actin would be polymerized and the cells immobile due to their high cytoplasmic viscosity. The steady state equilibrium between G-actin and F-actin is maintained by many actin binding proteins. Only a few of them are discussed below (Figure 1).

a) The presence of **G-actin sequestering proteins** like profilin (Carlsson et al., 1977; Christensen et al., 1996; Haugwitz et al., 1991; Rothkegel et al., 1996) or thymosin β 4 (Nachmias, 1993) keeps the G-actin concentration at about 50% of total actin and thus the ability for the cell to react quickly to external signals. Both profilin and thymosin β 4 bind to ATP-actin with higher affinity than to ADP-actin. Profilin competes with thymosin β 4 and is discussed as an actin shuttle from thymosin β 4 onto the free barbed ends. The ATP-actin pool is guaranteed by both profilin and thymosin β 4. However, one should keep in mind that lower organisms do not contain thymosin β 4, i.e. obviously other proteins or mechanisms are also able to sequester ATP-actin efficiently.

b) Another important class of actin-binding proteins is the **capping proteins**. They cap usually the fast growing end of an actin filament, inhibit elongation and keep cytoplasmic viscosity low (Hartmann et al., 1989). The complexity of cytoskeletal dynamics becomes obvious if one considers 'uncapping' of a locked filament upon a signal. In this case the cap is suddenly removed, the large number of now free filament ends triggers elongation at high speed due to by-passing the lag-phase (see above). Uncapping of filaments would be a reasonable mechanism to create in a few seconds a new moving front in a chemotaxis gradient.

c) A very well known example for a third class of actin-binding proteins is gelsolin whose name describes the transformation of an actin gel into a less viscous sol. Gelsolin severs the filaments into short fragments and leads to a weakening of sub-membranous actin cortices (Bryan and Kurth, 1984; Janmey et al., 1985). Actin Depolymerizing Factor (ADF)/cofilin is another class of severing proteins whose activity is responsible for the depolymerization of the actin filaments (Nishida et al., 1984).

Kinetics of actin polymerisation and function of actin-binding proteins

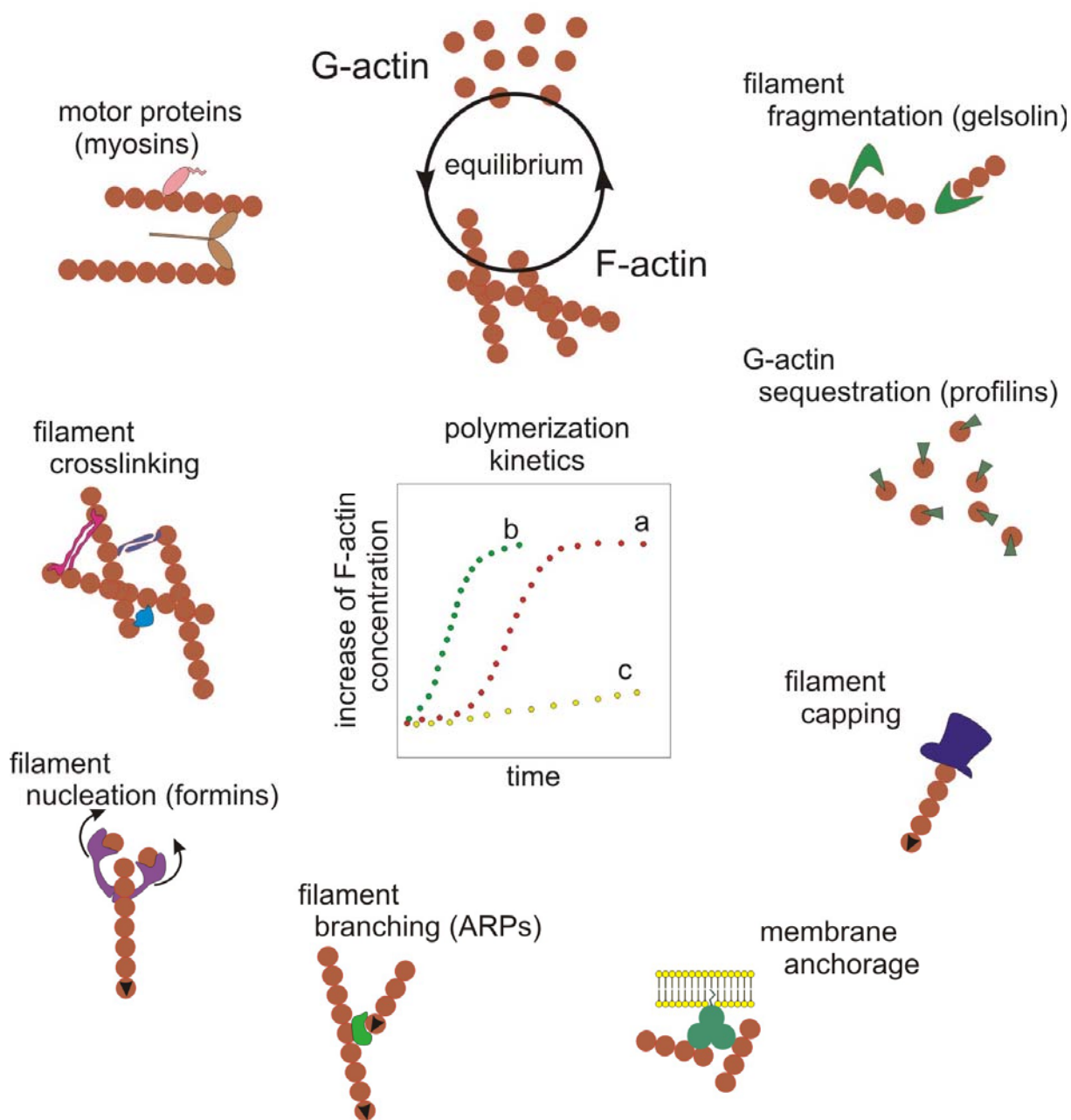


Figure 1: Schematic representation of different classes of actin binding proteins in eukaryotic cells and their behaviour in vitro

d) **Arp 2 and 3** were identified as part of a complex of 7 different proteins which functions as a *de novo* nucleator of filament formation and initiates branching of filaments (Amann and Pollard, 2001). The members of Wiskott-Aldrich-syndrome protein (WASP)/Suppressor of cAMP receptor (SCAR) family of proteins regulate the activity of the Arp2/3 complex probably by inducing a conformational change and bringing the two Arp

subunits close enough together to initiate nucleation (Blanchoin et al., 2000). Isolation of temperature sensitive mutants of the Arp2/3 complex with defects in the formation of actin patches revealed its contribution in their formation. However the other prominent actin structures, actin cables, remained undisturbed (Winter et al., 1997). This finding led to the identification of a second class of actin nucleators, the formins. Formins nucleate polymerization, elongate filaments from the free barbed ends, and remain associated like a processive capping protein.

e) In addition to the above mentioned actin binding proteins that regulate actin polymerization, a large and versatile number of other proteins like fimbrin (Prassler et al., 1997), α -actinin (Witke et al., 1986), filamin (Popowicz et al., 2006; Stossel et al., 2001), VASP (Bachmann et al., 1999) or cortexillin (Faix et al., 1996) regulate the 3-dimensional architecture of the filaments by **bundling or cross linking** the filaments.

1.2 Vasodilator Stimulated Phosphoprotein

Vasodilator-stimulated phosphoprotein (VASP), originally identified as the major substrate of cGMP- and cAMP-dependent kinases in platelets (Waldmann et al., 1987), is a member of the Ena/VASP family (Bear et al., 2001; Kwiatkowski et al., 2003; Reinhard et al., 2001). Ena/VASP proteins are a structurally conserved family found in vertebrates, invertebrates and also *Dictyostelium*. Ena/VASP proteins play an important role in cell adhesion and in the protrusive behaviour of the leading front in cell migration, and are involved in the regulation of actin-based functions (Bear et al., 2000; Gertler et al., 1996; Holt et al., 1998) such as axonal guidance, neural tube closure (Lanier et al., 1999), attenuation of platelet aggregation (Aszodi et al., 1999), T-cell activation (Krause et al., 2000), phagocytosis (Coppolino et al., 2001), cell-cell adhesion (Vasioukhin and Fuchs, 2001) and the intracellular movement of certain pathogens (Laurent et al., 1999). Though many different properties of these proteins were reported based on *in vitro* studies, the *in vivo* role and the mechanism of action remains elusive.

The Ena/VASP family contains *D. melanogaster* Ena (Enabled), *C. elegans* Unc-34, *D. discoideum* DdVASP, and the three mammalian family members VASP, Mena (Mammalian enabled), and EVL (Ena-VASP-like). All Ena/VASP family members share a conserved domain structure: an amino-terminal Ena/VASP homology 1 (EVH1) domain is

followed by a proline-rich central region and a carboxyl-terminal Ena/VASP homology 2 (EVH2) domain (see also Figure 3).

The EVH1 domain belongs to the PTB (phosphotyrosine binding) branch of the PH (pleckstrin homology) domain superfamily (Ball et al., 2000; Barzik et al., 2005; Beneken et al., 2000; Fedorov et al., 1999; Prehoda et al., 1999; Renfranz and Beckerle, 2002). A similar domain is also present in the WASP family of proteins hence also called 'WASP Homology 1' (WH1) domain'. The EVH1 domain binds to proteins with poly-proline stretches of the following consensus sequence: (F/W/Y/L)PPPPX(D/E)(D/E)(D/E) τ (X is any amino acid, τ is hydrophobic amino acid). Binding to this sequence targets the proteins to specific sites within cells, e.g. zyxin and vinculin to the focal adhesions, Fyb/SLAP (FYN binding protein/Src-like-adaptor) to phagocytic cups, and ActA to the ends of *Listeria monocytogenes*. Ablation of zyxin mislocalises the protein from the focal adhesion and retards cell motility. Other proteins that harbour this EVH1 binding site include pallidin, migfilin and ankyrin G (Mykkanen et al., 2001; Niebuhr et al., 1997; Parast and Otey, 2000).

All members of the VASP family harbour a central proline rich sequence of variable length. This region is responsible for the binding to the small G-actin binding protein profilin (Ahern-Djamali et al., 1999; Gertler et al., 1996; Lambrechts et al., 2000; Reinhard et al., 1995). In addition to profilin it also interacts with proteins with SH3 (Src Homology 3) and WW (the name WW derives from the presence of two signature tryptophan residues that are spaced 20-23 amino acids apart and are present in most WW domains known to date) domains, including those found in Abl (Abelson), Src Drk (Downstream of receptor kinase) (Ahern-Djamali et al., 1999; Comer et al., 1998; Gertler et al., 1995), IRSp53 (insulin receptor substrate p53) and FE-65 (amyloid beta (A4) precursor protein-binding) (Lambrechts et al., 2000). The physiological significance of this binding is not clear. Given the potent genetic interactions between Ena and Abl in flies (Gertler et al., 1990), it is possible that physical interactions between the PRO-region and the SH3 domain of Abl might play a role in connecting Abl signalling to Ena/VASP function.

The EVH2 domain contains three highly conserved regions: a G-actin-binding region, an F-actin-binding region (FAB), and a coiled-coil or tetramerisation domain (TD). *In vitro*, the EVH2 domain has been shown to bind to both G-actin and F-actin, induce actin

filament nucleation, promote filament bundling and mediate oligomerization (Ahern-Djamali et al., 1998; Bachmann et al., 1999; Walders-Harbeck et al., 2002).

Role of VASP in cell motility

Evidence for a role of Ena/VASP proteins in motility came from analysis of the effects of VASP deletion/overexpression on the motile behavior of living cells (Bear et al., 2000; Bear et al., 2002; Han et al., 2002; Rottner et al., 1999) and on actin-based propulsion of *Listeria* (Chakraborty et al., 1995; Laurent et al., 1999; Skoble et al., 2001; Smith et al., 1996).

Actin-based motility is mediated by site-directed activation of the Arp2/3 complex by the protein ActA (in *Listeria*) or by the proteins of the Wiskott-Aldrich syndrome protein (WASP) family in lamellipodia and filopodia extensions, which catalyse production of new filaments by barbed end branching, thus generating propulsive or protrusive forces (Boujemaa-Paterski et al., 2001). VASP and other members of the protein family, like the murine homologue of Ena (Mena) or Evl, greatly enhance the motility of *Listeria* in living cells (Smith et al., 1996) and in cell extracts (Laurent et al., 1999), indicating the function of VASP in *Listeria* motility. It is now known that VASP enhances motility by increasing the rate of dissociation of the branched junction, which is the rate-limiting step in the cycle of filament attachment-branching-detachment.

The effect of VASP on motility of living cells is less clear than its effect on *Listeria* propulsion owing to the conflicting reports from VASP mutant cell lines. While VASP was shown to be required for efficient chemotaxis in *D. discoideum* (Han et al., 2002) and a positive correlation of the amount of VASP at the leading edge and lamellipodial extension in fibroblasts, reports from VASP or Mena knockout cells showed an increase in cell motility in the absence of VASP. It is now proposed that VASP increases the transient protrusions of the lamellipodia but decreases the amount of branching, resulting in lower resistance against rearward force and overall cell motility.

1.3 Formins

Formins along with Arp2/3 complex and Spire belong to a class of actin binding proteins responsible for the *de novo* generation of actin filaments *in vivo*. While Spire and Arp2/3

complex bind to the pointed ends and allow growth from the free barbed ends, formins bind to the barbed ends. Formins are a highly conserved, ubiquitously expressed and multidomain proteins required for the assembly of actin filaments found in the cytokinetic contractile ring (Chang et al., 1997), yeast actin cables (Evangelista et al., 2002), adherence junctions between epithelial cells (Kobielak et al., 2004), filopodial protrusions (Schirenbeck et al., 2005), and in the establishment and maintenance of cell polarity (Sawin, 2002). The members of this family are characterised by two Formin Homology (FH) domains, FH1 and FH2. FH1 domain is characterised by a high density of proline residues. FH1 domain binds to profilin of the profilin-actin complex and increases the local concentration of the actin monomers in close vicinity of the nucleating FH2 domain (Kovar et al., 2006). The FH2 domain is approximately 400 amino acids and is the defining feature of this family and is sufficient for its nucleating activity *in vitro*. Some of the members also harbour sequences that are involved in the regulation of their activity and are grouped as Diaphanous Related Formins (DRFs). These domains include the Diaphanous Inhibitory Domain (DID), the Diaphanous Auto-regulatory Domain (DAD) and the small GTPases-Binding Domain (GBD). Interaction between the DID and the DAD domains keep the protein in an inhibitory state and the binding of small GTPases to GBD relieve the inhibition (Nezami et al., 2006; Vavylonis et al., 2006; Xu, 2006). This topology is typical for most formins

Mechanism of formin nucleation

Real time imaging and crystal structures of formin in complex with actin vastly contributed to our understanding of the molecular mechanism of formin action. While real time imaging (Higashida et al., 2004) of FH2 bound filament growth reveal that formins remain stably associated with the filament barbed ends as they grow, the insertion of actin monomers between the FH2 domain and the filament end was explained with the help of crystal structures. First, the structure of Bni1FH2 (Xu et al., 2004) alone suggested that the FH2 domain is a dimer with a donut shape. The crystal structure of Bni1FH2 associated with tetramethyl-rhodamine-labelled actin (TMR actin) (Otomo et al., 2005) demonstrated that flexibility in the FH2 dimer permits the actin filament to sit inside the donut hole, allowing each half of the FH2 dimer to interact with the two actin subunits at the end of the filament (a total of three subunits are bound since the penultimate subunit is bound by both FH2 molecules). This configuration allows both FH2 halves to remain continuously bound

during subunit addition because only one of the two contacts made by each half allows an alternating addition of a new monomer (Figure 2). In addition, it has been theorised that the FH2 domain dimer rotates in the direction opposite to the rotational direction of the elongating actin helices, thereby allowing the elongation of long filaments that do not accumulate torsion stresses and supercoil (Kovar, 2006; Kovar et al., 2006).

This model also predicts the existence of an FH2 dimer in equilibrium with two states: an open state allowing the addition of actin monomers and a closed state which does not allow any monomer addition. A transition from the closed state to an open state involves a stepping event of the lagging FH2 subunit to the barbed end allowing free space for the addition of actin monomers. The equilibrium between the open and the closed states ($K_{o/c}$) varies for every formin and this explains the differences in their elongation rates. Fission yeast formin Cdc12p, which completely inhibits barbed end elongation has a $K_{o/c}$ of ≤ 0.01 , and for mouse mDia1 that hardly influences the elongation rate and, consequently, has a constant of $K \geq 0.9$.

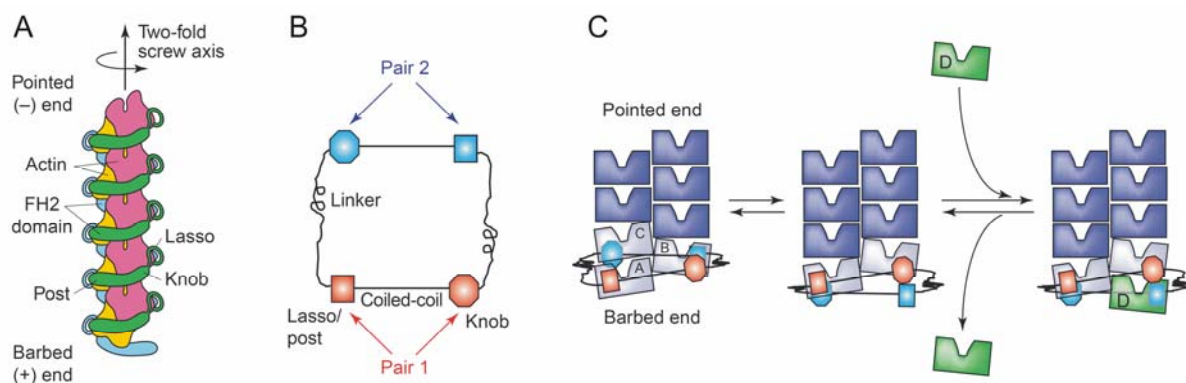


Figure 2: Model for processive movement of the formin homology 2 (FH2) domain with the barbed end.

(A) Model of Bni1 FH2 domain bound to actin based on the crystal structure (Otomo et al., 2005). The FH2 domain subunits are shown in green and blue. Actin monomers are pink and yellow. Actin monomers are oriented uniformly, with their pointed ends up and barbed ends down. (B) Schematic diagram of the FH2 domain dimer, represented as two ‘pairs’ of actin-interacting motifs. Each pair consists of one lasso–post dimerization interface and one knob region. The pairs are connected by linker regions, illustrated as squiggly lines to emphasize their flexibility. It is important to emphasize that each pair consists of sequence from both FH2 subunits. (C) Processive movement model. Each FH2 pair interacts with one face of the short-pitch helix of the actin filament. In the left panel, Pair 1 interacts with the front face, with the lasso–post region binding the barbed-end actin subunit (labeled ‘A’), and the knob region interacting with the barbed-end subunit of the adjacent protofilament (labeled ‘B’). Pair 2 binds the back face, its lasso–post interacting with subunit B, and its knob with subunit C. Due to interactions with FH2, the orientations of subunits A,

B and C on the filament are altered (denoted by gray as opposed to black for the non-FH2-bound subunits). In the center panel, the lasso–post of Pair 2 has released from subunit B and reoriented into an unbound position at the barbed end, the flexible linkers accommodating this change. In the right panel, a new actin subunit ('D', green) has added at the barbed end, with the lasso–post of Pair 2 binding it. All steps are reversible. The rate of barbed-end polymerization and depolymerization might be influenced by the on/off rate of individual pairs with actin subunits, by the flexibility of the linker regions or by monomer association rate for the altered barbed end. Reproduced from (Higgs, 2005)

1.4 Profilins

Profilins are small (12-15kDa) essential actin binding proteins that are present in animal cells (Carlsson et al., 1977), plant cells (Gibbon et al., 1997; Kandasamy et al., 2002; Valenta et al., 1993) and in viruses (Machesky et al., 1994b). Initial studies suggested that the main function was to bind actin monomers with 1:1 stoichiometry (Carlsson et al., 1977) and then release actin following cell stimulation and an increase in PIP₂ concentration, but are now known to have a far more complex influence on actin polymerization. One of the essential functions of profilin seems to be the nucleotide-exchange activity that accelerates the ADP-ATP exchange on G-actin 1000-fold thereby replenishing the pool of ATP-actin in the cell. Newly generated actin filaments consist of ATP-actin at the leading edge that is controlled in its elongation by the capping proteins CapG and CapZ. Profilins bind to the barbed end of an actin monomer, and function as a sequestering protein when the filaments are capped, but allow elongation of the free barbed ends of filaments at rates similar to free actin monomers. Profilins also block the elongation of the filaments from the pointed ends and inhibit spontaneous nucleation of actin filaments. In amoebae, the concentration of profilin and its affinity for actin are sufficient to account for majority of unpolymerized actin monomer pool (Kaiser et al., 1999; Vinson et al., 1998). Though the sequence homologies among profilins within and across species are not very high, the solved structure from bovine (Schutt et al., 1993), human (Metzler et al., 1995) or *Acanthamoeba* profilin (Fedorov et al., 1994; Vinson et al., 1993) showed very similar three dimensional folds. The structures of human profilin 1 and profilin 2 are almost superimposable (Nodelman et al., 1999). Both co-crystallization studies of bovine profilin:β-actin complexes (Schutt et al., 1993) and cross linking experiments (Vandekerckhove et al., 1989) showed that profilin binds to the sub domains 1 and 3 of G-actin in a 1:1 complex

Profilin has two other binding domains: one for phosphoinositides and one for poly-L-proline stretches seen in proteins such as Arp2/3 complex (Machesky et al., 1994a), formins (Kovar et al., 2006), VASP (Reinhard et al., 1995), and N-WASP (Fukuoka et al., 2001). The N-terminal and the C-terminal helices of profilin form a hydrophobic cleft that binds the poly-L-prolines. Aromatic residues on profilin intercalate with specific prolines of the polyproline helix. So far, all proteins that associate with profilin, have been found to contain the specific motif XPPPPP, where X is G, L, I, S or A. The PIP₂ binding site overlaps with both the actin- and the poly-L-proline binding site, and the binding of PIP₂ was shown to regulate both actin and poly-L-proline binding. Ability to bind both actin and poly-L-proline are essential for viability, at least in fungi (Lu and Pollard, 2001).

Complementation experiments in *D. discoideum* using plant profilins revealed the functional conservation of profilins (Karakesisoglou et al., 1996). Except for yeast most eukaryotic organisms express more than one profilin isoform. In mouse and human four profilin isoforms have been identified and characterized. Mammalian profilin I is expressed in all cells and tissue types except in skeletal muscle, whereas profilin II is expressed only in the developing and in the differentiated nervous system (Witke et al., 1998). Both these profilins differ slightly in their affinities for actin. An alternatively spliced form of profilin II, IIB, was recently reported that lacks the last 32 amino acids and has low affinities for actin and poly-L-proline. A third profilin isoform that is expressed mainly in the testis and in kidney was also reported (Braun et al., 2002). Though the presence of so many profilin isoforms with similar properties and structures is surprising, recent reports show that profilins are very specific in their interaction with different ligands probably contributed by the markedly different surface charge distribution (Schirenbeck et al., 2005; Witke et al., 1998).

In addition to actin regulation, profilins are associated with a large number of protein ligands. These include such different groups as nuclear proteins, Rac-Rho effector molecules, cell adhesion molecules. An interesting group of molecules that are gaining attention are the proteins involved in endocytosis and membrane trafficking that are coupled with actin polymerization. Previously it was shown that mouse profilin I is associated with exosomes in dendritic cells (They et al., 2001) and also with the Golgi compartments (Dong et al., 2000). In *D. discoideum* profilin null mutants show increased phagocytosis (Temesvari et al., 2000) and disruption of the endosomal/lysosomal protein

DdLMP can suppress the profilin null phenotype by a yet unknown mechanism (Karakesisoglou et al., 1999). Yeast profilin is also reported to be linked to membrane trafficking as suggested by the genetic interaction between *S. cerevisiae* profilin and Sec3p (Finger and Novick, 1997) and defective fluid uptake in profilin mutants.

Recently it was shown that mouse profilin 2 binds to dynamin1 and silences its function by inhibiting the binding of SH3-ligands that are necessary for the GTPase activity of dynamin (Gareus et al., 2006). The GTPase activity of dynamin is necessary for the recruitment of the endocytic machinery to the membranes (Gareus et al., 2006). Overexpression of wild type profilin 2 in HeLa cells reduced the receptor mediated endocytosis, but not the mutated protein deficient in dynamin1 binding.

D. discoideum has three profilin genes; two of them have been characterized in detail (Haugwitz et al., 1994; Haugwitz et al., 1991). Both profilin isoforms exhibit 55% identity in their amino acid sequences. *In vitro* studies showed that both isoforms bind G-actin with slightly differing affinities and are able to delay the onset of actin polymerization by shifting the critical concentration for actin polymerization to a higher level. Cells which lack only one isoform are indistinguishable from wild type cells. Only the disruption of both genes gave rise to an aberrant phenotype with an increased F-actin content, abnormal cytokinesis and development. These profilin deficient cells exhibit reduced motility, are up to ten times larger than wild type cells, often multinucleate, could grow on surfaces but not in shaking suspension and their development is blocked prior to fruiting body formation. The increase of F-actin by 60-70% suggests that *D. discoideum* profilin acts *in vivo* primarily as an actin sequestering protein.

1.5 Ste20 like kinases

Ste20 like kinases are serine/threonine kinases found in all eukaryotic species tested so far. Their catalytic domains are highly homologous to the Ste20 kinase of *S. cerevisiae*, the founding member of this group. The lack of Ste20 in yeast led to sterile cells due to the disruption of a MAP kinase pathway downstream of the pheromone receptor (Wu et al., 1995). The group of Ste20 like kinase is characterized by the presence of a signature sequence 'GTPY/FWAPY' (Dan et al., 2001). A subgroup of these kinases is defined by the presence of a p21 GTPase binding motif and therefore broadly classified as 'p21-activated kinase' (PAK) family (Hofmann et al., 2004). However, a larger number among the Ste20

like kinases do not harbour any well defined regulatory module and belongs to the germinal center kinase (GCK) family (Kyriakis, 1999). In addition, the topology of the kinases differs as well: PAKs have a C-terminal catalytic domain whereas the GCKs usually have their catalytic domain at the N-terminus. The increasing number of sequenced genomes allowed a fine tuning of phylogenetic relationships and further classification of Ste20 like kinases into eight different subfamilies based on conserved protein stretches within and outside the catalytic domain (Dan et al., 2001).

Recent data suggest that the Ste20 like kinases control key reactions in cell division, cell growth, cell polarity, apoptosis, and reorganization of the cytoskeleton. With the identification of Ste20 as a MAP4K, the role of other Ste20 like kinases in activating signaling pathways is not surprising (Drogen et al., 2000; Edmunds and Mahadevan, 2004; Wu et al., 1995). Following a phylogenetic analysis (Dan et al., 2001), kinases belonging to the GCK-I, -IV and -V subfamilies apparently regulate the JNK pathway, whereas members of the GCK-VI and -VIII subfamilies activate the p38 kinase cascade. MST1 and MST2 from the GCK-II subfamily were also shown to be part of MAPK pathways (O'Neill et al., 2005; Watabe et al., 2000).

The recently completed sequencing of the genome (Eichinger et al., 2005) helped to reveal four p21 activated kinases (Chung and Firtel, 1999; Lee et al., 2004a; Muller-Taubenberger et al., 2002) and thirteen highly homologous GCKs. The first *D. discoideum* GCK homolog was purified based on its ability to phosphorylate the F-actin fragmenting protein severin *in vitro* (Eichinger et al., 1998). Krs1 was the other member that was previously shown to phosphorylate severin as well. Phylogenetic analysis groups this kinase into the GCK-II subfamily along with mammalian MST1/KRS2, MST2/KRS1 (Creasy and Chernoff, 1995a; Creasy and Chernoff, 1995b; Taylor et al., 1996), and the *Drosophila* homolog Hippo (Harvey et al., 2003; Wu et al., 2003). This is in good agreement with a recent thorough *D. discoideum* kinome analysis which lists Krs1 in the MST subfamily (Goldberg et al., 2006).

1.6 *Dictyostelium discoideum* as a model organism

D. discoideum is a simple eukaryotic microorganism, which lives in forest soil and on decaying leaves, feeding on bacteria. The amoebae grow as separate, independent, single cells till the exhaustion of the nutrient source that triggers a developmental program, in

which up to 10^5 cells aggregate by chemotaxis towards cAMP (Gerisch, 1987; Loomis, 1996).

During the developmental cycle, amoebae migrate towards each other forming aggregates or mounds. Cells in these mounds undergo further differentiation into two major cell types, the prespore and prestalk cells that further develop into a mature fruiting body composed of a mass of spore cells supported by a thin long stalk made of vacuolated dead cells. Spores are oval, extremely resistant and germinate into amoebae again under favourable conditions. Under laboratory conditions, the entire developmental cycle can be completed within 24h (Chisholm and Firtel, 2004).

The growth and development of this organism can be separated and ease with which it can be grown in large quantities and be manipulated using powerful molecular genetic, biochemical and cell biological tools this micro organism provides a convenient model system to investigate cell motility, chemotaxis, cytokinesis, phagocytosis, endocytosis and signal transduction (Noegel and Schleicher, 2000). Recently, *D. discoideum* was also described as a suitable host for pathogenic bacteria in which one can conveniently study the process of infection (Skriwan et al., 2002).

A recent completion of the genome sequencing project provided the basis for a genome-wide survey of the microfilament system leading to the identification of a large number of new members of the microfilament system (Eichinger et al., 2005). Representatives of almost all classes of actin binding proteins were identified and the repertoire is most similar to metazoans followed by fungi and plants making *D. discoideum* a nice model system.

1.7 Goals of the project:

In the present work the following goals are addressed:

(1) The role of DdVASP in the formation of filopodia

Previously it was shown that VASP was required for filopodia formation in *D. discoideum* and in mammalian cells. It was reported to antagonise the activity of capping protein and promote the formation of filopodia. Recent studies showed that formins are necessary for the formation of filopodia and promote the growth of filopodia by antagonising the

capping protein. By employing *in vivo* and *in vitro* approaches and using *D. discoideum* amoebae the work should address the mutual roles of DdVASP and the formin dDia2.

(2) The *in vivo* role of a new profilin isoform

Among many activities profilins also interact with poly-proline regions in VASP and formins. The discovery of a third profilin in *D. discoideum* made it necessary to characterize this isoform in more detail and to obtain first data about its interaction with DdVASP or *D. discoideum* formins.

(3) Ste20-like kinases as members of signalling cascades

As a second project of this thesis, two selected Ste20 kinases should be investigated in more detail. Both of them were previously shown to phosphorylate the F-actin fragmenting protein severin *in vitro*.

All topics of this work aim at the characterization of signal transduction pathways which have their targets in the actin cytoskeleton.

2 Materials and Methods

2.1 Materials

Cell culture plates, 24 wells, flasks	Nunc
Cell culture dishes Ø 100 mm × 20 mm	Greiner bio-one
Cell culture dishes, Ø 3.5 mm with glass bottom	MatTek Corporation
Dialysis membranes Type 8, 20, 27, 25A	Biomol
Gel drying membrane	Festata
Gel-blotting-paper GB002	Whatman
Microconcentrators Centricon	Amicon
Nitrocellulose membrane Protran BA85	Schleicher & Schüll
Parafilm	American National Cal
PCR tubes 0.5 ml, Petri dishes, Ø 92 mm × 16 mm,	
Pipettes, 10 und 25 ml, 15 ml and 50 ml tubes ('Falcon'),	
1.5 ml centrifuge tubes	Sarstedt
Pipette tips	Braun Melsungen
Plasmid DNA Purification Maxi Kit	Macherey Nagel
QIAprep Spin Miniprep and Gel Extraction kits	Qiagen
Steel metal balls, Ø0.0025 inch, 440-C	New England Miniature
	Ball Company
Sterile filter, 0.22 µm Millex GV	Millipore
Ultracentrifuge tubes 1.5 ml	Beckman
X-ray film X-omat AR 5	Kodak

2.1.1 Computer programs

Adobe photoshop 5.5, Acrobat Reader 5.0,	Adobe Systems
Acrobat Distiller 5.0	
askSam 4.0	Seaside Software
AxioVS40 V4.3.101	Carl Zeiss Vision GmbH
CorelDraw 12 2003	Corel Corporation
DIAS 3.4.1	Solltech Inc.
DeepView/Swiss PdB Viewer	gsk GlaxoSmithKline
imageJ 1.34n	Wayne Rasband
Microsoft Office 2003	Microsoft Corporation
Openlab 2.2.5	Improvisation Ltd
Origin 7 SRI	OriginLab Corporation
Unicorn Software for Aekta	GE

2.1.2 Reagents

Unless and otherwise mentioned all laboratory chemicals used were purchased from Bio Mol, Fluka, Merck, Roth, Serva or Sigma and had the degree of purity "p.a."

Adenosine-3', 5'-cyclic Monophosphate (cAMP)	Sigma
Adenosine-5'-triphosphate-Na ₂ -Salt	Serva
Acrylamide (30% Acrylamide with 0,8% Bisacrylamide)	Roth
Agar-Agar, Type RG	Euler /BD
Agarose (SeaKem LE)	BMA

Ammonium persulfate (APS)	Roth
Bacto-Peptone/-Tryptone	Oxoid
BCIP (5-Bromo-4-chloro-3-indolylphosphate-p-toluidinsalz)	Gerbu
Bovine serum albumin Fraction V	Oxoid
Coomassie Brilliant Blue R 250, G 250	Roth, Sigma
Disodiumpyrophosphate	Sigma
DE52 (Diethylaminoethyl-Cellulose)	Whatman
DMSO (Dimethylsulfoxide)	Serva
DTT (1,4-Dithio-D,L-threitol)	Gerbu
EDTA (ethylenediaminetetraacetic acid)	Biomol
EGTA (ethylene glycol bis[2-aminoethyl ether]- -N,N,N',N'-tetraacetic acid)	Sigma
Ethidiumbromide	Sigma
[γ - ³² P] ATP	ICN
β -Glycerophosphate	Sigma
Glutaraldehyde	Serva
HEPES (N-2-Hydroxyethylpiperazide-N'-ethansulfonic acid)	Roth
IPTG (Isopropyl- β -D-thiogalactopyranoside)	Gerbu
β -Mercaptoethanol	Roth
NBT (Nitro Blue Tetrazolium)	Sigma
Nickel-NTA agarose	Qiagen
NP-40 (Nonylphenylpolyethylenglycol)	Fulka
Nucleotide	Peque labs
2-Propanol	Roth
Proteose peptone	Oxoid
Phenol/Chloroform	Roth
SDS (Sodium dodecylsulfate)	Serva
TEMED (N,N,N',N'-Tetramethylethylendiamine)	Pierce
Triton X-100 („surfact amps“)	Oxoid

2.1.3 Centrifuges and rotors

Centrifuges

Optima LE-80K, TL Ultracentrifuges,
GS-6KR Centrifuge, J2-21M/E Centrifuge,
J6-HC Centrifuge
Table top centrifuge 5415

Beckman
Eppendorf

Rotors

JA-10, JA-14, JA-20
Ti 35, Ti 45, Ti 70, TLA 100.3

Beckman

2.1.4 Media

All media and buffers used were prepared with deionised water, which had been filtered over an ion exchanger (Millipore) and were sterilized either by autoclaving or by passing through a micro filter.

AX-Medium (pH 6.7)
(Watts und Ashworth, 1970)
14.3 g peptone
7.15 g yeast extract

SM-Agar plates (pH 6.5)
9 g agar
10 g peptone

50 mM glucose
3.5 mM Na₂HPO₄

3.5 mM KH₂PO₄
made up to 1 l with H₂O

50 mM glucose
1 g yeast extract

4 mM MgSO₄
16 mM KH₂PO₄
5.7 mM K₂HPO₄
made up to 1 l with H₂O

Soerensen phosphate buffer (pH 6.0)
(pH 6.0)

(Malchow *et al.*, 1972)
14.6 mM KH₂PO₄
2 mM Na₂HPO₄

Phosphate agar plates

10 g Bacto-agar
dissolved in 1 l Soerensen
buffer

HL5-Medium (pH 7.5)

5 g yeast extract
10 g proteose peptone
50 mM glucose
8.5 mM KH₂PO₄
made up to 1 l with H₂O

PBS (pH 6.5)

70 mM Na₂HPO₄
30 mM KH₂PO₄
150 mM NaCl
0.1% NaN₃

LB-Medium for *E. coli* (pH 7.4)

(Sambrook *et al.*, 1989)
10 g bacto-tryptone
5 g yeast extract
86 mM NaCl

made up to 1 l with H₂O. pH was adjusted with NaOH and for agar plates the medium was cooled to 40°C before the addition of antibiotics.

LB rich medium (pH 7.0)

20 g bacto-tryptone
10 g yeast extract
86 mM NaCl

made up to 1 l with H₂O. 5 ml of 0.5 M sodium phosphate was added prior to autoclaving

2.1.5 Buffers

10 × Tris/Borate-Buffer (TBE, pH 8.3)

890 mM Tris/HCl
890 mM boric acid
20 mM EDTA
autoclave before use

TE-Buffer (pH 8.0)

10 mM Tris/HCl
2 mM EDTA
autoclave before use

TEDABP-Buffer (pH 8.0)

10 mM Tris/HCl
1 mM EGTA
1 mM DTT
0.02% NaN₃
prior to use the following
are mixed

MEDABP-Buffer (pH 6.5)

10 mM MES
1 mM EGTA
1 mM DTT
0.02% NaN₃
prior to use the follo-
wing are mixed

1 mM benzamidine
0.5 mM PMSF

1 mM benzamidine
0.5 mM PMSF

IEDANBP-Buffer (pH 7.6)

10 mM Imidazole
1 mM EGTA
1 mM DTT
0.02% NaN₃
prior to use the following are mixed:
1 mM benzamidine
0.5 mM PMSF
0.2 M NaCl

2.1.6 Instruments

Aekta FPLC system and Fraction collector RediFrac
Axiovert Microscopes 25, 35, M200
Dounce homogeniser
Eagle Eye II
Econosystem
Electroporator
Fluorescence-Spectrometer (FA-260-E1)
Heating block/Shaking Thermomixer 5436
Nuclepore-filter
Parr-bomb
Company
PCR-Thermocycler Uno
pH-Meter pH526
Photometer Ultrospec 2100 pro
Protein transfer Trans-Blot SD
Quartz cuvettes
Superdex 200 10/300 GL, Superose 6 10/300 GL and
Superose 12 10/300 GL
Ultrasonicator 820/H
UV-transilluminator IL-200-M
Vortex
Waterbath
Kühner

GE
Zeiss
Braun
Stratagene
BioRad
BioRad
Aminco Bowman
Eppendorf
Costar. Whatman
Parr Instrument

Biometra
WTW
Amersham
BioRad
Starna

GE
Elma
Bachofer
Bender & Hobein
GFL. Ika. Infors.

2.1.7 Bacteria strains

Klebsiella aerogenes

(Williams, 1976)

E.coli strains:

DH5α
JM 105
TOPO cells
XL-1 Blue

(Invitrogen)

Expression strains:

BL21 Rosetta	Stratagene
BL21 RIL	Stratagene
M15	Qiagen

***D. discoideum* strains**

AX2-214 (Laboratory wild type)	
pI/II minus strain	(Haugwitz et al., 1994)
Dd VASP minus strain	(Schirenbeck et al.,
2006)	
DST2 minus strain	this study
DST1 minus strain	generous gift from
	Dr. Meino Rohlf

2.1.8 Vectors

pDGFPXaMCS-Neo	(Dumontier et al., 2000)
pDEXRH	(Faix et al., 1992)
pGEX 5x-1	GE
pGEX 6P-1	GE
pLPBLP	(Faix et al., 2004)
pQE 30, 31, 32	Qiagen
pUC 18/19	(Yanisch-Perron et al., 1985)
pCR 2.1-TOPO	TOPO TA Cloning
Flag vectors	pDISC (Ralf Graef)

2.2 Molecular Biological Methods

2.2.1 Isolation of *D. discoideum* genomic DNA using a High Pure PCR Template Preparation Kit (Roche)

D. discoideum cells from Petri dishes or shaking cultures were harvested and washed with Soerensen buffer. The pellet was resuspended in 200 µl of PBS. 200 µl of binding buffer and 40 µl of proteinase K were added immediately to the cell suspension and incubated at 72°C for 10 min. 100 µl of isopropanol were added to the suspension which was then transferred into the upper reservoir of the filter set and centrifuged for 1 min at 8,000 g. The flowthrough was discarded. The filter tube was washed once with Inhibitor Removal buffer and twice with wash buffer (1 min / 8,000 g). Residual wash buffer was removed from the filter by centrifuging the empty filter tube for an additional minute at 13,000 rpm. The filter tube was transferred into a clean 1.5 ml Eppendorf tube and the DNA was eluted with 200 µl prewarmed (70°C) elution buffer by spinning the sample for 1 min at 8,000 rpm. The genomic DNA was stored at -20°C.

2.2.2 Isolation of total RNA by the Qiagen method

The Qiagen RNeasy Mini Kit was used for the isolation of total RNA from *D. discoideum* cells. Cells grown in axenic cultures or on a *Klebsiella* lawn were harvested and washed twice with Soerensen buffer (5 min / 1200 g). The cell pellet was resuspended in RLT buffer (600 µl for every 1x10⁷ cells) supplemented with fresh β-mercaptoethanol (dilution

1:1,000). One volume of 70% ethanol was then mixed with the lysate and the mixture was transferred onto a Qiagen RNA purification column. The column was spun at 13,000 rpm for 30 s and the flowthrough was discarded. The column was washed once with 700 µl of RW1 buffer, and twice with 500 µl RPE at 13,000 rpm for 30 s. Residual wash buffer was removed by centrifuging the empty column for an additional minute. RNA was eluted with 30 µl RNase free water. RNA was stored at -70°C for long term storage or it was used immediately.

2.2.3 RT-PCR

RT-PCR was carried out to amplify specific cDNAs from *D. discoideum* total RNA samples. Total RNA was isolated using the Qiagen RNeasy kit as described above. The reaction was set up in 0.5 ml PCR reaction tubes using the Qiagen One-Step RT PCR kit and the desired specific primers. This method employs an optimal combination of Omniscript Reverse Transcriptase, Sensiscript Reverse Transcriptase, and HotStarTaq DNA Polymerase.

Master mix (50 µl)

RNase-free water (provided)	—
5x QIAGEN OneStep RT-PCR Buffer	1x
dNTP Mix (containing 10 mM of each dNTP)	400 µM of each
Primer A	1 pmol/µl
Primer B	1 pmol/µl
QIAGEN OneStep RT-PCR Enzyme	2.0 µl
Template RNA	1-2 pg/tube

Reverse transcription was carried out at 45°-50°C for 30 min, followed by incubation at 95°C for 15 min and normal PCR cycles.

2.2.4 Polymerase Chain Reaction (PCR)

The amplification of DNA fragments and generation of site-directed mutagenesis was carried out by polymerase chain reactions. Taq polymerase (Roche), Taq buffer, dNTPs were used as usual. The reaction was performed on a thermocycler (Biometra UNO) in either a 50 µl or a 100 µl reaction. cDNA or genomic DNA were used as a template. A brief denaturation step was always done before the start of the actual 25-35 cycles for amplification. Annealing temperatures were calculated according to the formula of Suggs *et al* (Suggs *et al.*, 1981).

$$4(N_G+N_C) + 2(N_A+N_T) - 10 = T_a (\text{° C})$$

N = the number of Adenine (A), Thymidine (T), Guanidine (G) or Cytosine (C) in oligonucleotides.

Reaction conditions in most assays:

Denaturation:	95°C for 120 s
Denaturation:	95°C for 30s
Annealing:	variable temperature for 60s
Elongation:	69°C for 1 min for every 1000 bp
Final extension	70°C for 10 min
No. of cycles:	30

The annealing temparture is dependent of the primer sequences.

10x PCR buffer

200 mM Tris/HCl (pH 8.8)

100 mM KCl

100 mM $(\text{NH}_4)_2\text{SO}_4$
20 mM MgSO_4
1% Triton X-100
1 mg/ml BSA (Nuclease-free)

2.2.5 Agarose gel electrophoresis (Sambrook and Russell, 2001)

Electrophoretic separation of DNA was carried out using 0.7% (w/v) agarose gels prepared in 1 x Tris-borate EDTA buffer at 1-5 V/cm. Running and gel buffer were identical. The gels were cast in chambers of various sizes (4 x 7 to 20 x 20 cm), the DNA to be separated was mixed with 0.2 vol of DNA sample buffer and loaded onto the gels. At the end of the run, the gel was stained in a solution of ethidium bromide (5 $\mu\text{g}/\text{ml}$) for 10- 30 min, followed by destaining in water for about 30 min. Subsequently the gels could be observed under UV light at 312 nm and photos taken with the Eagle Eye CCD camera system (Stratagene, Heidelberg).

DNA sample buffer

40% sucrose
0.5% SDS
0.25% bromophenol blue
-Taken up in TE buffer

2.2.6 Determination of DNA concentration

DNA was diluted 100 times in sterile H_2O and the absorbance was measured at 260 nm and 280 nm. An O.D._{260} of 1.0 corresponds to 50 $\mu\text{g}/\text{ml}$ of double stranded DNA. An $A_{260:280}$ ratio of 1.80 indicated highly pure DNA free from contaminating protein. Alternatively, the DNA concentration could also be estimated by comparing the intensity of bands after agarose gel electrophoresis with the bands in the Mass Ruler lane.

2.2.7 Isolation of DNA fragments from agarose gels

Extraction and purification of DNA from agarose gels in Tris-borate buffer were performed using the QIAquick gel extraction kit (Qiagen) according to the manufacturer's instructions. The kit provides buffers and all centrifugation steps were carried out at 14,000 rpm at room temperature using a tabletop microcentrifuge. The DNA was excised from the agarose gel with a clean scalpel, the gel slice weighed, and 3 vol buffer QG were added to 1 vol gel (100 mg~100 μl). The tube was then incubated in a heating block at 50°C for 10 min or until the gel slice was entirely dissolved. To increase the yield of DNA fragments (< 0.5kb and > 4kb), 1 gel vol isopropanol was added to the sample and mixed. The sample was then loaded onto a QIAquick spin column (Qiagen) and centrifuged for 1 min in order to bind DNA to the resin. The flowthrough was collected in a 2 ml collection tube and discarded. For washing, 750 μl of buffer PE was added to the column and spun for 1 min. The flowthrough was discarded and the column was centrifuged for an additional 1 min to remove residual ethanol completely. The column was then placed into a clean 1.5 ml tube and the DNA was eluted by the addition of 30-50 μl of elution buffer (10 mM Tris/HCl, pH 8.5) or dH_2O to the column followed by a centrifugation for 1 min.

2.2.8 Purification of PCR products

For cloning purposes, the PCR products were purified using the QIAquick PCR Purification Kit from Qiagen following the manufacturer's protocol. The kit provided

buffers were used and all centrifugation steps were done at 14,000 rpm at room temperature using a table top microcentrifuge. 5 vol of PB buffer were added to 1 vol of the PCR product and mixed. The mixture was applied to a QIAquick spin column and centrifuged for 1 min to bind DNA to the column while the flowthrough collected in 2 ml collection tube was discarded. DNA was washed with 750 μ l of PE buffer by a centrifugation for 1 min. Residual ethanol was removed by an additional centrifugation for 1 min. The spin column was then placed into a clean 1.5 ml tube and the DNA was eluted with 50 μ l of EB buffer. The purified DNA was subsequently used for restriction digestion

2.2.9 DNA cleavage with restriction enzymes

For cloning purposes usually 1 μ g of DNA (plasmid or PCR product) was digested in a 50 μ l reaction with 10 U of each enzyme. The buffer suitable for the restriction enzyme(s) was added and the volume was adjusted with dH₂O. The tube was incubated at the 37°C overnight. The digestion of the vector was monitored on an agarose gel. For screening of putative clones, the reaction tubes were incubated at 37°C for 45-60 min with 0.1-0.25 U of enzyme / 2 μ g of DNA.

2.2.10 Mini preparation of plasmid DNA using Qiagen Miniprep Kit

The plasmid DNA from *E. coli* was isolated with the QIAprep Spin Miniprep Kit from Qiagen. All buffers were supplied with the kit. Single colonies from LB plates were inoculated and grown in LB medium with appropriate selection pressure. Cells were pelleted and resuspended in 250 μ l buffer P1 containing RNase. The cells were lysed by adding 250 μ l alkaline lysis buffer P2 and the suspension was mixed gently by inverting the tube 4-6 times. The suspension was then neutralized by mixing the suspension with the addition of 350 μ l buffer N3. The mixture was centrifuged (10 min / 13,000 rpm). The plasmid containing supernatant was passed through the QIAprep spin column to allow binding to the resin. The column was washed with 750 μ l buffer PE, and centrifuged for an additional minute to remove residual wash buffer. The QIAprep column was then placed into a clean 1.5 ml tube and DNA was eluted with 50 μ l of EB buffer.

2.2.11 Mini preparation of plasmid DNA by the method of Holmes and Quigley

Overnight cultures of *E. coli* in LB medium (with ampicillin; 10 μ g/ml) were spun and the pellet was resuspended in 200 μ l of STET/lysozyme buffer. The suspension was boiled in a water bath for 1 min, centrifuged (13,000 rpm, 10 min, room temperature) and the insoluble cell debris was removed using a sterile tooth pick. The nucleic acids in the supernatant were precipitated with 200 μ l of isopropanol for 5 min at room temperature and sedimented using a table top centrifuge (13,000 rpm, 30 min, room temperature). The DNA pellet was washed with 70% ethanol, air dried and the pellet was resuspended in 50-100 μ l sterile H₂O or in TE (Holmes and Quigley, 1981).

2.2.12 Phosphatase treatment (Sambrook and Russell, 2001)

In order to prevent self-ligation of a linearised vector, the phosphate group at the 5' end was removed using alkaline phosphatase from calf intestine. Dephosphorylation was performed in a 50 μ l reaction volume, whereby 1-5 μ g of linearised DNA vector was incubated with 1-2 U of alkaline phosphatase in 1 x phosphatase buffer at 37°C for 1 h. To inactivate the enzyme, the DNA was purified over a Qiagen column as described above.

2.2.13 Ligation of DNA into a plasmid vector

Ligation of CIP treated vector and insert was carried out overnight at 16°C using 1.5 U of enzyme, in a minimum volume usually in not more than 30 µl. The vector and the insert were mixed at a molar ratio of 1:3.

2.2.14 Preparation of chemically competent cells

250 ml LB medium were inoculated with overnight preculture, and grown in a 37°C shaker, 220 rpm until an OD₆₀₀ of 0.4-0.6 was reached. Cells were put on ice for 30 min and then centrifuged for 20 min (4°C, 4,000 rpm). Cells were washed twice with ice-cold CaCl₂/glycerol. Finally the pellet was resuspended in 2 ml of CaCl₂ / glycerol buffer and kept on ice in 200 µl aliquots for 30 minutes, shock-frozen in liquid nitrogen and stored at -70°C.

Transformation buffer (CaCl₂/glycerol):

60 mM CaCl₂

15% glycerol

10 mM PIPES

pH was adjusted to 7.0

2.2.15 Transformation of *E. coli*

For transformation, competent *E. coli* cells were thawed on ice and incubated with the ligation mix on ice for 20 min followed by a heat shock at 42°C for 90 s. The cells were immediately placed on ice for 1 min and revived with LB medium. Cells were kept in 37°C with agitation for 45-60 min and plated on LB plates containing the appropriate antibiotic. Plates were incubated at 37°C overnight to obtain *E. coli* colonies harbouring the transformed plasmid. Single clones were inoculated into tubes containing 2-5 ml LB with antibiotics. Cells were grown on a 37°C shaker for 7 h or overnight. The positive transformants were detected by mini preparation of DNA plasmid.

2.2.16 Transformation of *E. coli* by electroporation

For transformation, electrocompetent *E. coli* cells were thawed on ice. Ligation mix was precipitated to remove the salt present in the ligation buffer and the DNA pellet was resolubilised in a minimum volume of deionized water. Electrocompetent cells were mixed with the DNA and placed in a pre-cooled electroporation cuvette (BioRad; Gene Pulser Cuvette). After a pulse of 1.8 kV, 200 Ω and 25 µF, 1 ml of LB or SOC medium was immediately added and the cells were regenerated at 37°C for an hour. Cells were spun down, resuspended in 200 µl of LB, plated onto LB plates with appropriate selection pressure and incubated overnight at 37°C.

2.2.17 Transformation of *E. coli* using the TOPO TA Cloning kit

To transform *E. coli* cells with pCR 2.1-TOPO vector the TOPO TA Cloning kit was used. This method allows cloning of undigested PCR products by transformation of TOPO *E. coli* cells. *Taq* polymerase adds a single deoxyadenosine (dA) to the 3' ends of PCR products. The vector supplied in the TOPO TA Cloning kit had single, overhanging 3' deoxythymidine residues. This allowed PCR inserts to ligate efficiently with the vector by a topoisomerase.

The ligation and transformation were done following the manufacturer's protocol.

Ligation:

0.5 – 4 µl of the fresh PCR product

1 µl of salt solution

sterile water added to a total volume of 5 µl

1 µl TOPO vector

final volume 6 µl

Ligation was carried out at room temperature for 20 min.

Transformation:

2 µl of ligation mix was added to the One Shot Chemically Competent *E. coli* cells supplied with the kit. The mixture was incubated on ice for 20 min and then cells were heat shocked for 30 seconds at 42°C. The tubes were transferred to ice and 1 ml of LB medium was added. Cells were incubated at 37°C for 1 h. 10-15 µl from each transformation was spread onto prewarmed LB-Amp plates and incubated overnight at 37°C to get colonies.

2.2.18 *E. coli* permanent cultures

Overnight grown cultures of bacteria were centrifuged and the pellets were resuspended in fresh LB medium containing 7% DMSO. The cells were shock frozen in liquid nitrogen and stored at -70°C.

2.2.19 Maxi preparation of plasmid DNA

To isolate large quantities of plasmid DNA, DNA was isolated from 250-400 ml cultures using a DNA Maxi-kit. The cells were harvested by centrifugation (4,000 g; 5 min; 4°C). The cell pellet was resuspended in 12 ml of buffer S1+RNase A, lysed by adding 12 ml of buffer S2 and mixed gently by inverting the vial 6-8 times. The mixture was incubated at room-temperature for not more than 5 min. The lysate was neutralized by carefully adding 12 ml of pre-cooled buffer S3, incubated on ice for 15 min, transferred to the centrifugation tubes and spun down (12,000 g, 40 min, and 4°C). The supernatant was passed through the NucleoBond AX 500 column that was pre-equilibrated with 6 ml of buffer N2. The column was washed with 35 ml of wash buffer. The plasmid DNA was eluted with 15 ml of buffer N5 and precipitated with 11 ml of isopropanol at room temperature. DNA was pelleted by centrifuging at 15,000 g, 4°C, for 30 min. The DNA pellet was washed with 5 ml of 70% ethanol (centrifuged at 15,000g; room temperature; 10 min), air-dried and dissolved in 500 µl 10 mM Tris.

Buffer S1: 50 mM Tris-HCl
10 mM EDTA
100 µg/ml RNase A
pH 8.0

Buffer S3: 2.8 M potassium acetate
pH 5.1

Buffer N3: 100 mM Tris
15% ethanol
1.15 M KCl
pH adjusted to 8.5 with H₃PO₄

Buffer S2: 200 mM NaOH
1% SDS

Buffer N2: 100 mM Tris
15% ethanol
900 mM KCl
0.15% Triton X-100
pH adjusted to 6.3 with H₃PO₄

Buffer N5: 100 mM Tris
15% ethanol
1 M KCl
pH adjusted to 6.3 with H₃PO₄

2.3 Biochemical Methods

2.3.1 SDS-Polyacrylamide Gel Electrophoresis (SDS-PAGE)

Protein mixtures were separated by discontinuous SDS-PAGE (Laemmli, 1970). For this purpose, 10, 12 and 15% acrylamide resolving gels with 3% stacking gels were used (7.5 x 10 x 0.05 cm). The stacking gel deposits the polypeptides to the same starting level at the surface of the resolving gel, and subsequently the SDS-polypeptide complexes are separated in the resolving gel according to size under uniform voltage and pH. Prior to SDS-PAGE, 3 x SDS gel loading buffer was added to the protein samples to be separated. The mixture was boiled for 3-5 min. Electrophoresis was carried out at a constant voltage of 150 V, after which the gel could be stained with Coomassie Blue dye and destained for direct observation of the protein bands. Proteins from the gel could also be blotted onto a nitrocellulose membrane and detected indirectly via antibodies. As standard, a mixture of proteins of defined molecular masses was electrophoresed.

3 x SDS-PAGE sample buffer

150 mM Tris/HCl (pH 6.8)
30% Glycerol
6% (^{w/v}) SDS
15% β-mercaptoethanol
0.3% bromophenol blue

10 x SDS-PAGE running buffer

250 mM Tris
1.9 M glycine
1% (^{w/v}) SDS

2.3.2 Coomassie Blue staining of proteins

Following SDS-PAGE, gels were stained in Coomassie Blue solution by shaking for 15-30 min, after which the unbound dye was removed by shaking in a destaining solution.

Coomassie Blue solution

0.1% Coomassie Brilliant Blue R 250
50% methanol
12% glacial acetic acid
Solution filtered through a Whatman filter

Destaining solution:

10% ethanol
7% glacial acetic acid

2.3.3 Silver staining

The acrylamide gels were fixed in a solution containing 50% methanol and 12% acetic acid for 30 min at room temperature. The fixative was removed and washed 2 x 30 min with 5% methanol and 7% acetic acid. The gels were soaked in 10% glutaraldehyde solution for 30 min, washed a number of times in water for 2 h, incubated in silver nitrate solution (Sol. A), and then washed briefly for 10 s in water. The gel was developed with Sol. B and the reaction stopped after 5 min with 10% ethanol and 7% acetic acid

Solution A

2 ml NaOH (1N)
1.4 ml NH₃ (25%)
92.6 ml H₂O
4 ml AgNO₃ (0.2mg/ml)

Solution B

10 ml methanol
1 ml formaldehyde
50 mg citric acid
90 ml H₂O

2.3.4 Drying of SDS-PAGE gels

For permanent recording, SDS-polyacrylamide gels after Coomassie Blue staining were washed in water with agitation with a couple of changes of water to remove the destaining solution. The gels were then shaken in a drying solution for 20 min, after which each gel was sandwiched between two dialysis membranes pre-wetted in the drying solution and then air-dried overnight.

Drying solution for polyacrylamide gels

24% ethanol

5% glycerol

2.3.5 Western blotting

Following separation of protein by SDS-PAGE, the proteins were transferred from gels onto nitrocellulose membranes (Schleicher & Schuell BA85) according to a modified protocol of Towbin *et al* (Towbin et al., 1979) by the means of a protein transfer apparatus (Trans-Blot SD, BioRad). In this “semi-dry” method, the gel and its attached nitrocellulose membrane were sandwiched between several pieces of Whatman 3MM filter paper which had been soaked in transfer buffer, and protein transfer was carried out at room temperature at 15 V for 45 min, after which the nitrocellulose filter was blocked for at least 1 h or overnight at room temperature in 5% (w/v) milk powder in NCP buffer. The membrane was then washed five times with NCP. The membrane was then incubated with primary antibody diluted in 0.1% BSA solution in NCP overnight or at least for 3 h. After washing 3 times with NCP buffer, the membrane was incubated with a secondary antibody conjugated with alkaline phosphatase (diluted 1:2,000 in NCP buffer + 1% BSA) for at least 3 h. The membrane was washed 5 times (15 min each) with NCP and once with 0.1 M Na₂CO₃-buffer, pH 10.2. Finally, the protein bands were detected by using 25 ml of 0.2 mg/ml BCIP diluted in 0.1 M Na₂CO₃.

Transfer buffer (pH 8.5):

25 mM Tris/HCl

190 mM glycine

20% methanol

0.02% SDS

20x NCP buffer (pH 7.2)

200 mM Tris/HCl

3 M NaCl

20 ml Tween 20

2% NaN₃

2.3.6 GST-tagged protein expression

Constructs in pGEX vectors were transformed into DH5 α or Rosetta BL21 cells (Novagen). Cultures were inoculated and grown overnight at 37°C, diluted tenfold and grown at 21°C to an OD₆₀₀ of 0.4 - 0.8. Expression was induced with usually 0.5 mM IPTG and cells were grown overnight at 21°C. After harvesting and washing following routine procedures, cells were resuspended in lysis buffer, opened by sonication in the presence of 0.5 mg/ml lysozyme. Lysates were centrifuged at 10,000 g for 45-60 min at 4°C and the supernatants were coupled to Glutathione-Sepharose 4B (Sigma) by recycling for 3-4 h. The matrix was washed with 10-20 column volumes of lysis buffer and the bound proteins were eluted with lysis buffer containing 20 mM reduced glutathione. The presence of protein in different fractions was tested by Bradford's method (Bradford, 1976). Protein containing fractions were analysed on SDS-PAGE. The appropriate fractions were pooled and dialysed against PBS.

Lysis Buffer:

1 x PBS

1 mM DTT
5 mM benzamidine
1 mM PMSF
protease inhibitor cocktail (Sigma)

2.3.7 Cleavage of the GST tag

If pGEX-6P vectors were used for expression, the GST tag could be removed by PreScission Protease. Following elution of the GST fusion protein from Glutathione Sepharose, the eluate was dialysed extensively against PBS containing 1 mM EDTA and 1 mM DTT in order to remove reduced glutathione and protease inhibitors from the sample. 10 µg of enzyme were used to cleave 1 mg of GST fusion protein. Cleavage was carried out at 4°C overnight on a rotatory shaker. Once digestion was complete, the sample was passed through a washed and equilibrated Glutathione Sepharose to remove free GST and the PreScission Protease from the protein of interest.

2.3.8 Purification of histidine-tagged constructs

For the expression of proteins with His-tag, the cDNA were cloned into pQE vectors (Qiagen). Cultures were inoculated and grown overnight at 37°C, diluted tenfold and grown to an OD₆₀₀ between 0.4 - 0.8 at 21°C. Expression was induced with 1 mM IPTG, cells were grown, harvested, lysed and centrifuged essentially as described above. The resulting supernatants were coupled to Ni-NTA beads (Qiagen) and incubated for 3-4 h. The matrix was washed with 10-20 column volumes of lysis buffer supplemented with an additional 10 mM Imidazole and the bound proteins were eluted with lysis buffer containing 250 mM Imidazole. The protein fractions were pooled and dialysed against PBS.

2.3.9 Preparation of actin from rabbit skeletal muscle

Actin was prepared from rabbit skeletal muscle according to the methods described by Spudich and Watt (Spudich and Watt, 1971) as well as by Pardee and Spudich (Pardee and Spudich, 1982). The back and upper thigh muscles of a freshly bled rabbit or breast muscle of chicken were sliced into pieces, minced and extracted with high-salt extraction buffer for 10 min with agitation. The mixture was centrifuged (4,000 g, 10 min) and re extracted after which the sediment was resuspended in water and the pH adjusted to between 8.2 and 8.5 with 1 M Na₂CO₃ solution. Following centrifugation (4,000 g, 10 min), the supernatant was discarded and the process was repeated until swelling of the sediment was observed. The sediment was then washed with cold acetone, dried overnight. Finally the acetone powder was stored at -20°C for subsequent actin preparation.

10 g muscle acetone powder were extracted with 200 ml of G-buffer at 0°C for 30 min, filtered through nylon nets and re-extracted at 0°C for 10 min. The filtrate was centrifuged (30,000 g, 30 min, 4°C) and the actin in the supernatant allowed to polymerize for 2 h at room temperature or overnight at 4°C after addition of KCl (50 mM), MgCl₂ (2 mM) and ATP (1 mM). For removal of tropomyosin, solid KCl was then slowly added till a final concentration of 0.8 M was reached. The actin filaments were then sedimented by centrifugation (150,000 g for 3 h, at 4°C). For depolymerization, the F-actin pellet was dialysed against several changes of G-buffer and further purified using a Sephacryl S300 gel filtration column (2.5 x 45 cm Pharmacia). From its optical density at 290 nm, the G-actin concentration could be calculated easily (1mg/ml pure actin: 0.65 O.D.₂₉₀) (Wegner, 1976). The G-actin prepared could be stored on ice up to 3 weeks for most applications.

Extraction buffer

0.5 M KCl
0.1 M K₂HPO₄

G-buffer (pH 8.0)

2 mM Tris/HCl
0.2 mM CaCl₂
0.2 mM ATP
0.02% NaN₃
0.5 mM DTT

2.3.10 Pyrene-labelling of actin

Actin was labeled with N-(1)pyrenyliodoacetamide (pyrene) following the protocol of Kouyama and Mihashi (Kouyama and Mihashi, 1981). After the ultracentrifugation step in the course of preparation of actin from acetone powder as described above, 2/3 of the supernatant were carefully collected and dialysed against buffer P. Actin polymerization was initiated by the addition of KCl (150 mM) and MgCl₂ (2 mM), and 3-5 fold molar excess of pyrene (in DMSO) was added immediately to the vigorously stirred actin solution. From this step onwards, all activities were carried out in the dark since pyrene is light sensitive. The solution was turned end-over-end in a 50 ml tube at room temperature overnight after which the actin filaments were sedimented (150,000 g, 3 h, 4°C). The F-actin pellet was homogenized in G-buffer and dialysed against G-buffer to allow depolymerization. After a second centrifugation step (150,000 g, 3 h, 4°C), the pyrene-labelled G-actin was purified by gel filtration as described above and later stored at -70°C.

Buffer P (pH 7.6)

1 mM NaHCO₃
0.1 mM CaCl₂
0.2 mM ATP

2.3.11 Pyrene actin assays

Pyrenyliodoacetamide-labeled actin monomers (pyrene actin) provide a fluorescent readout of actin filament polymerization because a 30-fold increase in fluorescence occurs on incorporation of a labeled actin subunit into the polymer. Only low levels (5–10%) of pyrene labeled actin are required for a strong signal. For actin assembly, a final concentration of 2 μM actin was routinely used. The reaction (800 μl) was started by addition of actin

Nucleating activity of dDia2 or Dd VASP

To test the nucleating activity of dDia2 or DdVASP the chosen concentrations of the actin / pyrene-actin was so low (usually 1-2 μM total actin) that an extended lag phase occurred in the control sample. For actin assembly under physiological salt conditions the reaction mixture was supplemented with 100 mM KCl.

Uncapping of F-actin seeds

F-actin seeds: F-actin seeds were usually prepared by polymerizing actin and mechanically shearing the filaments by vortexing. 0.1 μM actin seeds were used per assay. No lag in actin polymerization should be observed when polymerization was initiated in the presence of seeds.

Capping of F-actin seeds: Recombinant His-tagged *D. discoideum* capping protein Cap32/34 or the mouse macrophage capping protein CapG were routinely used in the assays. The amount of capping protein needed to saturate the barbed ends was determined by titrating the F-actin seeds with different amounts of capping proteins. The concentration that exhibited very high but not complete inhibition was used for the subsequent assays

Uncapping: Uncapping of the F-actin seeds should result in rapid actin polymerization. This was done by adding different proteins to the capped seeds.

Depolymerization assays

Actin filaments when diluted below the critical concentration of the barbed ends (0.1 μM) depolymerize rapidly. This can be monitored by the decrease in fluorescence over time. Depolymerization of F-actin is a very rapid reaction and measurement of actin depolymerization for the first 0-50 sec is very critical. Therefore, the F-actin solution was added to the dry cuvette in the fluorimeter and diluted by forceful addition of the actin-free reaction mixture. For pre-capping the barbed ends capping protein was mixed gently with the F-actin solution and incubated for 120 sec before depolymerization was induced by dilution as described above. The effect of DdVASP on the capped filaments was tested by diluting them with DdVASP in the actin-free mixture to avoid bundling of filaments during preincubation.

2.3.12 Immunoprecipitation

For immunoprecipitations the cells were harvested by centrifugation at 1,200 g for 3 min, washed twice with phosphate buffer and resuspended at a density of 1×10^8 cells/ml in cold 25 mM HEPES buffer pH 7.4. One ml of the cell suspension was sedimented for 2 min at 2,000 g and the pellets incubated with lysis buffer containing 25 mM HEPES pH 7.4, 50 mM NaCl, 1 mM EGTA, 5 mM benzamidine, and 1 mM DTT, 5% glycerol, 1% *n*-octylpolyoxyethylene (Bachem), 1 mM PMSF and protease inhibitor cocktail (Sigma). The crude lysates were spun for 10 min at 15,000 g and the clear lysates were each supplemented with 100 μg of polyclonal antibodies together with 150 μl of protein A-Sepharose CL-4B (Sigma) slurry equilibrated in lysis buffer. After 2 h of incubation at 4°C, the beads were sedimented, washed seven times with 1 ml lysis buffer, and bound proteins eluted with SDS sample buffer.

2.3.13 F-actin bundling assays

For F-actin bundling assays, G-actin and DdVASP or HsVASP solutions were cleared at 100,000 g for 30 min in a Beckman benchtop ultracentrifuge at 4°C to remove aggregates. The reaction mixtures were incubated for 30 min at room temperature in 1.5 ml centrifuge tubes in polymerization buffer (10 mM Imidazole containing 3 mM MgCl_2 , 1 mM ATP and 0.2 mM CaCl_2 pH 7.0). The samples were then centrifuged for 15 min at 10,000 g to separate F-actin bundles present in the pellet from unbundled F-actin filaments and G-actin present in the supernatant. The supernatant was then transferred into Beckman Ultra-Clear centrifugation tubes and centrifuged at 100,000 g for 15 min, mainly to separate single filaments and actin monomers. All the samples were then dissolved in SDS sample buffer. Sample volumes were normalized and analysed on SDS-polyacrylamide gels.

2.3.14 Preparation of profilin III affinity resin

For covalent coupling of profilin III to an agarose resin Affigel 10 from Bio-Rad was used. Affigel 10 contains N-hydroxysuccinimide esters on a derivatized cross-linked agarose gel. A major advantage of Affigel is the mild conditions that permit coupling. Coupling can be achieved between pH 3.0 to 10.0. Upon addition of ligand, N-hydroxysuccinimide is opened and a stable amide bond is formed. Recombinant profilin III (approximately 25 mg/ml of resin) was dialysed extensively against 0.1 M MES-buffer, pH 5.5 to remove any primary amine containing compounds such as Tris. At first, the uniform slurry of the affinity matrix was transferred to a glass fritted funnel. The preservative was drained and

the gel was washed with three bed volumes of cold (4°C) deionised water by applying vacuum. Care was taken, not to allow the gel bed to fall dry. The moist gel cake was transferred to a clean glass flask; the cold ligand solution was added (0.5:1.0 ratio of protein solution to the gel volume) and mixed on an end-over-end wheel for 2 h at room temperature. The free active esters were completely blocked by mixing 0.1 ml 1 M ethanolamine per ml gel for 1 h. After 1 h of blocking the gel was washed with coupling buffer followed by water to remove free reactants. Before storage or the actual application, the column was washed with all the solvents that were subsequently used to elute the substances specifically bound to the column. The gel material was stored at 4°C in the starting buffer containing 0.2% NaN₃ or with 20 mM MES buffer pH 5.5.

MES buffer (pH 5.5)

Between 20-100 mM MES

0.2 mM DTT

1 mM benzamidine

0.5 mM PMSF

0.02 % NaN₃

2.4 Cell Biological Methods

2.4.1 Growth in liquid medium and on agar plates

Wild type AX2 strain was cultured axenically in either AX medium or in HL5 medium in Erlenmayer flasks. The media were supplemented with the appropriate antibiotics when cultivating the mutants. The generation time for the wild type at 21°C and 150 rpm is about 8-10 h. Cells were also cultured on Petri dishes. For this purpose AX2 wild type cells were suspended in 12 ml HL5 medium. For all cell biological studies, cells were allowed to grow maximally up to a cell density of 5×10^6 cells/ml to avoid the stationary phase. For large scale preparations cells were cultivated in 4 x 2.5 l cultures up to a cell density between 5×10^6 to 1.2×10^7 cells/ml.

2.4.2 Preservation of spores

Cells from liquid culture were harvested by centrifugation at 830 rpm for 10 min, washed once with cold Soerensen buffer, resuspended at a cell density of about 2×10^8 cells/ml, and 500 µl of the cell suspension were spread out per phosphate agar plate. The cells were able to develop into fruiting bodies within 2-3 days. The spores were then harvested by knocking onto the lid of the Petri dish and taken up in 10 ml of cold Soerensen buffer. 1 ml aliquots were dispensed into Nunc tubes (2.2 ml), shock-frozen in liquid nitrogen and stored at -70°C. For inoculation with spores, an aliquot was thawed at room temperature and cultured either in AX or in HL5 medium, whereby after 3 days at 21° C and 150 rpm, a cell density of about 5×10^6 cells/ml was reached.

2.4.3 Storage of *D. discoideum* cells at -70°C

For preservation of *D. discoideum* cells, axenic cultures were harvested and resuspended at a cell density of about 5×10^7 cells/ml in ice-cold freezing medium (1.1 ml containing 900 µl of HL5 or AX medium, 100 µl of horse serum and 100 µl of DMSO). Cells were distributed as 1.1 ml aliquots into sterile tubes, pre-cooled on ice. The tubes were incubated at 4°C for one hour, -20°C for 2-4 h and then stored at -70°C.

2.4.4 Transformation of *D. discoideum* cells

D. discoideum cells were transformed with the appropriate plasmids by electroporation. Approximately 10^7 growth-phase cells were washed at 0°-4°C, twice in 17 mM K-phosphate buffer, pH 6.0 and once in electroporation buffer (EP; 50 mM sucrose, 10 mM Na-K-phosphate buffer, pH 6.1). The cell pellet was then resuspended in 700 μ l EP and the suspension gently mixed with ~35 μ g of DNA at 0°C in a 4 mm electroporation cuvette. Electroporation was performed for 1 ms, at 1 kV and 10 μ F with the Gene Pulser Xcell (Biorad); two pulses were applied at 5 s intervals. After electroporation, the cells were transferred to a 9 cm plastic Petri dish and shaken at ~40 rpm for 15 min at 20°C. The suspension was adjusted to 2 mM CaCl₂ and 2 mM MgCl₂ and shaking was continued for another 15 min. Finally, 12 ml axenic growth medium was added, and the cells were allowed to recover for 24 h. After the 24 h recovery period, the cells were placed in axenic medium containing the appropriate selection pressure to select for transformants.

Electroporation buffer (pH 6.1)

50 mM sucrose

10 mM KH₂PO₄

pH was adjusted to 6.1 with KOH solution, and the buffer was sterilized by filtration

2.4.5 Cloning of transformants

Following 10-15 days of selection, the transformants were washed from the Petri dishes, diluted and plated together with an aliquot of *K. aerogenes* suspension onto SM agar plates. The transformants were diluted to about 50-100 cells per plate for better isolation of single colonies. Within 2-3 days at 21°C, single round clearing plaques were visible. These were picked with sterile toothpicks and cultured in 24-well plates in HL5 medium containing selection pressure for transformants (G418; dilution 1:1,000) and antibiotics mixture (ampicillin/streptomycin 1:1000) to remove the contaminating bacteria. The axenic cultures were then grown in larger quantities, harvested and further analysed.

2.4.6 Analysis of cell shape and cell migration

Aggregation competent wild type and mutant cells (knock out and rescue) were plated onto glass coverslips in small plastic dishes, and cell migration was recorded at intervals of 10 s by using an Axiovert-200 inverted microscope and the Axiovision software (Carl Zeiss, Jena, Germany). The time-lapse movies were analysed with the DIAS program (Solltech, Oakdale, IA). For shape analysis, the outlines of the single cells were drawn manually. Chemotaxis experiments were performed with micropipettes and a micromanipulator system (Eppendorf, Hamburg, Germany) essentially as described previously (Gerisch and Keller, 1981)

2.4.7 Phagocytosis assay

D. discoideum cells of strain AX2 and the DST-1 deficient mutant cell lines were grown to densities below 5×10^6 cells/ml, harvested, washed, and resuspended in Soerensen phosphate buffer to a density of 2×10^6 cells/ml in a 100 ml Erlenmeyer flask. Tetramethyl rhodamine isothiocyanate (TRITC)-labeled yeast cells (120 μ l; 10^9 cells/ml) were added to 20 ml of the *D. discoideum* cell suspension. Samples of 1 ml were withdrawn every 20 min and added to 100 μ l of trypan blue solution (20 mg/ml dissolved in 20 mM sodium citrate containing 150 mM NaCl), which quenches the fluorescence of non-internalized yeast cells. After 3 min of agitated incubation, cells were spun and the supernatant was removed

carefully. After resuspension in Soerensen phosphate buffer, fluorescence was measured in a fluorimeter using 544 nm light for excitation and recording emission at 574 nm. The measured fluorescence was calculated as relative fluorescence to AX2.

2.4.8 Expression of Cre and selection of Bsr minus clones

Bsr knockout mutants were transformed with pDEX-NLS-cre as described previously. After the 24 h recovery period, the cells were placed in axenic medium containing 10–20 µg/ml of G418 (Invitrogen Life Technologies) to select for pDEX-NLS-cre transformants. Selection in G418 is continued for 3–10 days. The cells were then plated for clonal isolation by standard dilution. The clones were subsequently picked in replica onto two different plates. The first was a standard SM agar plate using growing *K. aerogenes* as the nutrient source. The second was a non-nutrient phosphate (30 ml) agar plate (17 mM Na/K-phosphate, pH 6.0 in 1.5% agar) layered with 500 µl of a concentrated *K. aerogenes* suspension in Na/K-phosphate buffer and 120 µl of Blasticidin S at 10 mg/ml; the final concentration of Blasticidin S in the agar plate was 40 µg/ml. All *D. discoideum* cells grow on SM *K. aerogenes* plates, but only *D. discoideum* that have retained the *Bsr* cassette grow rapidly in the presence of Blasticidin S. A wild type parental cell was always used for growth control. Cells not growing in Blasticidin S were replica plated into 24 well microtitre plates containing axenic media, axenic media with Blasticidin S or axenic media with G418. Each transformation gave different frequencies for selective and optimized growth. Genomic DNA from Blasticidin- and G418-sensitive cell lines was analysed by PCR.

2.4.9 Phototaxis

Phototaxis efficiency of the wild type and mutants was tested as described previously (Darcy et al., 1994) by using a sterile inoculation loop to transfer cells to water agar plates from the edges of colonies growing on *K. aerogenes* lawns. The plates were wrapped in a dark coloured box with a 2 mm wide opening for the entry of light. Plates were incubated at 21°C for at least 48 h. To visualise the slugs and their tracks, cells were transferred onto a nitrocellulose membrane and were stained with an actin antibody.

2.4.10 Indirect immunofluorescence

Studies of subcellular localisation were also performed via indirect immunofluorescence. For this assay, coverslips to be used were washed with 3.6% HCl followed by dH₂O. Exponentially growing *D. discoideum* cells were harvested, washed twice with Soerensen buffer, and 1×10^6 were allowed to attach to the coverslips for 15 min, after which excess fluid was removed and the cells were fixed in cold methanol for 10 min at -20°C followed by 30 min air drying. Alternatively, cells could be fixed with paraformaldehyde/picric acid solution (2% paraformaldehyde, 10 mM Pipes, 15% saturated picric acid, pH 6.0) for 15 min and then washed several times with PBS/glycine and PBG. The cells were then permeabilised with 70% ethanol for 5 min at room temperature and washed with PBS/glycine followed by PBG.

After fixation, cells were incubated with undiluted hybridoma supernatants for at least 2 h before being washed with PBG and then subjected to 1 h incubation with fluorescently labelled goat anti-mouse IgG (diluted in PBG). F-actin was labelled either with Alexa 488, TRITC-labelled phalloidin or a monoclonal antibody against *D. discoideum* actin (Simpson et al 1984). Nuclei were stained either with DAPI (4, 6-diamidino-2-phenylindole, Sigma) or TO-PRO diluted in PBG. After incubating with the secondary antibody cells were

washed several times with PBG, PBS and briefly with dH₂O before being embedded in gelvatol and kept at 4°C overnight.

10x PBS (for immunofluorescence, pH 7.4)

1.37 M NaCl

0.027 M KCl

0.081 M Na₂HPO₄

0.015 M KHPO₄

PBG

0.5% BSA

0.05% fish gelatine

in 1x PBS, sterilised by passing through a 0.5 µm filter

2.4.11 Reflection Interference Contrast Microscopy

Reflection Interference Contrast Microscope imaging (RICM) was performed with either an inverted Zeiss LSM 510 laser scanning confocal microscope (LSM). Images were obtained using the 633 nm line of a He-Ne laser, a reflection mirror in place of the dichroic beam-splitter, a fully open pinhole, and a 100×/1.6 NA oil-immersion Neofluor lens. The second dichroic beam-splitter was removed from the light path. Cultures for the inverted microscope were prepared by attaching a glass coverslip over a hole in the bottom of a 35 mm tissue culture dish. The cells were either in Soerenson buffer or in nutrient rich media. The parameters of the laser scanning system were adjusted so that focal contacts appeared black. For time lapse movies, about 100 images were collected at 10 s intervals.

2.4.12 Yeast strains, maintenance, recovery from frozen stocks, and routine culturing

The two yeast strains used for all yeast two hybrid purposes were AH109 and Y187. These strains were supplied with the Match Maker 3 system (BD Biosciences). Yeast strains are stored indefinitely in YPD medium with 25% glycerol at -70°C. To prepare new glycerol stock cultures of yeast an isolated colony from the agar plate was scraped with a sterile inoculation loop and resuspended in 20–50 ml of YPD medium (or the appropriate SD medium) and incubated on a shaker at 30°C and 200 rpm overnight. Usually it takes longer for cells to grow in selection media. The culture was spun in 1.5 ml microcentrifuge tubes. The pellet was vortexed vigorously to thoroughly disperse the cells. The cells were resuspended in YPD medium with 25% glycerol and stored at -70°C in freeze vials.

2.4.13 Yeast plasmids

Two shuttle plasmid vectors for *E.coli* and yeast were supplied along with the kit. pGBKT7 harbours the DNA-binding region of the Gal4 transcription factor and a kanamycin resistant marker for selection in *E.coli*. The fused cDNA is expressed as a myc-tagged protein and can be used for immunoprecipitations and immunoblots. The pGADT7 vectors harbour the activation domain of the Gal4 transcription factor and an ampicillin resistance marker. The fused cDNA was expressed as a HA-tagged protein.

2.4.14 Yeast transformation

To test the interaction between two proteins, the bait and the target vectors carrying the appropriate genes were transformed into either Y187 or AH109 yeast strains using the THE Liac/SS CARRIER DNA/PEG METHOD. Briefly, the yeast strains were innoculated into 5 ml of liquid medium (2x YPAD) and incubated on a shaker at 30°C and 200 rpm. 2 ml of an overnight YPAD culture (titer between 1 and 2 x 10⁸/ml) were harvested in a sterile 1.5 ml microcentrifuge tube by centrifuging for 30 s. To the cell pellet the following components of the transformation mixture were added in the order listed below

<u>Component</u>	<u>Volume (μl)</u>
PEG 3500 50% w/v	240 μ l
LiAc 1.0 M	36 μ l
Boiled SS-Carrier DNA (2 mg/ml)	50 μ l
Plasmid DNA (0.1 to 1 μ g) plus water	34 μ l
Total volume	360 μ

The carrier DNA must be boiled in a water bath for five days, snap cooled on ice/water and vortexed before addition. The tubes were incubated in a water bath at 42°C for 40 to 60 min. The transformation mix is then removed by centrifugation for 30 s, the cell pellet was resuspended in 1.0 ml of sterile water and plated onto the appropriate selection plates

2.4.15 YPAD medium (YPD plus adenine)

(Yeast Extract - Peptone - Dextrose plus Adenine medium)

6.0 g	yeast extract (Difco)
12.0 g	peptone (Difco)
12.0 g	glucose
60 mg	adenine hemisulphate
600 ml	distilled water

For agar medium 10 g of Bacto-agar was added and sterilised by autoclaving at 121°C for 15 min. To grow the Y187 strain the media was prepared without the addition of adenine hemisulphate.

2.4.16 Synthetic Complete drop out (SC drop-out) Medium

4.0 g	Difco Yeast Nitrogen Base (w/o amino acids)
12.0 g	glucose
0.50 g	Synthetic Complete Drop Out Mix
600 ml	distilled water
10.0 g	Difco Bacto Agar (add for solid medium)

The ingredients (except Agar) were mixed in water and the pH was adjusted to 5.6 with 10 N NaOH. (This step is important for highest efficiency transformation). The media were sterilised by autoclaving at 121°C for 15 min.

Synthetic complete drop-out medium mix (SC drop-out)

2.0 g	Adenine hemisulfate
2.0 g	Arginine HCl
2.0 g	Histidine HCl
2.0 g	Isoleucine
2.0 g	Leucine
2.0 g	Lysine HCl
2.0 g	Methionine
3.0 g	Phenylalanine
6.0 g	Homoserine
3.0 g	Tryptophan
2.0 g	Tyrosine
1.2 g	Uracil
9.0 g	Valine

Omit the appropriate component(s), indicated in bold type, to prepare SC-Ade, SC-His, SC-Leu, SC-Trp, SC- Trp/Leu, and SC-Trp/Leu/His. Combine the ingredients in a clean

250 ml plastic bottle. Add three or four clean glass marbles and shake vigorously to mix. This quantity will be sufficient for approximately 100 (600 ml) batches of SC drop-out medium. Homoserine can be replaced by the addition of serine and threonine (2 grams each).

2.4.17 Constructs used for the yeast two hybrid

The activation domain (AD) of pGADT7 was fused to full length VASP (1-380), EVH1 (1-113), PRD (114-192), EVH2 (193-380), EVH1 PRD (1-192), PRD EVH2 (114-380). All the three profilin isoforms were fused with the Gal4-binding domain (BD) in plasmid pGBKT7. All the fragments were cloned as BamHI and Sall fragments.

3 Results

3.1 Characterisation of DdVASP

3.1.1 The VAsodilator Stimulated Phosphoprotein DdVASP from *Dictyostelium discoideum*

The microorganism *Dictyostelium discoideum* contains only one *vasP* gene as indicated by the genome project (Eichinger et al., 2005) (www.dictybase.org). Sequence analysis of the gene revealed the presence of only one intron in the 5' region with 145 nucleotides and therefore, the entire coding sequence was amplified by RT-PCR from total RNA of vegetative cells. The full-length cDNA clone coded for 380 amino acids (Figure 3A) which gave rise to a protein with a molecular mass of 39,107 Da and a calculated pI of 10.5. DdVASP showed a moderate degree of homology to VASPs from other species.

3.1.2 Domain structure of DdVASP

The derived protein sequence of DdVASP (Figure 3A) showed that the domain architecture (Figure 3B) of this protein is well conserved and can be divided into three distinct domains: an N-terminal Ena/VASP homology domain 1 (EVH1 domain), also termed as a WH1 domain, spanning about 113 amino acids [1-113] and a 188 amino acids C-terminal EVH2 or WH2 domain [193-380]. Both these domains are separated by a stretch of about 79 amino acids rich in prolines. The EVH2 domain contains the following three highly conserved blocks: G-actin binding domain (Walders-Harbeck et al., 2002); the F-actin binding (FAB) motif (Bachmann et al., 1999; Huttelmaier et al., 1999; Laurent et al., 1999), and the C-terminal Tetramerisation Domain (TD). The G-actin binding site of DdVASP is especially similar to the WH2 domain seen in WASP, WIP and other members of this family of proteins. The tetramerisation domain forms a predicted coiled-coil domain and is necessary for multimerisation of the molecule, a key property for a number of different functions of VASP.

A] DdVASP Sequence

```

1  MSETAIFNAT  GQVFTYSPQT  RNWVPSSNVP  ATLQMYFNNSG  ANTYRVIGRA  EVH1
51  GDDPNNFLIN  FAVKSEVVYS  RASEIFHQFT  DQRTHFGINF  TSKQDADTFG
101  GGFENVLRSL  KGGPQQPPPQ  VPKPQPQP  QPQPPQRP  STVIAKPVAP  PRD
151  QAPVAPPQAP  AAAPQAPAPP  AAPPAPPKPP  GPPPPPPAPK  PPAAGGGTGR
201  NALLGSIENF  SKGGLKKTVT  VDKSAGVPTK  TTPSANSAAS  NAGSEPSSGG  EVH2
251  STPAPAPKSS  GGGGGDLMA  EVMAKRAKMK  AAASQPKEES  SAPTPAPTPA
301  PTPAPTPSST  SFKPPQSFSK  PATKTAAANK  PPSPSLSAPL  PSTVANEDLQ
351  SLKEEILTEV  RKEIQAKDE  ILEAIRASQH

```

B] Domain Structure of DdVASP

```

Dd VASP      GGTGRNALLGS IENFSKGLKK-TVTVDKSAGVPTKTTTPSANSAA
Mm WIP       EQAGRNALLSD ISKG-K-KLKK-TVTNDRSAPILDKPKGAGASAG
Mm WIRE      EQRNRGALLQD ICKGT--KLKKVTNVNDRSAPVIEKPRGSSGGYG
Hs NWASP-1  TAGNKAALLDQ IREGAQ--LKKV-EQNSRPVSCSGDALLDQIRQ
Sc Vpr       VMQGRDALLGD IRKGM--KLKKA-ETNDRSAPIVGGGVSSASGS
Hs Thyβ4    MSDKPGMAE-IEKFDKSKLKK-TETQEKN-PLSSKETIEQEROA

```



```

Dd VASP      GGGDLMAEVMAKRAKMKAAASQPKEE
Hs VASP      GGGGLMEEMNAMLARRRKAT.QVGEK
Mm VASP      TGGGLMEEMNAMLARRRKAT.QVGEK
Mm Ev1      GGGGLMEEMNKLLAKRRKAASQ.TDK

```

Figure 3: Domain structure of DdVASP

(A) Amino acid sequence of DdVASP. The three functional domains of DdVASP were indicated by a colour code, EVH1 (Blue), PRD (Red), EVH2 (Green). The predicted coiled-coil domain is highlighted by underlining the amino acids. (B) The domain organization of DdVASP. EVH: Ena/VASP homology; PRD: proline-rich domain. The C-terminal EVH2 domain contains three regions: A G-actin binding motif (G), an F-actin binding motif (F) and a region required for tetramerization (T). Top: Alignment of its G-actin binding site to WH2 (Wasp homology domain 2) domains from other G-actin binding proteins (accession numbers/residues: DdVASP CAH05068 / 196-239, Mm WIP NP694778 / 29-70, Mm WIRE NP922922 / 33-75, HsNWASP-1 NP003932 / 402-442, Sc Vpr NP013441 / 27-68, Hs Thy-β4 NP066932 / 1-41). Identical residues are shown in red, conserved charged residues in blue. Bottom: The alignment of the F-actin binding regions of VASP from *D. discoideum* and Ena/VASP-like (Evl) proteins from other species is shown (accession numbers/residues: DdVASP CAH05068 / 264-289, HsVASP P50552 / 297-321, Mm VASP P70460 / 293-317, Mm Evl P70429 / 261-285).

3.1.3 Complementation of VASP null cells with GFP-DdVASP

The *vasP* gene was disrupted by inserting a blasticidin resistant cassette into the wild type gene as shown in Figure 4A. For construction of the *vasP* targeting vector, a 510-bp 5' BamHI/PstI fragment and a 540-bp 3' HindIII/SalI fragment were amplified from genomic AX2 WT DNA by PCR. Both fragments were cloned into the corresponding sites of pLPBLP containing the blasticidin S resistance cassette. The resulting vector was cleaved with BamHI and SalI and used to disrupt the *vasP* gene in WT cells. The null mutants were screened by PCR using two sets of primers as shown in Figure 4B. DdVASP-null mutants were transformed with GFP-tagged VASP to complement the wild type gene.

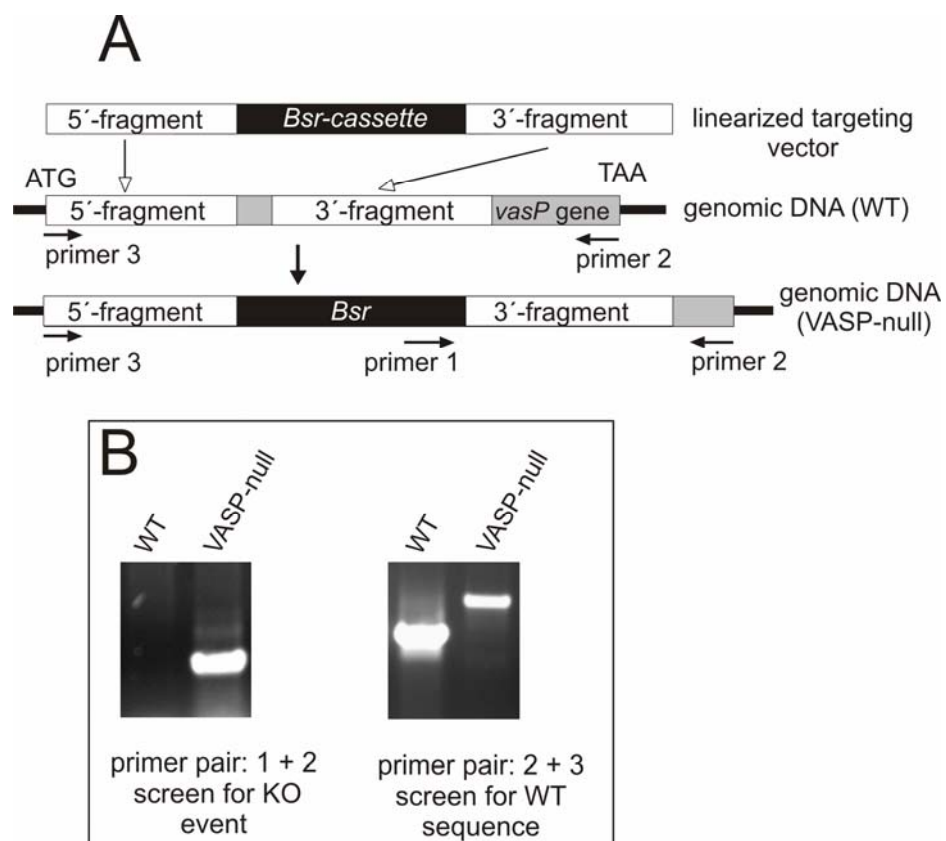


Figure 4: Generation of VASP-null mutants.

(A) Schematic view of the linearized targeting construct used to inactivate the *vasP* gene in wild-type cells. (B) DdVASP-null mutants were identified by PCR using specific primer pairs as indicated by arrows in A.

It was previously shown that GFP-HsVASP was localized to the tips of protruding lamellipodia, membrane ruffles and also to the filopodial tips. The localization is independent from the level of GFP protein expression (Rottner et al., 1999). In order to investigate the role of DdVASP, DdVASP was overexpressed as a GFP tagged protein

under a constitutive actin15 promoter. Clones expressing GFP-DdVASP and wild type AX2 cells were tested in an immunoblot with a DdVASP polyclonal antibody (Figure 5A and B). The localization of the protein was examined in live cells in a Laser Scanning Microscope to distinguish retraction fibers from true filopodia. GFP-DdVASP cells were resuspended in Soerensen-Phosphate buffer to induce the generation of filopodia. DdVASP was diffused throughout the cell body and with strong staining at the tips of filopodia (Figure 5C).

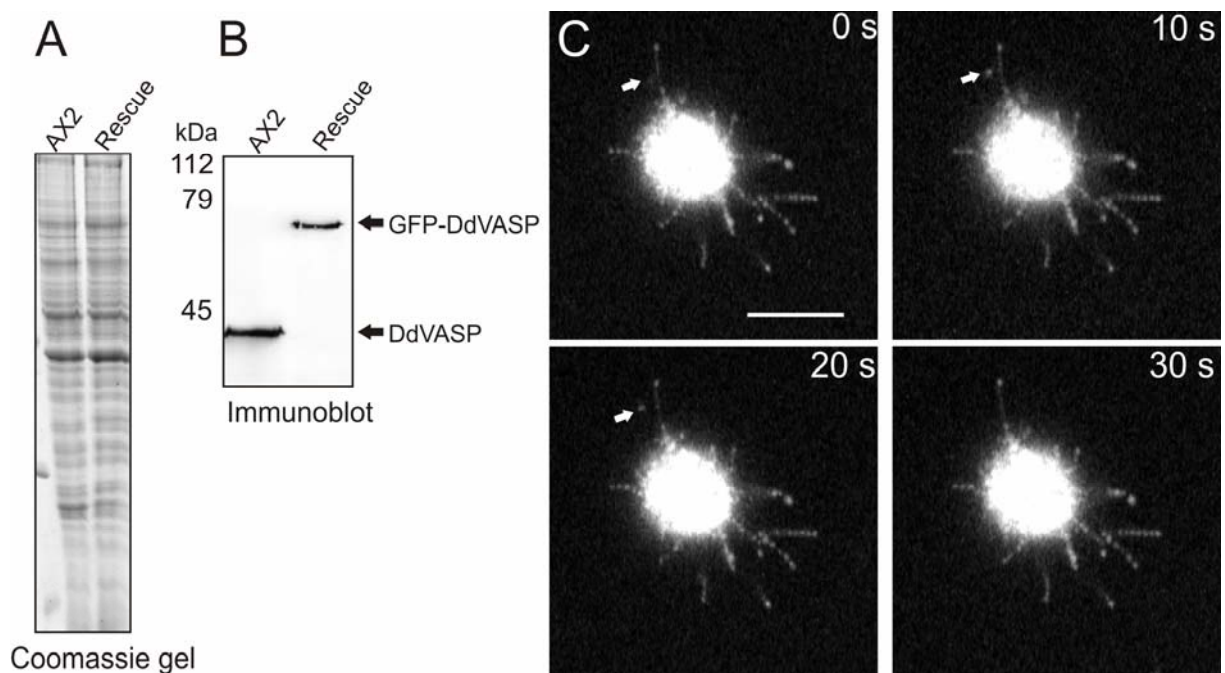


Figure 5: DdVASP localizes to filopodial tips

(A, B) Expression of GFP-DdVASP in VASP-null mutant. Equal amounts of wild type and DdVASP rescue cells were loaded (Coomassie gel, A) and the expression was detected in an immunoblot with anti DdVASP polyclonal antibodies (Immunoblot, B). (C) Full length GFP-DdVASP localizes to the tips of substrate-attached and free filopodia (indicated by a white arrow). A time-lapse series on GFP-DdVASP cells in phosphate buffer at a 10 sec interval in one confocal plane was recorded.

3.1.4 Cell dynamics

To comprehend the structure of the cytoskeleton during filopodia formation, the dynamics of cell movement as well as cell/glass contacts Reflection Interference Contrast Microscopy (RICM) was used. In this method the image is based on the positive interference of the reflected light from the glass coverslip and from the cell surface. Only one optical section is imaged and the light reflected from the stray areas is suppressed using a confocal microscope. The structures close to the surface appear darker whereas structures farther away appear white. The dynamic motile behavior and the filopodium

structures were compared with those of the GFP-DdVASP cells (Figure 6). The cells overexpressing GFP-DdVASP produce filopodia that are far greater in number and in length compared to those produced by the wild type cells. The adhesion area of the wild type cells is much more dynamic as they form more transient contacts with the glass surface compared to DdVASP overexpressing cells.

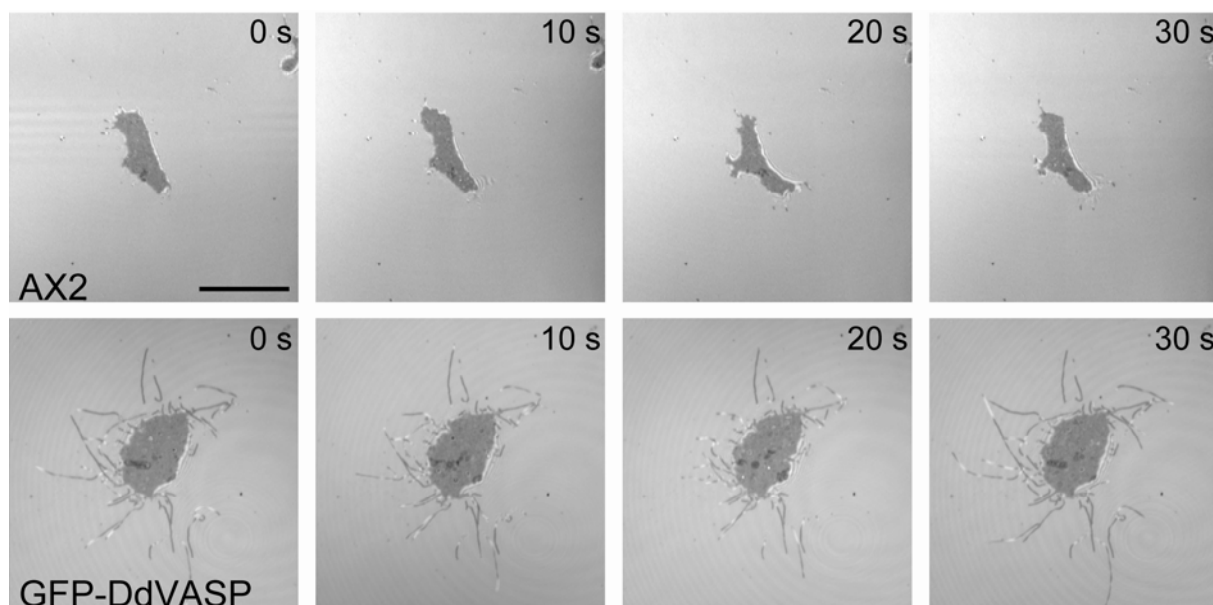


Figure 6: RICM analysis of wild type and GFP-DdVASP mutants

Reflection Interference Contrast Microscopy was employed to analyse the adhesion surface and cytoskeletal structures such as filopodia that are very close to the substrate (<100 nm). The dynamic behaviour of both wild type AX2 cells and DdVASP null cells expressing GFP-DdVASP on glass surface was visualized. GFP-DdVASP cells generate filopodia that are more in number and are longer in length compared to the wild type cells. Scale Bar: 10 μ m

3.1.5 Purification of capping proteins Cap32/34 and CapG

For uncapping experiments, an N-terminal 6x His-tag fusion of recombinant *D. discoideum* capping protein Cap32/34 and mammalian capping protein CapG were used. Cap32/34 is composed of two subunits, an α subunit of 34 kDa and a β subunit of 32 kDa, each encoded by a distinct gene. Cap32/34 was originally purified based on its prominent viscosity decreasing activity (Schleicher et al., 1984). For expression and purification of the recombinant dimeric capping protein, the Cap34 and 32 cDNA fragments were cloned in tandem with an additional Shine-Dalgarno sequence inbetween to facilitate expression of both the subunits from a bicistronic operon in *E. coli*. Both proteins were expressed in M15 cells (Qiagen) carrying an additional plasmid expressing a repressor. The complex of 34 and 32 was purified using the His-tag on the 34 kDa subunit (

Figure 7A). The purified protein was dialysed against PBS supplemented with 1 mM DTT, 1 mM benzamidine, 5 mM PMSF and stored on ice till tested. CapG is a monomeric capping protein expressed abundantly in macrophages (Witke et al., 2001a). It is a member of the gelsolin family with high affinity to barbed ends of the F-actin filaments and no severing activity. The cDNA was cloned and expressed as a His-tag protein (Figure 7B). The activity of CapG was more stable compared to that of Cap32/34.

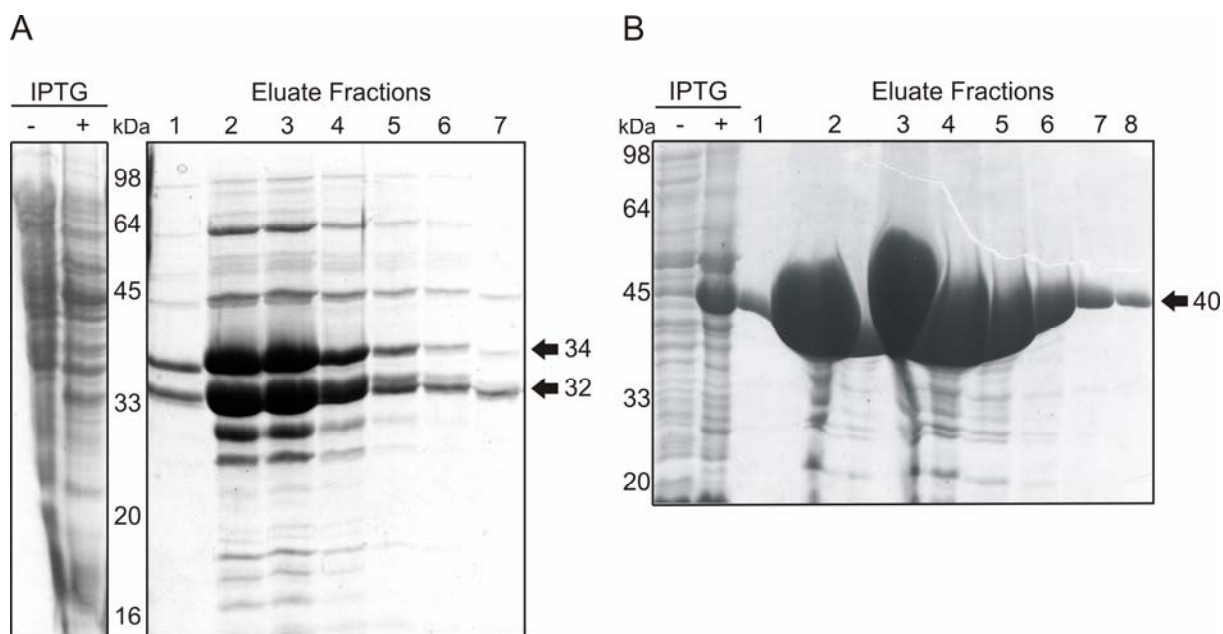


Figure 7: Purification of the recombinant capping proteins

(A) Purification of His-Cap32/34 from M15 cells. Uninduced and overnight induced cells were boiled in SDS sample buffer and loaded onto a 10% acrylamide gel. Lysate from 4 l of culture was bound to Ni-NTA agarose beads, washed and the bound protein was eluted with 250 mM Imidazole. An aliquot from the eluted protein fractions were loaded onto the gel. The 32 and 34 kDa proteins are indicated. (B) Purification of CapG. The 40 kDa His tagged macrophage capping protein CapG was purified on a Ni-NTA column. The purified protein aliquots were separated on a 10% SDS-polyacrylamide gel.

3.1.6 Purification of GST DdVASP

For biochemical characterization of DdVASP, the protein was purified as a GST fusion protein with a PreScissionTM protease cleavage site in between. The protein was expressed either in DH5 α or in BL21 Rosetta, a strain that expresses additional tRNAs from a pRARE plasmid. A high level of protein expression was seen at 21°C compared to 37°C. Protein fractions eluted from the GST column always contained protein species running with faster mobility which was a result either from the breakdown of full length protein or by premature termination of translation in the central proline rich domain (Figure 8A). Undialysed protein was active when tested for the activity in pyrene assays. The protein

was not stable for longer periods in G-buffer hence for long time storage the protein was stored in PBS containing 1 mM PMSF, 5 mM benzamidine and 1 mM DTT. To rule out possible artifacts due to the presence of GST, in some cases the tag was removed after cleavage with PreScissionTM Protease (Fig. 7B). No significant differences could be detected.

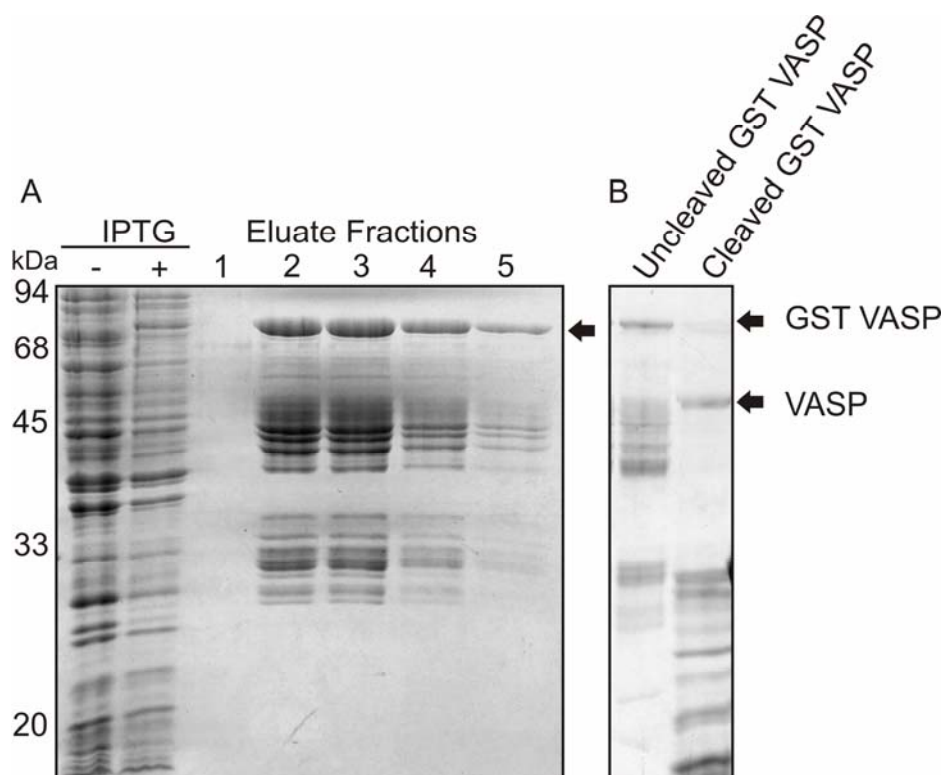


Figure 8: Expression and purification of recombinant DdVASP

(A) Expression of GST DdVASP. The recombinant GST-fusion protein (~ 70 kDa) was bound to Glutathione Sepharose beads and the bound proteins were eluted with 30 mM reduced glutathione. The eluted fractions were analysed by SDS-PAGE (10% acrylamide). Peak fractions 2, 3 and 4 were dialysed against PBS supplemented with 1 mM EDTA for the cleavage of the GST tag. (B) Removal of the GST-tag. The GST-DdVASP was incubated with PreScissionTM protease at 4°C overnight. Cleavage was monitored by comparing the protein before and after cleavage by SDS-PAGE (10% acrylamide)

3.1.7 dDia2 interacts directly with DdVASP

In mammalian as well as in *D. discoideum* cells VASP localises to the filopodial tip complex and was found to play an important role in the formation of lamellipodia and filopodia (Han et al., 2002). In this respect, the DRF dDia2 shows similar properties and, therefore, a possible interaction between dDia2 and DdVASP was studied using the yeast-two-hybrid technique. In contrast to the proline-rich FH1 domain alone and the N-terminus

of dDia2 (Δ FH1FH2), the FH1FH2 and the FH2 regions of dDia2 showed interaction with DdVASP (Figure 9). This indicated that the interaction between the formin dDia2 and DdVASP was mediated by the actin-binding FH2 domain. The observation that yeast cells expressing the FH1FH2 construct grew faster than those expressing FH2 alone suggested that FH1 might facilitate binding of FH2 to DdVASP. These findings are consistent with a previous study that showed an interaction of mouse mDia1 FH2 with full-length murine VASP, and an enhancement of this interaction in the presence of the FH1 domain (Grosse et al., 2003). The absence of any interaction between dDia2 FH3 and DdVASP as reported for other formins like mDia1 was not surprising because they represent different isoforms in this protein family, they are from different organisms and exert different functions. While mDia1 is a Rho-effector, dDia2 more likely reflects the features of mDia2 (DRF3), having a function downstream of Cdc42 or Rif in filopodia formation.

A direct binding between dDia2 and DdVASP was tested in pull-down experiments using recombinant His-tagged FH1FH2 from dDia2 and GST-tagged full length DdVASP. GST-DdVASP alone showed only a non-specific interaction with Ni-NTA-agarose, but coprecipitated in the presence of His-tagged FH1FH2 at an approximately equimolar ratio (Figure 9B, upper panel). Moreover, in the *vice versa* approach His-tagged FH1FH2 was specifically retained on glutathione resin loaded with GST-tagged VASP (Figure 9B, lower panel). These results provide conclusive evidence for a direct interaction between dDia2 and DdVASP *in vitro*.

To confirm the data obtained by *in vitro* experiments, *in vivo* immunoprecipitations of dDia2 from cell lines expressing GFP alone, GFP-DdVASP or GFP-dDia2 employing polyclonal antibodies specific for dDia2 was performed. GFP-DdVASP was co-immunoprecipitated with dDia2 while GFP alone that served as the negative control, was absent from dDia2 immunoprecipitates (Figure 9C). These findings define DdVASP as a dDia2 interacting protein *in vivo*.

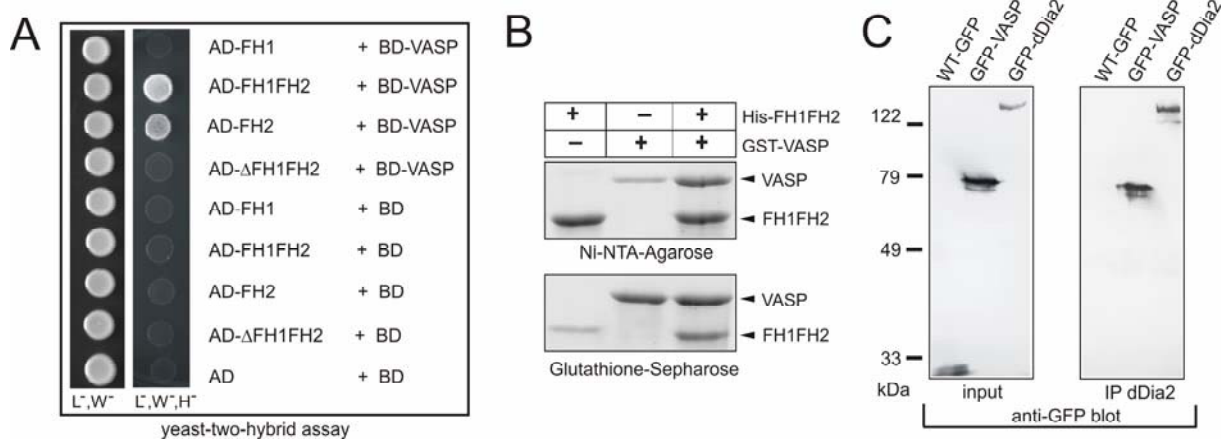


Figure 9: dDia2 interacts with DdVASP

(A) dDia2 specifically interacts with VASP through its FH2 domain in a yeast-two-hybrid assay. Yeast were transformed with the indicated constructs and tested for interaction by growth on selective media lacking leucine (L), tryptophane (W) or histidine (H) as indicated; activation domain (AD); binding domain (BD). (B) Direct interaction between dDia2 and DdVASP. Purified His-tagged FH1FH2 and GST-VASP were incubated alone or in combination (2 μ M each) with either 100 μ l Ni-NTA-Agarose or glutathione-Sepharose slurry each in a buffer containing 25 mM Tris/HCl, pH 7.0, 30 mM NaCl, 1 mM DTT. After repeated washing of the beads bound proteins were monitored by SDS-PAGE and Coomassie Blue staining. (C) Co-immunoprecipitation of dDia2 and VASP. Cell lines expressing GFP, GFP-DdVASP or GFP-dDia2 (left panel) were used for immunoprecipitation with anti-dDia2 polyclonal antibodies. The immunoprecipitates were analyzed in Western blots with anti-GFP antibody mAb 264-449-2.

3.1.8 Regulation of actin polymerization by dDia2 and DdVASP *in vitro*

To explore the nature of the interaction between these two proteins, we characterized DdVASP on a biochemical level and compared its properties with those of dDia2 FH1FH2.

A] Nucleation activity of DdVASP: The nucleating activity of DdVASP was measured using the fluorimeter based ‘pyrene-actin’ assay. The nature of the polymerization curve reflects the nucleation and elongation rates in the system. As shown in (Figure 10) with actin monomers alone as starting material (black curve), a polymerization lag was observed, reflecting the unfavorable nucleation process. With increasing concentration of GST-DdVASP (10-500 nM) more and more filaments built up eliminating the lag, and the polymerization rate increased to a maximum. The GST-tag did not affect polymerization kinetics. The nucleating effect of VASP is due to electrostatic interaction with actin monomers and is highly dependent on ionic strength of the buffer. In low ionic strength buffers such as G-buffer, DdVASP readily induces polymerization of actin but is inefficient in high ionic strength buffer (100 mM KCl). In addition, Mg-actin (Carrier et

al., 1986) or a lower pH (Zimmerle and Frieden, 1988) were shown to favour actin nucleation.

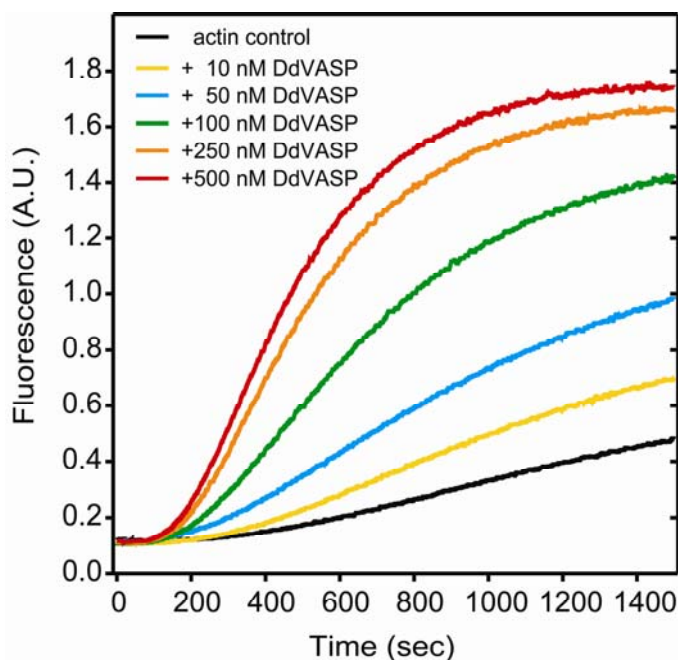


Figure 10: DdVASP nucleates actin

Actin ($1.1 \mu\text{M}$) was polymerized in the presence of 0 nM (black line) to 500 nM (red line) DdVASP in polymerization buffer containing 50 mM KCl. A dose dependent increase in actin polymerization is observed.

B] Uncapping activity of DdVASP: The ability of VASP to compete with the capping protein in binding to the barbed ends is controversial. Though it has recently been proposed that VASP could interact with barbed ends, thus preventing them from being capped and promoting barbed end growth (Bear et al., 2002), these results were challenged by other findings (Samarin et al., 2003). The putative uncapping activity of DdVASP was challenged in a series of experiments:

First, the ability of DdVASP to remove capping proteins cap32/34 and capG from the barbed ends of short actin filaments and promote elongation was tested (

Figure 11A). Addition of $0.1 \mu\text{M}$ F-actin seeds to free G-actin induced spontaneous actin elongation (black curve) that is inhibited by the addition of the capping protein. The amount of capping protein needed was determined by titration and the amount that inhibited nucleation almost completely was further used. Addition of increasing amounts of DdVASP (10-500 nM) did not enhance actin elongation that would be expected from uncapped F-actin seeds. The slight increase in polymerization was most likely the result of

de novo nucleation of G-actin by DdVASP, independent of the presence of capped F-actin seeds. Due to some controversy in the field and with regard to the observation that both dDia2 and DdVASP localize to tips of filopodia, the nucleating and uncapping activities of these two proteins were compared in a combinatorial approach (Figure 11B). A pyrene-actin based polymerization assay that was started in the presence of capped F-actin seeds resulted in a long lag-phase, whereas the control with uncapped F-actin seeds showed immediate polymerization. The addition of 100 nM DdVASP after 400 sec to capped actin seeds caused a slow but significant actin polymerization. However, further addition of 100 nM FH1FH2 after 800 sec resulted in a steep burst of fluorescence, which indicated the uncapping of the F-actin seeds and enhanced elongation. The assumption drawn from this observation was confirmed in another assay, in which an excess of free capping protein was added to polymerizing actin in the presence of either DdVASP or dDia2 (Figure 11C). The slope of the curve in the presence of DdVASP or dDia2 prior to the addition of capping protein was defined as 100% arbitrary fluorescence and compared with the slope after the addition of capping protein. This result showed that capping protein can inhibit actin polymerization in the presence of DdVASP but not of dDia2. From this we conclude that DdVASP nucleates actin polymerization, most likely as a tetramer through its G-actin binding sites, and that efficient elongation of the *de novo* nuclei is inhibited by free capping protein. Conversely, FH1FH2 successfully competed with the capping protein at the barbed ends resulting in uninterrupted elongation.

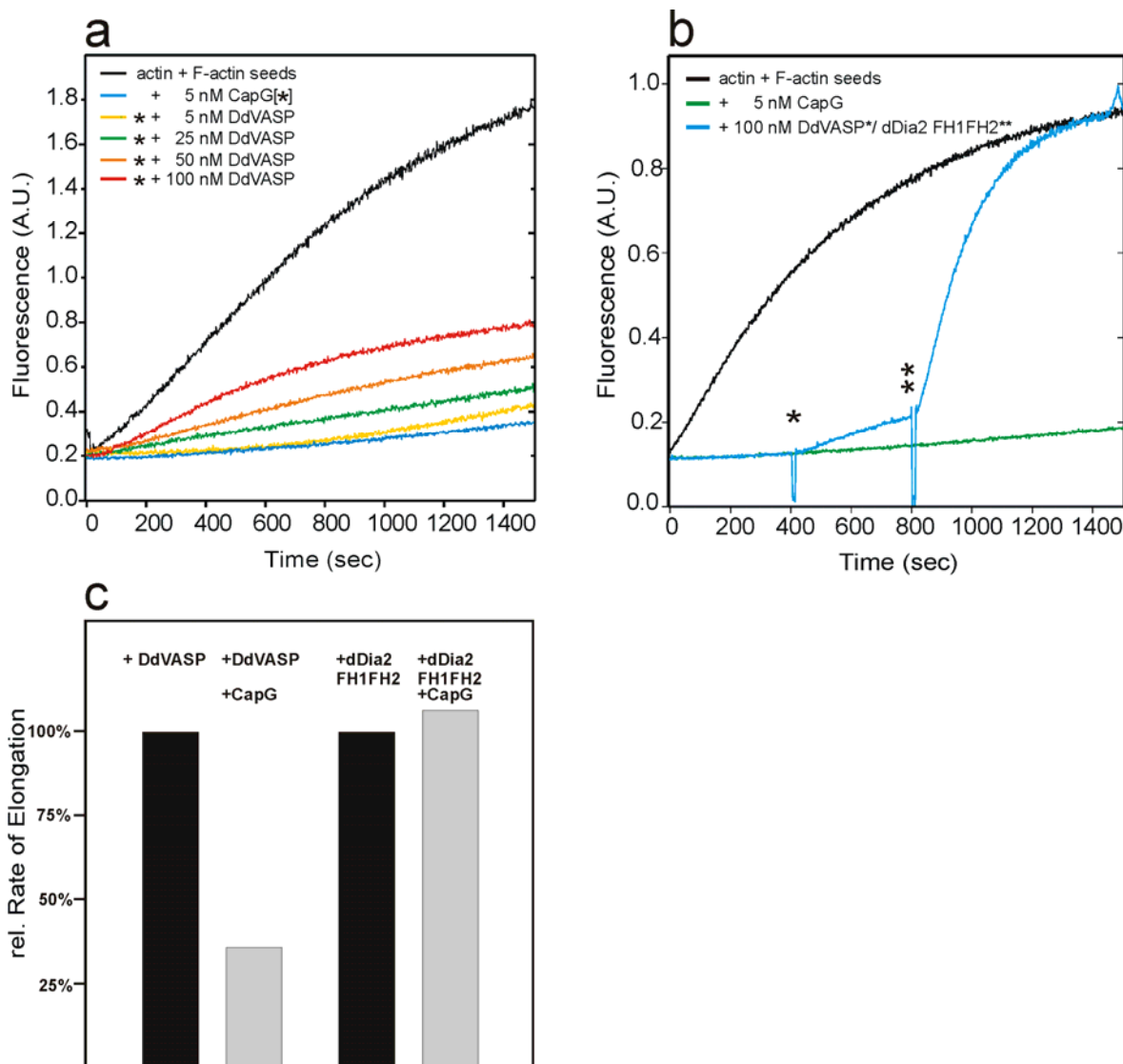


Figure 11: DdVASP does not compete with capping protein

(A) Actin ($1.4 \mu\text{M}$) was polymerized in the presence of F-actin seeds to avoid *de novo* nucleation (black line). The presence of 5 nM capping protein strongly inhibited actin polymerization (light blue line). Addition of increasing amounts of DdVASP to capped filaments showed that DdVASP cannot remove the cap and merely nucleates polymerization of the remaining G-actin. (B) Direct comparison of DdVASP and formin activities. Actin was polymerized in the presence of actin seeds (black line) or capped actin seeds (green and blue lines). After 400 sec (one star) 100 nM DdVASP was added, and after 800 sec (two stars) 100 nM dDia2 FH1FH2 was added to the same sample. The slope between 400 and 800 sec reflects normal DdVASP-induced *de novo* nucleation, whereas after addition of dDia2 FH1FH2 the capped seeds were efficiently uncapped and elongated, leading to a fast increase of F-actin as indicated by the steeper slope. (C) Analysis of nucleating and uncapping activities. The intrinsic nucleation activity of 50 nM DdVASP was measured in the pyrene actin assay, and the slope of fluorescence increase was set to 100% (first bar). After addition of 30 nM CapG the fluorescence increase was strongly inhibited because the newly formed filaments were immediately capped at their barbed ends (second bar). This inhibition was not observed in the presence of dDia2 FH1FH2 (third and fourth bars) because the formin competes with capping protein and supports elongation also in the presence of capping protein.

C] DdVASP cannot compete with capping protein for barbed end binding: In a fourth experimental setup the depolymerization kinetics of pyrene-labelled F-actin were monitored. This assay allows the analysis of the molecular organization at the barbed end. Depolymerization occurs after dilution of F-actin solutions below the critical concentration of the barbed ends ($0.1 \mu\text{M}$), i.e. under these conditions nucleating activity is irrelevant. The interaction of a protein of interest with the barbed end, however, should change the kinetics of actin monomer dissociation. (Figure 12A) shows that dilution of F-actin to $0.1 \mu\text{M}$ into solutions containing even high concentrations of DdVASP did not inhibit depolymerization whereas the addition of FH1FH2 from dDia2 considerably inhibited the depolymerization of actin. These findings indicate that DdVASP does not directly interact with barbed ends and thus is not able to compete with capping protein. Consistent with these data, actin filaments that were capped with Cap32/34 did not depolymerize from the barbed ends even at high concentrations of DdVASP (Figure 12B). CapG, another type of barbed end capping protein, could also not be removed by DdVASP under these conditions (Figure 12C).

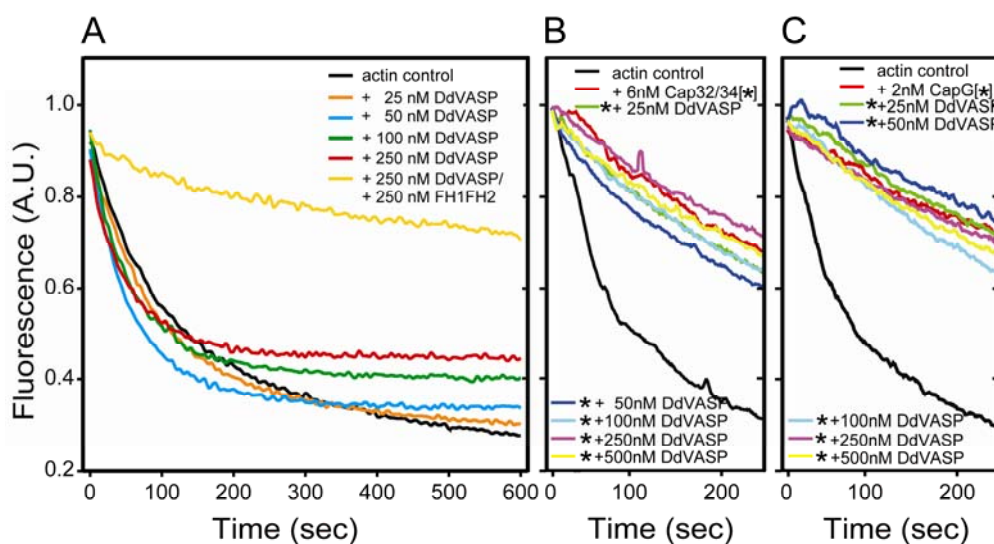


Figure 12: DdVASP does not uncap the filaments

(A) Polymerized actin (63% pyrene-labeled) was diluted to $0.1 \mu\text{M}$ in polymerization buffer alone or in polymerization buffer containing DdVASP or DdVASP and dDia2 FH1FH2. Note that depolymerization is not attenuated by the addition of DdVASP indicating that it cannot alter barbed end kinetics. (B and C) DdVASP cannot remove capping proteins from the barbed ends. Polymerized actin with either free barbed ends or with the barbed ends capped by either Cap32/34 or CapG was diluted to $0.1 \mu\text{M}$ in

polymerization buffer containing 100 mM KCl and the amounts of DdVASP indicated. Neither Cap32/34 nor CapG were removed by DdVASP from the filament ends otherwise this would trigger fast depolymerization.

3.1.9 DdVASP bundles F-actin filaments in high salt

VASP was shown to associate with F-actin structures like stress fibers in platelets and to cosediment with F-actin suggesting that it binds to actin filaments (Reinhard et al., 1992). To define this interaction and investigate the salt dependency of this interaction, cosedimentation experiments with F-actin and DdVASP with and without GST-tag were done. The assay was carried out in different salt concentration and at room temperature. After polymerization the protein samples were subjected to low speed sedimentation to separate F-actin bundles from unpolymerized actin and unbundled actin filaments (Figure 13A). In the presence of 0 mM KCl most of the filaments were bundled and DdVASP remained associated with the bundles. However, with increasing salt concentration the amount of F-actin in a 10,000 g pellet was slightly reduced. When the supernatants were subjected to high speed sedimentation at 100,000 g, DdVASP was still found to be associated with actin filaments even in high salt. Thus unlike nucleation, the bundling activity is essentially insensitive to higher salt concentration indicating that it is likely to persist *in vivo*. It was previously shown by deletion experiments that in HsVASP, a stretch of 20 amino acids [259-278] was necessary for F-actin binding and cross linking property. Deletion of the corresponding amino acids in DdVASP impaired its ability to bundle F-actin and to cosediment with the bundles (Figure 13B). To exclude the possibility of a misfolded protein resulting from the deletion of the F-actin binding region, the nucleation activity of the protein in low salt concentration was tested. Similar to the wild type protein, Δ FAB still nucleated actin filaments (Figure 13C) suggesting that this multidomain protein still retained some of its activities.

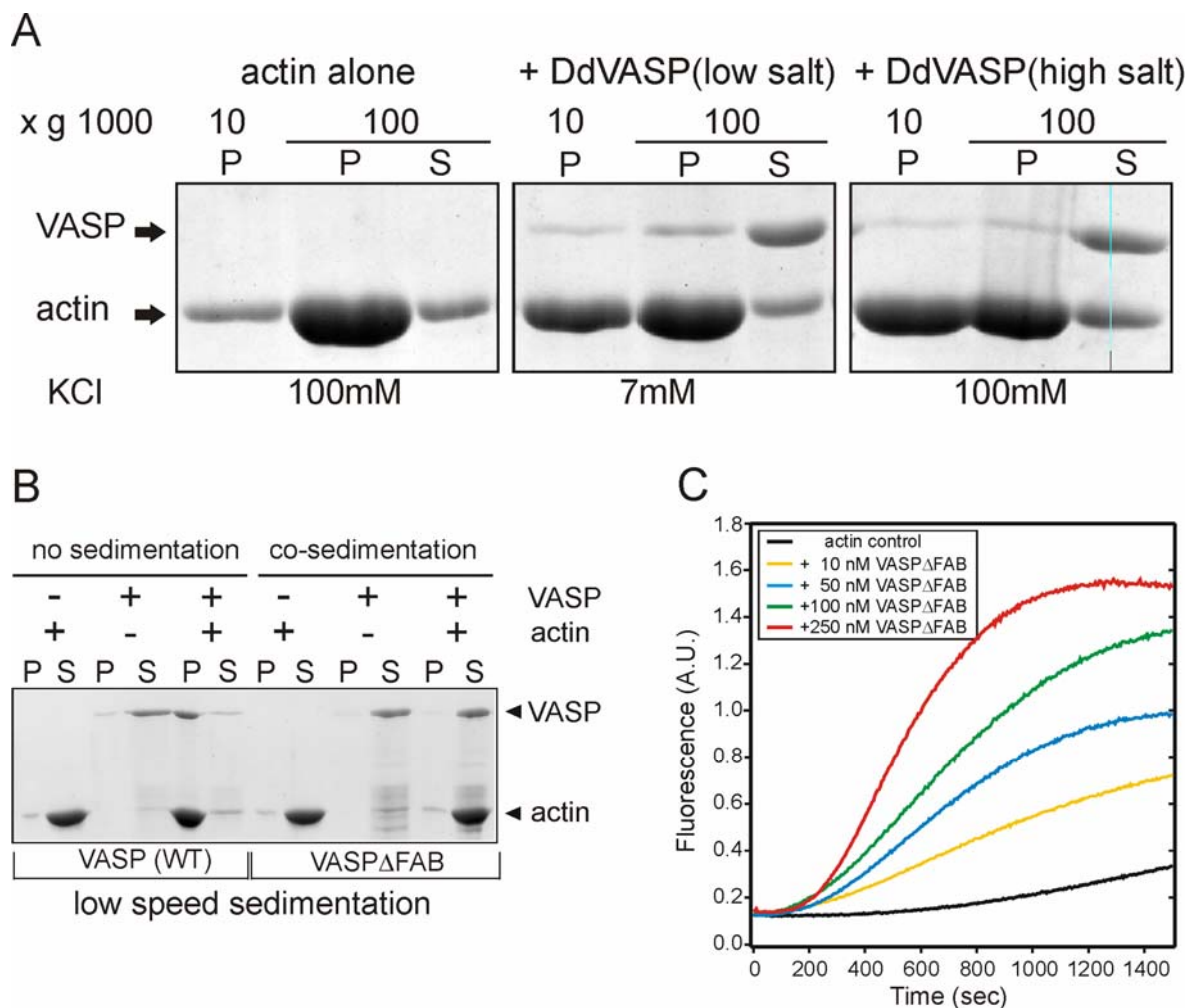


Figure 13: DdVASP bundles F-actin filaments in high salt conditions

(A) The gel shows a sedimentation assay at 10,000 g and 100,000 g to distinguish bundles and actin filaments. Lanes 1, 2, and 3 shows 10,000 g actin pellet, 100,000 g pellet and supernatant of actin alone; lanes 4, 5 and 6, actin plus DdVASP at low salt conditions (7 mM KCl); lanes 7, 8 and 9, actin plus DdVASP plus 100 mM KCl. The amount of actin sedimented at 10,000 g in the presence of DdVASP and 100 mM KCl (lane 7) shows clearly that DdVASP maintains its bundling activity at higher salt concentrations. (B) Deficiency of F-actin bundling activity by DdVASP Δ FAB in a low-speed sedimentation assay. Recombinant WT DdVASP and DdVASP Δ FAB (1 μ M) were incubated alone or with G-actin (5 μ M) in polymerization buffer and spun at 15,000 g. In contrast to WT DdVASP (left blots), DdVASP Δ FAB (right blots) does not cosediment with the F-actin. P, pellet; S, supernatant. (C) DdVASP Δ FAB nucleates actin polymerization. Actin (1.1 μ M) was polymerized in the absence and the presence of increasing amounts of DdVASP Δ FAB. Deletion of the F-actin binding side did not hamper the nucleating activity.

3.1.10 F-actin bundling activity is required for filopodia formation *in vivo*

To test whether the bundling activity of DdVASP is also required for filopodium formation *in vivo* DdVASP-null mutants were complemented with GFP-tagged WT and mutant

DdVASP Δ FAB. Subsequent analysis of these cells revealed that only WT DdVASP but not DdVASP Δ FAB could rescue their ability to form filopodia (Figure 14). Taken together, these findings clearly demonstrate the importance of the actin bundling activity of DdVASP for filopodium formation *in vivo*.

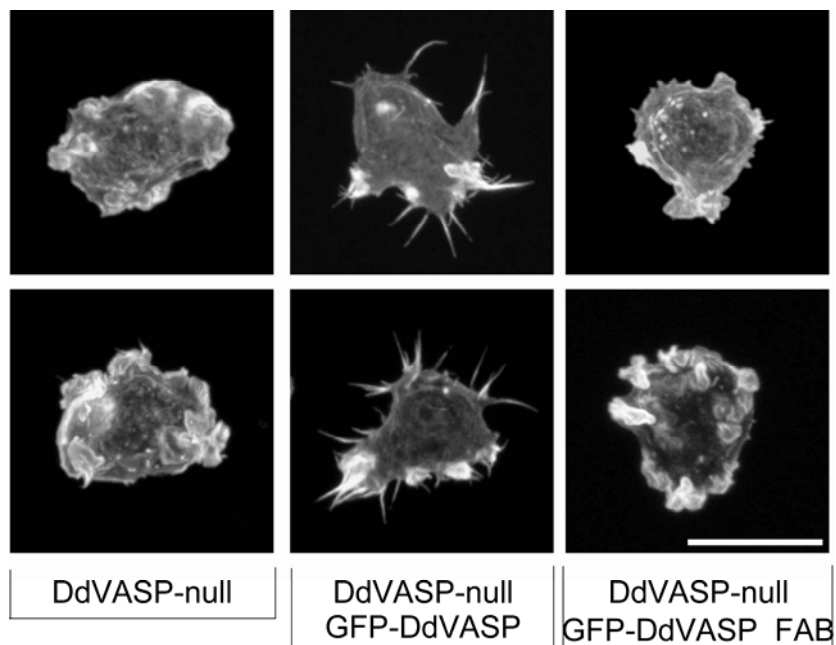


Figure 14: The F-actin bundling activity of DdVASP is required for filopodium formation *in vivo*.

3D reconstruction of tetramethylrhodamine B isothiocyanate–phalloidin-labeled knockout and reconstituted cells as indicated. (Scale bar: 5 μ m.) Only cells reexpressing WT DdVASP display normal filopodia.

Finally, to test for a mutual recruitment of DdVASP and dDia2, the localization of GFP-dDia2 in DdVASP-null cells as well as the localization of GFP-DdVASP (WT) in dDia2-null cells was examined. As shown in

Figure 15 both cell lines largely lacked filopodia and the GFP signals in both cell lines were predominantly confined to the cortical region. Interestingly, analysis of the few filopodia in these mutants revealed that both GFP-DdVASP and GFP-dDia2 in the opposite null-strains still localized to filopodial tips. This strongly suggested that the targeting of these two proteins to filopodial tips is not mutually dependent, whereas the formation of filopodia requires both.

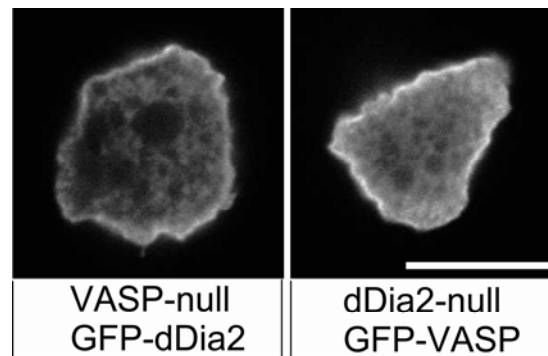


Figure 15: The targeting of dDia2 and DdVASP to filopodial tips is not mutually dependent

Cellular distribution of GFP-tagged dDia2 or DdVASP in mutants lacking DdVASP or dDia2. Confocal sections are shown. (Scale bar: 5 μ m.)

3.1.11 Human VASP (HsVASP) displays virtually identical properties as *Dictyostelium* VASP

To test whether the functions of DdVASP identified in this study are specific to *D. discoideum* or if they can be extended to higher organisms, some of the key features of HsVASP were analysed. Similar to DdVASP recombinant HsVASP did not inhibit actin depolymerization or compete with capping protein (Figure 16A-C). In analogy to DdVASP, HsVASP- Δ FAB failed to bundle actin filaments as demonstrated in the low speed sedimentation assays (Figure 16D).

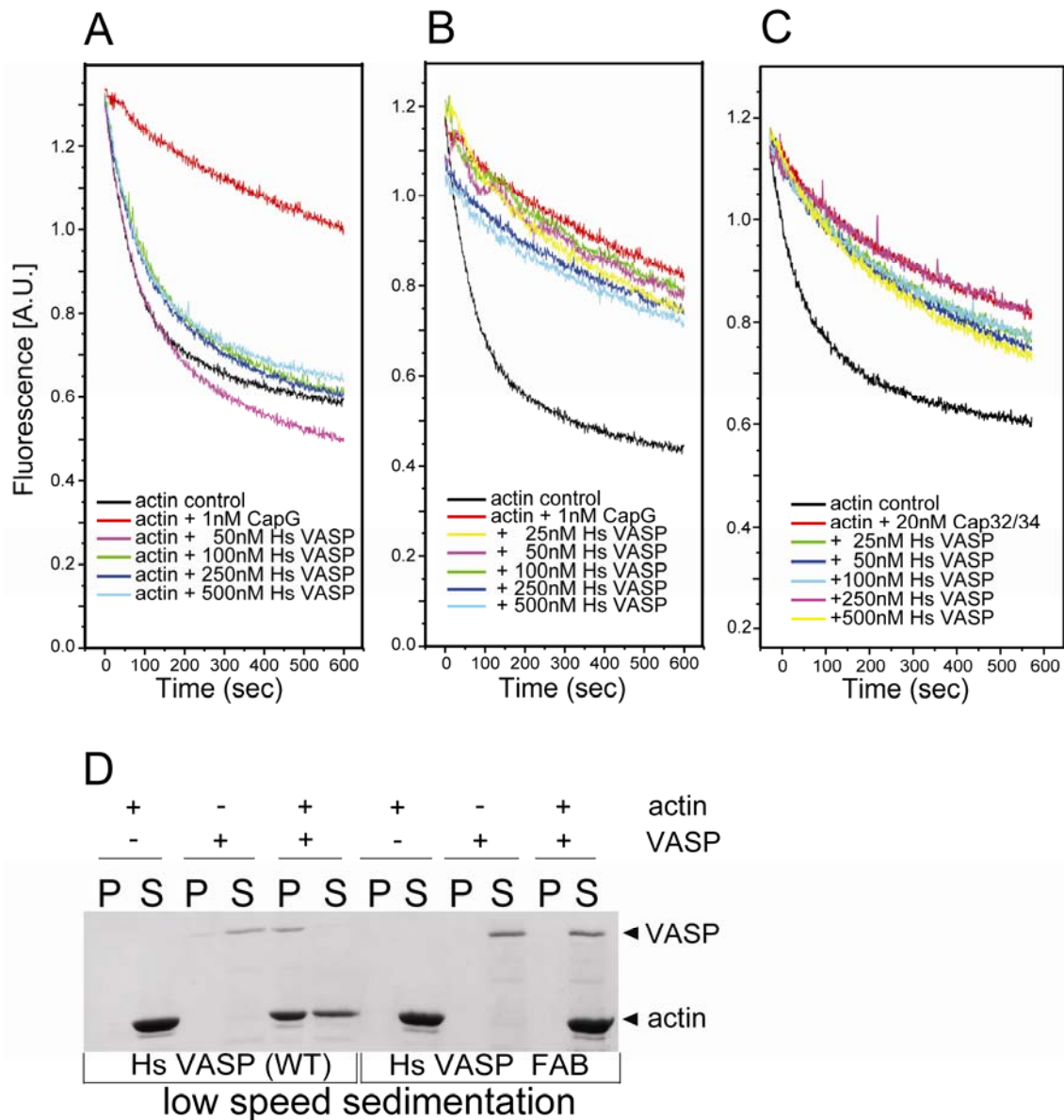


Figure 16: *In vitro* and *in vivo* analysis of HsVASP

(A) HsVASP does not interact with barbed filament ends. Polymerized pyrene-labeled actin was diluted to $0.1 \mu\text{M}$ in polymerization buffer alone or in polymerization buffer containing increasing concentrations of HsVASP. Whereas the addition of CapG inhibits depolymerization (red line), even high concentrations of HsVASP do not slow down depolymerization. (B and C) Polymerized actin with either free barbed ends (black lines) or with the barbed ends capped by CapG (B) or Cap32/34 (C) was diluted to $0.1 \mu\text{M}$ in polymerization buffer containing 100 mM KCl and the amounts of HsVASP indicated. Neither CapG nor Cap32/34 was removed by HsVASP from the filament ends. (D) Deficiency of F-actin bundling activity by HsVASP Δ FAB in a low-speed sedimentation assay. Recombinant WT HsVASP and HsVASP Δ FAB ($1 \mu\text{M}$) were incubated alone or with G-actin ($5 \mu\text{M}$) in polymerization buffer and spun at $15,000 \times g$. In contrast to WT HsVASP (left blots), HsVASP Δ FAB (right blots) does not cosediment with the F-actin. (P, pellet; S, supernatant). Lanes 1, 2, 7, and 8, actin alone; lanes 3, 4, 9, and 10, HsVASP alone; lanes 5, 6, 11, and 12, actin plus HsVASP.

3.2 Characterisation of *D. discoideum* profilin III

3.2.1 DdVASP interacts with the profilin III isoform through its polyproline domain

Members of the VASP family of proteins were previously shown to interact with profilin (Gertler et al., 1996; Reinhard et al., 1995; Watanabe et al., 1997) and preferential binding of profilin isoforms with other ligands was previously reported. A possible interaction between DdVASP and the three profilin isoforms was tested in a yeast two hybrid assay. The coding sequences of all *D. discoideum* profilin isoforms were fused to the DNA binding domain of the yeast transcription factor GAL4, and each of these were transformed into the yeast strain AH109 along with the full length DdVASP cDNA fused to the activation domain of the yeast transcription factor GAL4. The interaction was tested for the activation of transcription of the reporter genes *HIS3* and *lacZ*. Only the cells that were transformed with profilin III and DdVASP grew under the appropriate selection (Figure 17A), suggesting a specific interaction with profilin III. Cells that were transformed with DdVASP and control vector containing lamin C did not grow.

The profilin III interacting domain of DdVASP was identified by testing domains of DdVASP in the yeast two hybrid assay. DNA encoding the domains EVH1, EVH1-PRD, PRD, PRD-EVH2 and EVH2 were fused to the activation domain of the yeast transcription factor GAL4 (Figure 17B). Yeast cells were cotransformed with profilin III and one of the above listed constructs, and tested for interaction as described above. An interaction was detected when profilin III was cotransformed with constructs containing the polyproline domain (Figure 17C), suggesting that this interaction is mediated by proline-rich sequences in DdVASP. No significant growth was observed in cells cotransformed with the profilin III and PRD domain probably due to the improper folding of the PRD alone.

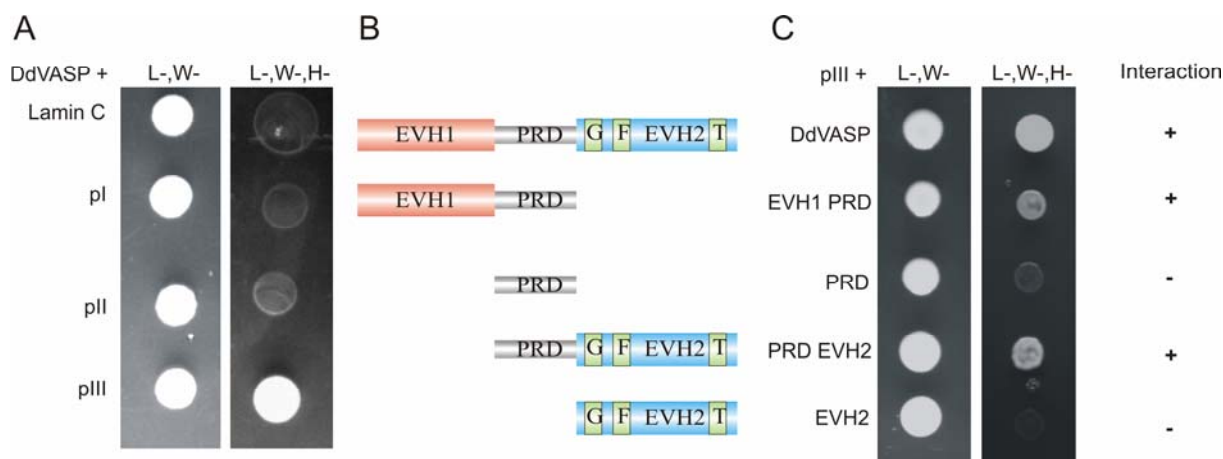


Figure 17: DdVASP interacts via its proline rich domain (PRD) with profilin

(A) DdVASP specifically interacts with pIII. Yeast cells were transformed with vectors coding for DdVASP and the indicated profilin isoform, and tested for interaction on selective media lacking leucine (L), tryptophane (W) or histidine (H) as indicated. Cells transformed only with pIII grew normally, indicating a specific interaction. (B) pIII interacts with the PRD of DdVASP. Yeast cells were transformed with pIII and the indicated constructs. (C) Both EVH1 and EVH2 constructs with an additional PRD interacted with pIII as indicated by the growth on the selective media. Activation domain (AD); Binding domain (BD)

3.2.2 Isolation of a *profilin III* minus mutant

The biological function of profilin III was investigated by characterising a *profilin III*-minus mutant. A *profilin III*-minus strain was created by homologous recombination in the wild-type strain AX2. For this purpose, a gene replacement vector containing a 400 bp homologous fragment upstream of the 5' end of the *profilin III* gene, and a 600 bp homologous fragment downstream of the *profilin III* gene was constructed (Figure 18A). The vector was digested with the restriction enzymes BamHI and SalI to separate the integration cassette from the vector backbone, to facilitate double crossover. The digested DNA was transformed into AX2. The transformants were selected for 15 day with blasticidin S. Clones were isolated by serial dilution onto *K. aerogenes* plates. The integration of the gene replacement knockout cassette at the right place was analysed by PCR using two sets of primers (Figure 18B, left panel). In each set one primer bound in the *blaR* gene and the other primer to regions beyond the 5' and 3'- regions of the gene replacement construct. Additionally the clones were tested in an immunoblot for the absence of profilin III using profilin III specific polyclonal antibodies (Figure 18B, middle

panel). Profilin III rescue mutants were generated by expressing full length profilin III tagged with a FLAG peptide at its N-terminus (Figure 18C, right panel).

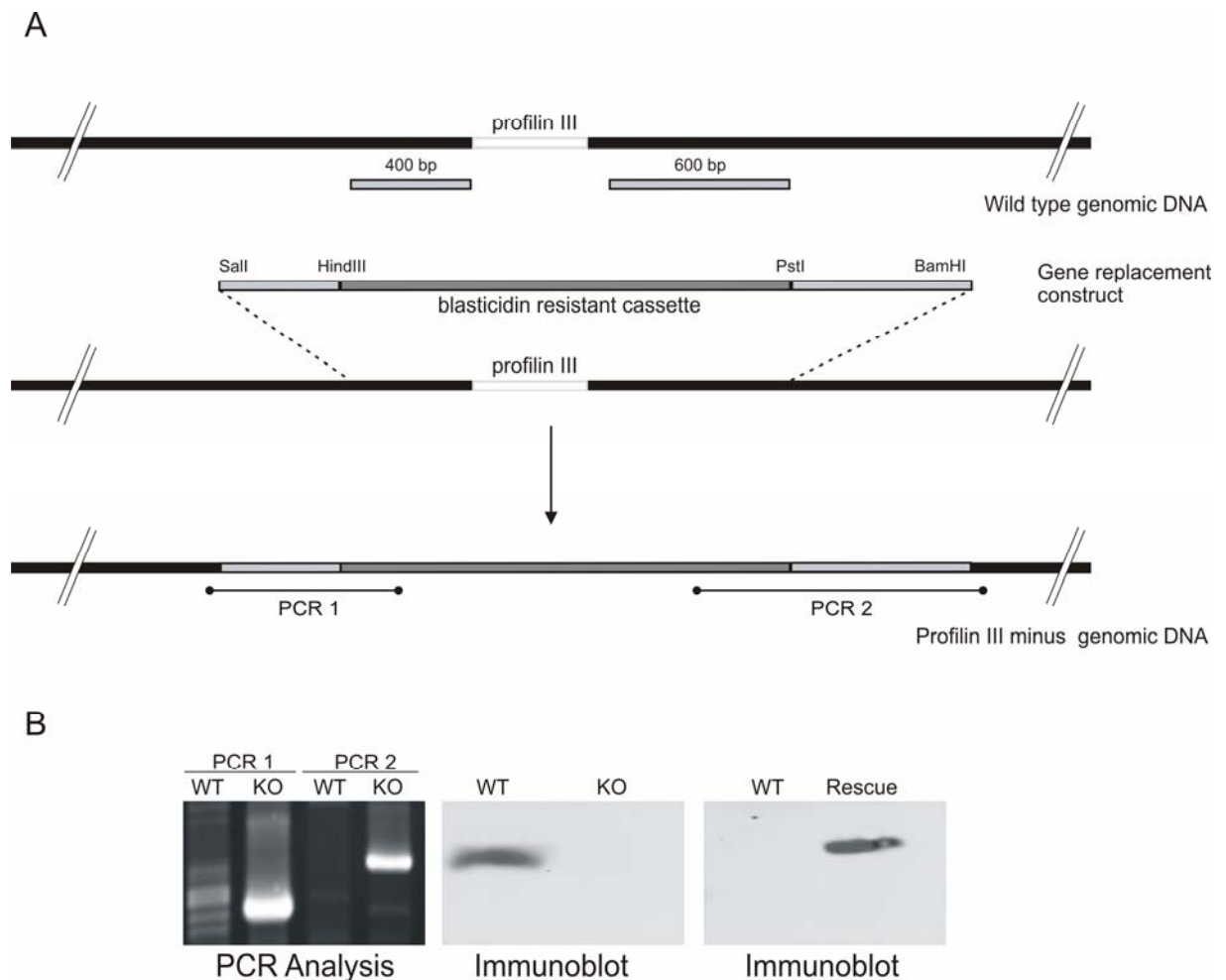


Figure 18: Isolation of *profilin III*-null and N-FLAG profilin III rescue mutants

(A) Schematic view of the linearised targeting construct used to inactivate the *profilin III* gene in wild-type (WT) cells. (B) Screening of *profilin III*-null mutants. A PCR screen (left panel) was done at both the 5'- and 3'-ends to score for gene replacement. The clones were tested in an immunoblot for the absence of endogenous profilin III (middle panel). The minus mutants were rescued by the expression of N-Flag pIII (right panel).

3.2.3 Estimation of profilin III concentrations in wild type AX2 and in pI/II minus cells

D. discoideum mutants lacking the profilin isoforms I and II have a severe and complex phenotype: single cells were impaired in cytokinesis, were up to 10 times larger than wild type cells and development ceased at early culmination (Haugwitz et al., 1994). However, a few clones were observed by serendipity to have a partially rescued fruiting body formation and cytokinesis defect. These mutant clones were picked and the expression of

profilin III was quantified. The amount of profilin III expressed in vegetative cells [t0], of AX2 (Figure 19A) and spontaneous pI/II minus revertents (Figure 19B) was quantified by comparing the amount of cellular protein in a known number of cells with different amounts of recombinant protein. Total cell lysate and recombinant protein were subjected to SDS-PAGE, transferred to a nitrocellulose membrane and analysed using specific polyclonal antibodies generated against profilin III. Recombinant protein concentrations were determined using Bradford's assay. The signals on the immunoblot were quantified by ImageJ software and compared to published data on profilin I and II concentrations in *D. discoideum* (Haugwitz et al., 1994). AX2 wild type cells express about 200 fold less profilin III ($\sim 0.23\mu\text{M}$) than profilin (I + II, $\sim 47\mu\text{M}$). Expression of profilin I and II was not detected in the pI/II minus revertants (data not shown), but the expression of profilin III was upregulated suggesting that profilin III behaves as a conventional profilin *in vivo*, if it is expressed at higher levels.

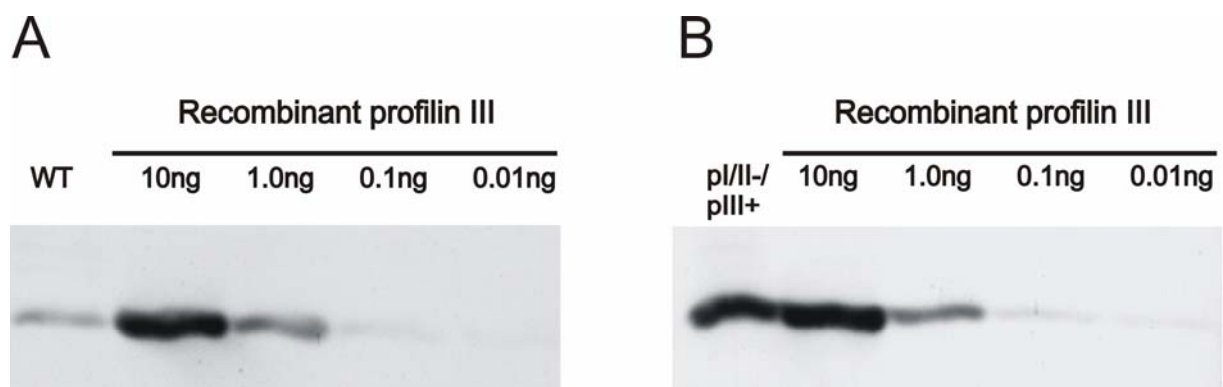


Figure 19: Quantification of profilin III expression

(A) Analysis of profilin III protein expression levels in wild type AX2 cells. Lysate from WT cells (lanes 1) and as a calibration standard, recombinant profilin III protein (1; 0.1 and 0.01 ng, respectively) were resolved by SDS-PAGE, western blotted and probed with anti-profilin III antibody. (B) Analysis of profilin III protein expression levels in pI/II-spontaneous revertents overexpressing pIII. Lysate from the overexpressing cells (lanes 1) and recombinant profilin III protein (10, 1; 0.1 and 0.01 ng, respectively) were resolved by SDS-PAGE, western blotted and probed with anti-profilin III antibody. Bands on western blots were quantified using ImageJ software.

3.2.4 Cellular distribution of profilin III

Profilin I and II were shown to be major *in vivo* regulators of the actin cytoskeleton and present in much higher concentrations as compared to profilin III. The antibody directed against the profilin III isoform could not be used successfully in immunolocalisation

studies in both wild type and pI/II minus cells, owing to the low abundance of profilin III in both strains.

To overcome this problem we were forced to analyse the distribution by overexpressing the protein under the control of a constitutive promoter (actin15). It is known since many years that profilins as a fusion to comparable larger proteins very often lose their actin binding activity. As an example, use of GFP as a tag to investigate the localisation in live cells proved to be unproductive as the GFP-tagged profilin III despite its overexpression could not effectively rescue the severe defects of the pI/II mutant, probably owing to the size of GFP (26 kDa) as compared to the profilin moiety (14 kDa).

Therefore, profilin III was fused to a FLAG tag at the N-terminus with a short linker sequence inbetween. Fusion constructs were transformed into AX2 cells and the transformants expressing the fusion protein were screened by immunoblots. Equal amounts of total cell homogenates were subjected to SDS-PAGE after immunoblotting the protein was visualised with profilin III specific polyclonal antibodies. AX2 and pI/II minus cells were used as controls for normal profilin III expression (Figure 20A). In comparison, the fusion protein appeared to be present in excess quantities compared to wild type or pI/II minus cells. Both, the untagged protein and protein tagged with FLAG tag at the N-terminus, were localised to filopodia consistent with the profilin III and DdVASP interaction (Figure 20B). However, different procedures left some doubts about the validity of this cellular localisation of profilin III. When cells were fixed using much milder fixatives such as ice cold methanol, the protein was uniformly distributed throughout the cell, probably with a slight enrichment at the cell cortex. However, no filopodia could be detected using this method.

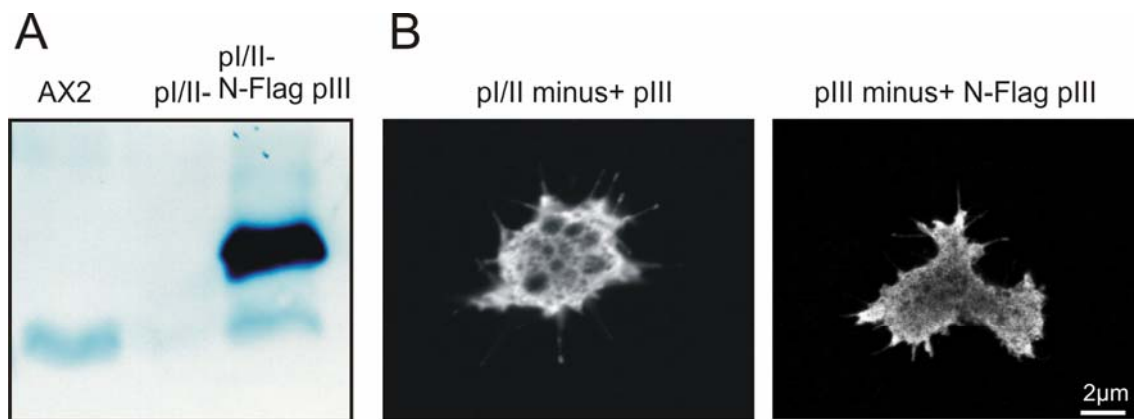


Figure 20: Profilin III is localised to the filopodia when overexpressed

(A) Wild type and pI/II- cells expressing N-Flag profilin III were analysed in an immunoblot using profilin III specific antisera. In comparison to the endogenous protein N-Flag protein was expressed in much higher quantities. (B) Localisation of profilin III in pI/II- cells. Untagged profilin III overexpressing pI/II- cells and wild type cells overexpressing N-Flag profilin III were fixed with picric acid and stained for profilin III specific polyclonal antibodies. The cells were imaged in a confocal microscope with an optical section of 0.02 μm . Scale bar: 2 μm

3.2.5 Overexpression of profilin III rescues the cell morphology and cytokinesis defect of pI/II- cells

Ectopic expression of either profilin I or profilin II could revert the most severe defects in the pI/II-minus mutant. To test if profilin III is *in vivo* a functional profilin as well, profilin III was overexpressed in pI/II- cells under the control of the actin15 promoter. Among the most sensitive assays a putative rescue could be identified either by addressing the defect in cytokinesis or the block of late development. Overexpression of profilin III clearly rescued the cytokinesis defect (Figure 21).

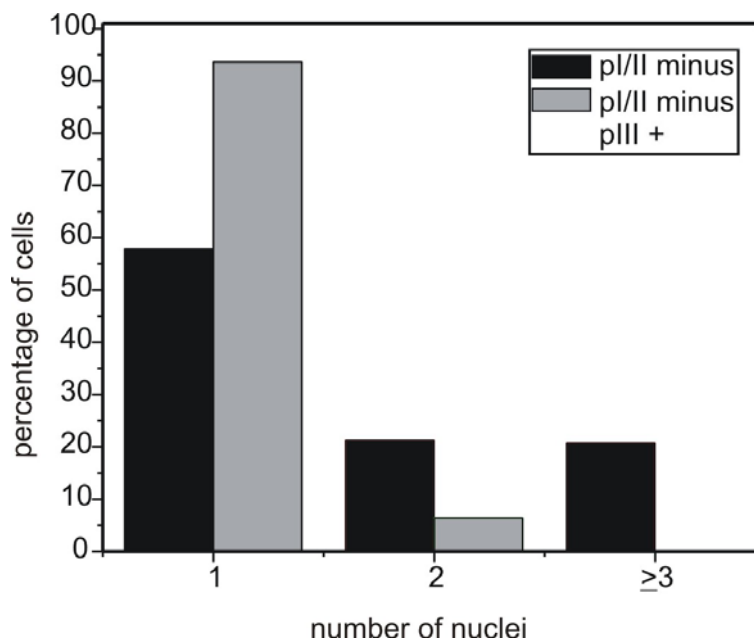


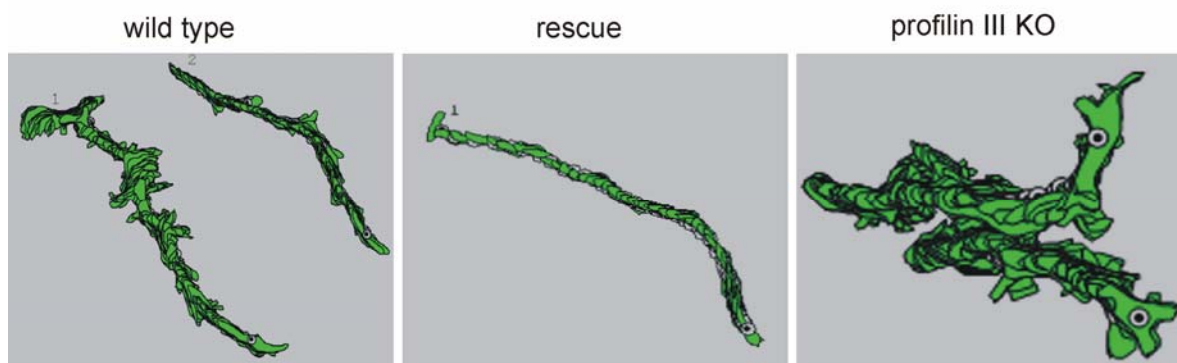
Figure 21: Overexpression of pIII in pI/II- cells rescued the cytokinesis defect of the pI/II-cells

pI/II minus cells with and without pIII overexpression were fixed on a glass coverslip with ice-cold methanol and stained with DAPI for visualising the nuclei. Their number was counted in approximately 200 cells. When overexpressed, pIII complemented the role of pI or pII and rescued the cytokinesis defect.

3.2.6 *Profilin III*-null cells exhibit motility defects

In *D. discoideum*, DdVASP showed enrichment at the leading edge of an actively moving cell during chemotaxis and deletion of the gene resulted in cells that have defects in chemotaxis and in the ability to suppress lateral pseudopods. Since profilin III interacts specifically with DdVASP a possible role in motility during chemotaxis was examined. Chemotaxis of profilin minus cells was examined during the aggregation phase in detail. Any differences in the timing of the early development between the wild type AX2 and the profilin-null mutants was monitored by analyzing the presence of the contact site A protein, a developmentally regulated cell adhesion molecule that is expressed during early development. The expression pattern in both the wild type and the mutant is similar (data not shown). After 7 hours of starvation, the migratory pattern of both the wild type and the mutant towards the external cAMP supplied with a microcapillary filled with 10^{-3} M was monitored. Images were recorded as described in materials and methods. Speed, direction change, roundness and persistence were calculated. The mutant cells were less polarised. They lacked the ability to suppress lateral pseudopods resulting in cells with irregular migratory tracks and reduced overall speed. However as the cells approached the tip of the

capillary these cells tend to move in a more directed fashion. The shape changes of two *profilin III*-null and AX2 cells were analysed from the chemotaxis movies. The outlines were drawn manually after manifesting the images using the DIAS program. Every other image was used for tracing and the images were superimposed to show the changes in the cell shape during the movement. The cell shapes suggest a lack of polarity and a continuous change of direction. The expression of a FLAG-tagged full-length profilin III reverted the cell polarity and motility defect completely. In addition, the cells underwent considerably more directional changes than AX2 cells, and the speed of movement was reduced significantly (Figure 22). These defects could be rescued by the expression of N-Flag pIII.



	Speed [$\mu\text{m}/\text{min}$]	Persistence [$\mu\text{m}/\text{min-deg}$]
wild type	13.2 \pm 0.5	4.4 \pm 0.1
pIII rescue	18.2 \pm 7.1	8.7 \pm 4.9
pIII KO	5.8 \pm 5.4	1.7 \pm 2.0

Figure 22: Chemotaxis analysis of profilin III- null cells and cells expressing N-Flag profilin III

Cells were developed in 1X phosphate buffer for 7 h. Cells were plated on a Petri dish with a glass bottom and visualized by using an inverted microscope and a micropipette filled with 10^{-3} M cAMP. Cell movements were recorded with Axiovision software and analyzed using the DIAS program. Comparison of cell shape, direction change, and speed of the movement of different cells is shown. A representative cell from each type of cells is shown. The recordings are made at 6 frames/min. The image was obtained by superimposing the frames.

3.3 Characterisation of *D. discoideum* Ste20-like kinases

In a general search for homologs of the severin kinase which was the first identified Ste20-like kinase in *D. discoideum* (Eichinger et al., 1998) we found among many others also the gene *krsA*. Original cloning and studies on kinase activity were done by Hyun-ju Son during her time as graduate student in the laboratory (Son, 2003) (<http://edoc.ub.uni-muenchen.de/archive/00001552/>), further and more detailed characterization of *krsA* and its gene product Krs1 and severin kinase null mutant are part of this thesis.

3.3.1 Sequence analysis of Krs1

The gene itself was first mentioned by Hideko Urushihara and coworkers as FC-AV09 cDNA from the sexually mature stage of the *D. discoideum* strain KAX3 (GenBankTM accession number AF061281) and designated as *krsA* for 'kinase responsive to stress 1-like kinase'. The gene contains five exons, the four introns have a size of 77, 119, 77 and 175 bp, respectively. The full length cDNA (1386 bp) was obtained by RT-PCR using RNA isolated from vegetative cells. The complete Krs1 kinase consists of 461 amino acids with a molecular mass of 52.5 kDa. The topology shows an N-terminal catalytic (287 aa) and a C-terminal regulatory domain (174 aa) which is typical for the Germinal Centre Kinase (GCK) family among Ste20 like kinases. Besides all canonical subdomains which characterize Ser/Thr-kinases, the so-called Ste20-signature 'GTPY/FWAPE' is present in Krs1 as well. In database searches the highest degree of sequence homology was observed in kinases from the GCK-II subfamily such as mammalian MST1 and MST2 (Figure 23) or Hippo from *D. melanogaster* with more than 60% identity in the catalytic domain. Phylogenetic analysis revealed Krs2 (DDB0216375) and *Dictyostelium* Ste20 kinase A (DstA) (DDB0216377) as the closest relatives in *D. discoideum* with 58% and 56% identity in the catalytic domain (Figure 24). Kinases in the GCK-II subfamily are key players in apoptosis (Edgar, 2006; Hay and Guo, 2003; O'Neill et al., 2004) and were for example shown to phosphorylate histone 2B during programmed cell death (Cheung et al., 2003).

Though in many cases the regulatory domains in Ste20-like kinases do not show distinct domain structures with known functions, in Krs1 the putative inhibitory domain (aa 330-379) and a possible multimerization/SARAH domain (aa 412-458) are well conserved (Figure 23). The Krs1 SARAH domain (named after a similar region in Sav / Rassf / Hpo) (Scheel and Hofmann, 2003) spans about 50 amino acid residues and is located at the extreme carboxyl terminus. Most likely, this stretch forms an α -helical coiled-coil motif

characterized by a seven-residue periodicity. Interestingly, Krs1 also contains a putative caspase cleavage site 'DEQD' (aa 287-290) similar to the one important for regulation of MST1 and MST2 during caspase mediated cell death. The significance of this is unclear, as there were no true caspases identified in *D. discoideum*. The only known paracaspase had no protease activity towards known caspase substrates (Uren et al., 2000) and as the gene knockout had no effect on vacuolar autophagic cell death (Kosta et al., 2004), paracaspases in *D. discoideum* seem to have functions that do not involve apoptosis or similar forms of cell death. It is therefore unlikely that Krs1 is a functional homolog of its mammalian counterparts. However, since proteolytic cleavage of MST1 regulates its subcellular localization and its function (Ura et al., 2001), a similar mechanism of activation of Krs1 by a specific protease might exist. Proteolytic activation of kinases was described for *D. discoideum* before

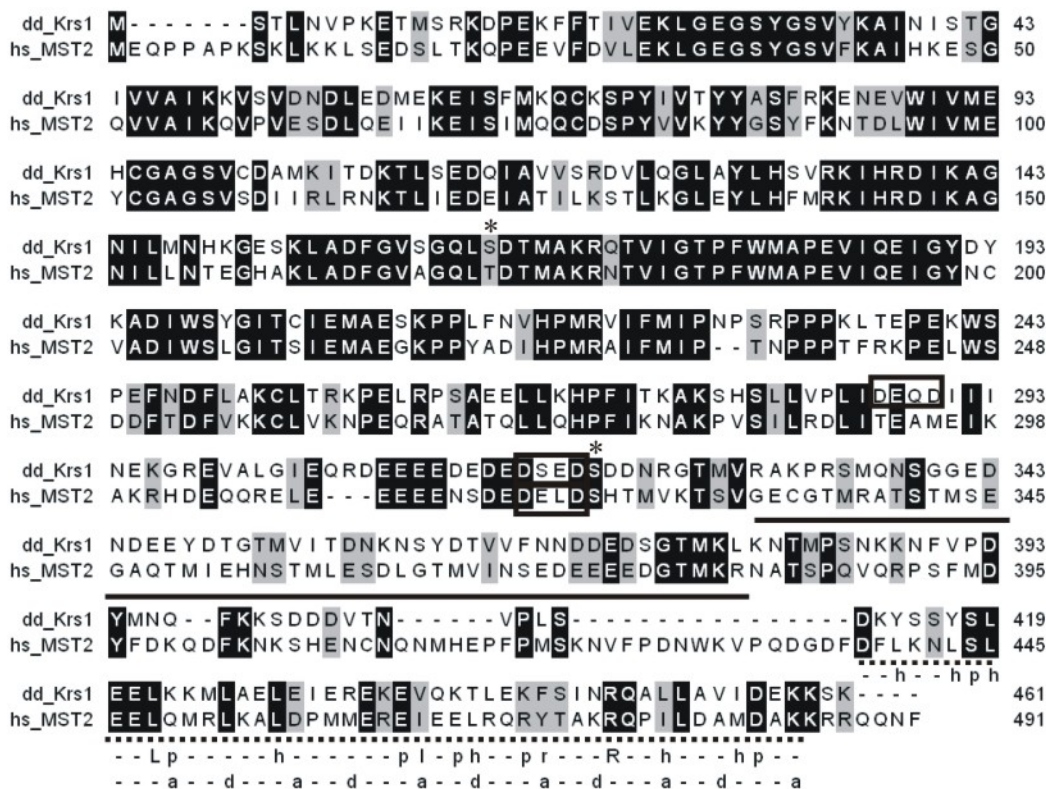


Figure 23: The N-terminal catalytic domain (1-287) of Krs1 exhibits high homology to MST2

The sequence alignment was done with the program MultiAlign (Corpet, 1988). The regulatory domain (288-461) of Krs1 contains two distinct domains, the inhibitory domain (underlined) and the SARAH domain (broken underlined). The invariant and conserved residues in the 50 amino acid residue SARAH domain as well as the heptad repeat of the coiled-coil motif necessary for protein-protein interactions are indicated (hydrophobic (h), polar (p), aliphatic (l) and aromatic (r)). The putative caspase sequences are boxed and the postulated autophosphorylation sites are marked (*).

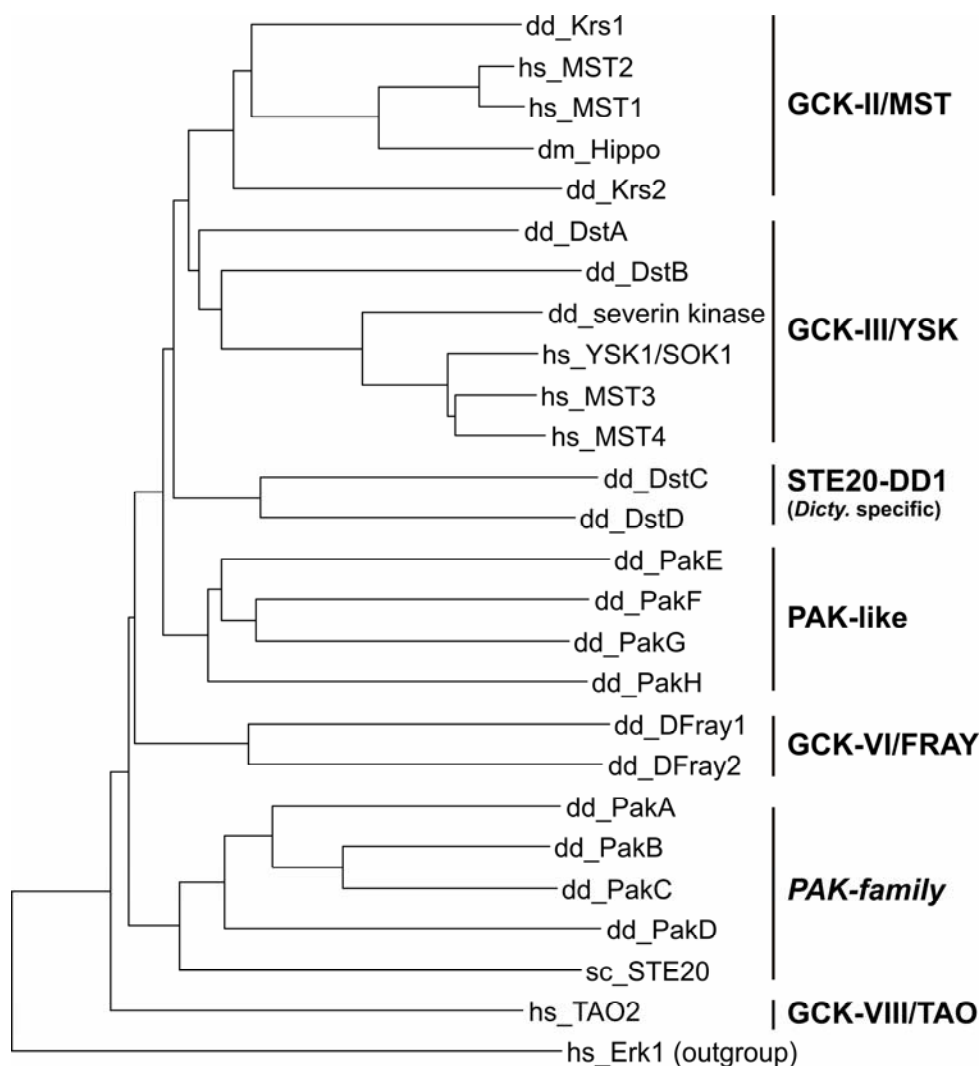


Figure 24: The phylogenetic analysis of *krsA*

The phylogenetic tree is based on ca. 260 amino acids of the kinase domain using the ClustalW program (Chenna et al., 2003) with default settings. The tree was drawn with njplot. The sequences used have the following accession numbers: DDB0191176/*svkA* (*dd_severin_kinase*), DDB0191170/*krsA* (*dd_Krs1*), DDB0229410 (*dd_PakF*), DDB0229408 (*dd_PakH*), DDB0216375 (*dd_Krs2*), DDB0216379 (*dd_DstC*), DDB0216374 (*dd_DstD*), DDB0229414 (*dd_PakE*), DDB0229411 (*dd_PakG*), DDB0216377 (*dd_DstA*), DDB0216378 (*dd_DstB*), DDB0230012 (*dd_DFray1*), DDB0229911 (*dd_DFray2*), AAA83254 (*hs_MST1*), AAB17261 (*hs_MST2*), AAH65378 (*hs_MST3*), CAI42079 (*hs_MST4*), BAA20420 (*hs_YSK1/SOK1*), AAH51798 (*hs_TAO2*), NP_611427 (*dm_hippo*), AAB69747 (*sc_STE20*), AAK52329 (*hs_ERK1* (outgroup)).

3.3.2 *In vitro* kinase activity of Krs1

It was previously shown by Hyun-Ju Son (Son, 2003) that

- (i) Krs1 phosphorylates the actin-binding protein severin and its domains 2+3,
- (ii) the kinase activity is more prominent in Mn^{2+} , a feature shared by the human GCK-III subfamily member human MST3,

- (iii) the catalytic domain (aa 1-287) as defined through the 12 subdomains (Hanks and Hunter, 1995) is inactive and needs a seven additional amino acids for activity,
- (iv) the regulatory domain in the C-terminal half inhibits kinase activity, and stepwise truncations increase drastically the kinase activity,
- (v) the regulatory domain is a substrate for autophosphorylation, and that
- (vi) a fusion with maltose-binding protein allowed purification of an active recombinant kinase.

The main focus of the present work was the further characterization of the *in vitro* activity and the isolation of a kinase knockout mutant.

3.3.3 Subcellular localization of Krs1

The subcellular localization of endogenous Krs1 was assayed in immunoblots using the polyclonal anti-Krs1 antiserum (Son, 2003). Nearly all of the Krs1 was detected in the soluble fraction, neither the 10,000 x g nor the 100,000 x g nor the Triton-X 100 insoluble cytoskeleton contained significant amounts. Consistent with these data, wild type cells showed an overall distribution of Krs1 in immunofluorescence experiments. Overexpression of a GFP-tagged full length Krs1 in the wild type background however, showed in addition a bright signal at the cell cortex (Figure 25).

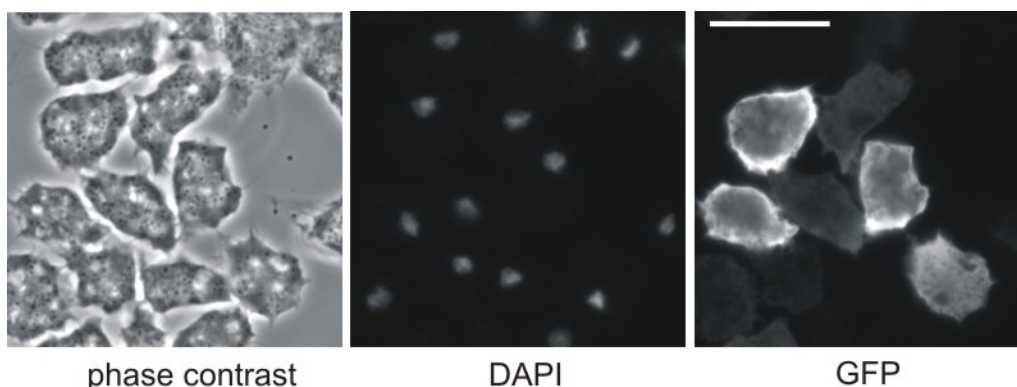


Figure 25: Intracellular distribution of Krs1

GFP-tagged full length Krs1 in wild type cells showed an enrichment of the kinase at the cell cortex. The cells were fixed with ice cold methanol, nuclei were stained with DAPI, the GFP kinase was detected with a polyclonal anti GFP serum. The images were recorded in an Axiovert200 fluorescence microscope. The bar represents 10 μm

3.3.4 Isolation and characterization of *krsA*-null mutants and GFP overexpressors

To learn more about the *in vivo* function of Krs1, we generated *krsA*-null mutants where the gene was disrupted by introducing a blasticidin resistance cassette that terminates translation between subdomains IX and XI of the kinase domain Figure 26A. Transformants were selected and tested for the presence of endogenous Krs1 protein by western blots (Figure 26B). Several independent negative clones were isolated. Growth of *D. discoideum* cells in axenic cultures and on *K. aerogenes* lawns were normal as compared to AX2. Also phagocytosis of fluorescently labeled yeast cells was undisturbed.

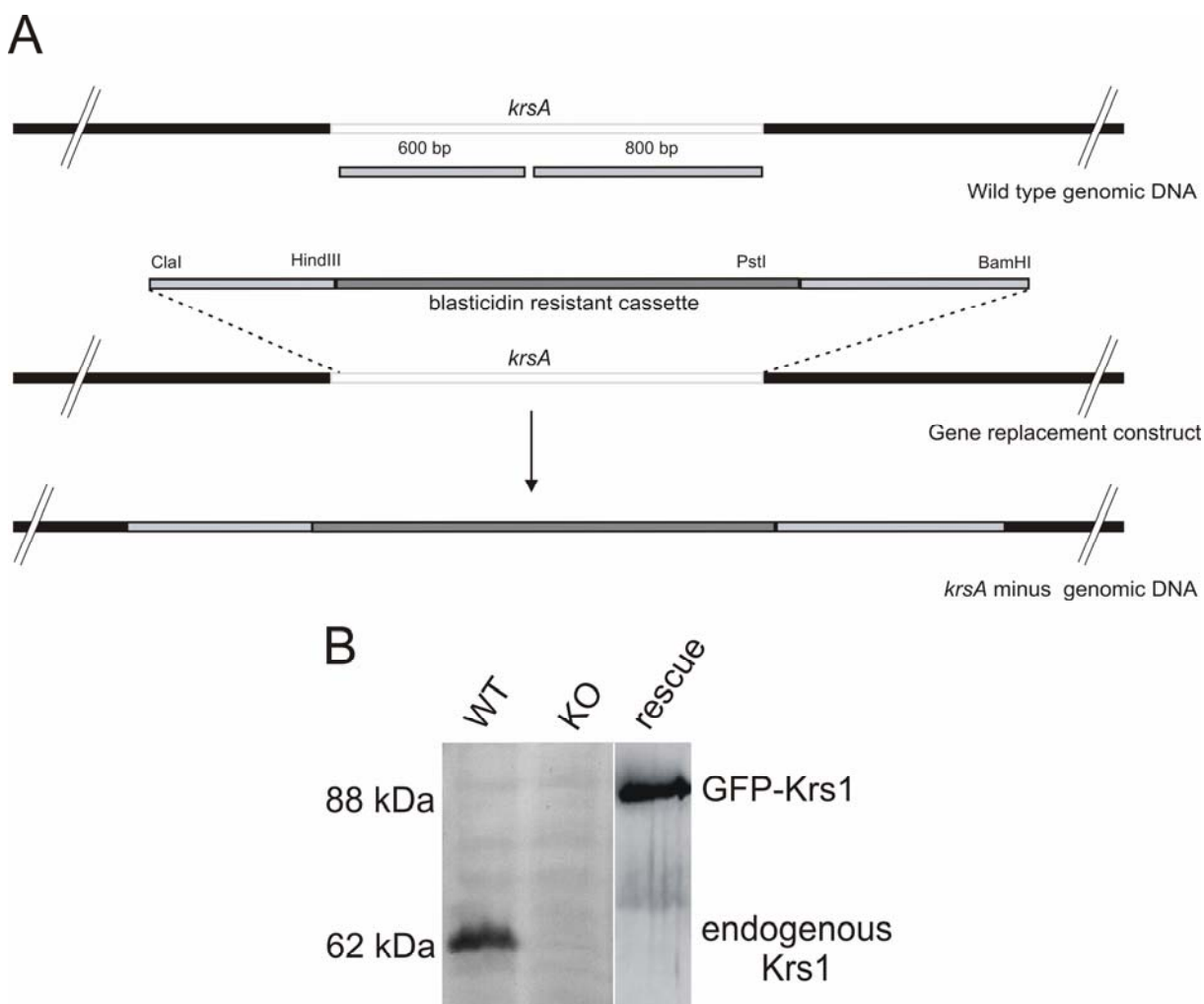


Figure 26: Generation of *krsA*-null and rescue mutants

(A) A gene disruption vector was constructed by cloning a 5' and a 3' fragment on either side of the blasticidin resistance cassette. (B) Western blot analysis showed that in the isolated mutants a gene disruption had occurred, the endogenous protein was seen only in the wild type and not in Krs1 null cells or the rescue which expresses the GFP-Krs1 fusion construct

3.3.5 Development of *krsA*-null mutant on phosphate agar and in suspension

Upon starvation, *D. discoideum* cells enter a developmental cycle that leads from single amoebae to the formation of a multicellular fruiting body. This cycle involves differentiation into at least two cell types, prespore and prestalk cells, which sort to give rise to a mature fruiting body consisting of stalk and spore cells. This process requires locomotion and chemotaxis by single cells, as well as morphogenesis, pattern formation, and motility of multicellular structures. *krsA* was previously shown to be developmentally regulated and the transcript was upregulated at t_{12} (Son, 2003). However, similar changes were not seen at the protein level using the Krs1-specific antibody, developmental markers like contact site A or the Mud1 antigen were present at the appropriate developmental stages (data not shown).

To investigate the development under submerged conditions where cells are subjected to a much shallower cAMP gradient, both *krsA*-null mutant and wild type cells were plated in phosphate buffer onto 1 cm diameter cell culture dishes at different cell densities. Wild type cells developed into well formed streams when plated at a density of 5×10^6 cells or more. In contrast, the null mutant cells could not form streams at these densities but formed irregular aggregates (Figure 27).

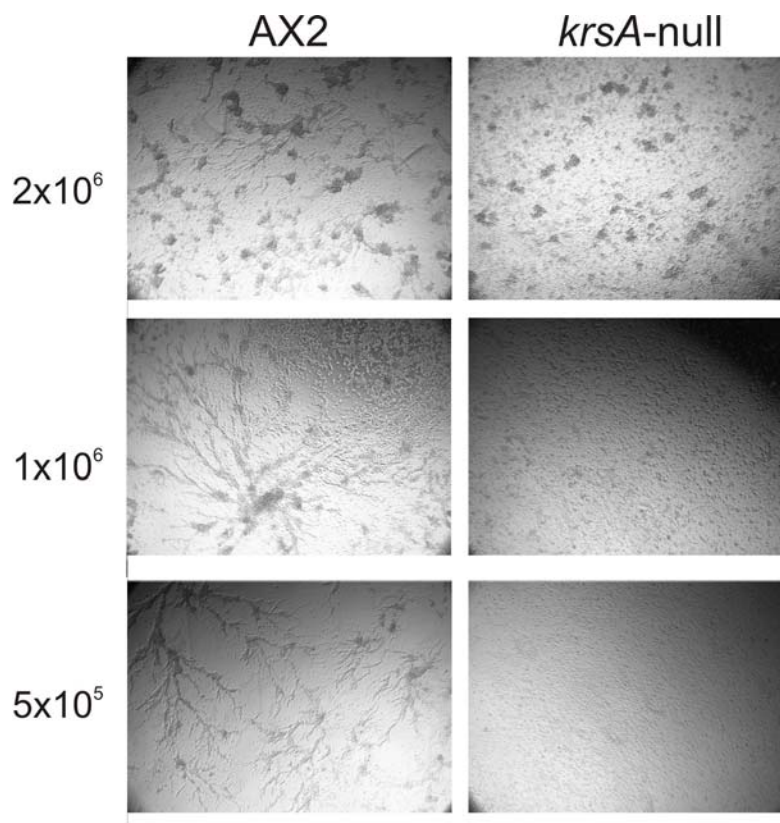


Figure 27: Development of *krs1*-null mutants in submerged cultures

The *krs1*-null cells when plated at a low cell density fail to form streams in submerged cultures compared to AX2.

3.3.6 Properties of severin kinase

A second kinase that was investigated during the course of this study was severin kinase (*svkA*). Severin kinase was previously isolated from the cytosolic fraction of *D. discoideum* based on *in vitro* phosphorylation assays (Eichinger et al., 1998). Severin kinase phosphorylates the Ca^{2+} dependent F-actin fragmenting protein severin (Eichinger et al., 1991). The kinase was isolated as a protein with a molecular mass of about 300 kDa, harbouring 62 kDa active subunits. The cDNA coding for severin kinase was isolated from the cDNA library based on partial peptide sequence information. Analysis of the coding sequence of *svkA* identified this kinase as a member of the Ste20-like kinase family. The catalytic domain of the kinase harbours 12 subdomains which are typical for serine/threonine and tyrosine kinases, and also the signature sequence of the Ste20 like family in subdomain VIII.

3.3.7 Isolation of *svkA*-null mutants

To investigate the function of severin kinase, a null mutant generated by gene disruption via homologous recombination using the *Cre-loxP* recombination system (Faix et al., 2004) was a generous gift from Dr. Meino Rohlf. A 800bp fragment from the 5'-end with introns 2 and 3, and a 600bp fragment from the 3'-end were used for the construction of the knockout cassette. The disruption was confirmed by immunoblot using antisera generated against recombinant severin kinase (Figure 28).

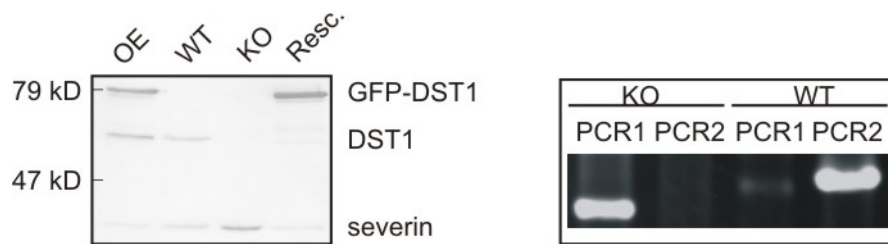


Figure 28: Isolation of *svkA*-null and GFP-SvkA expressing mutants

Blasticidin resistant colonies were screened for the disruption of the *svkA* gene by an immunoblot (left panel) using SvkA specific antisera. As seen in the blot the 62kDa SvkA is present in the wild type cells and in the GFP-SvkA overexpressing cells, but is absent in the null mutant. A high molecular mass GFP-SvkA protein is seen only in the rescue and in the overexpressing mutants. The right panel shows a PCR based screen. In PCR1 the reverse primer binds only to the blasticidin cassette, hence the amplicon is present only in the null mutants. In PCR2 the whole *svkA* gene is amplified and since the gene after the disruption is too large to be amplified under these conditions the amplicon is seen only in the wild type and not in the mutant.

3.3.8 *svkA*-null mutants exhibit growth defects

The growth of *svkA*-null cells on bacterial lawns was measured in comparison to wild type AX2 cells. Deletion of the severin kinase gene led to a drastic reduction in the growth of these cells (Figure 29). Expression of GFP-SvkA rescued the growth defect of these cells.

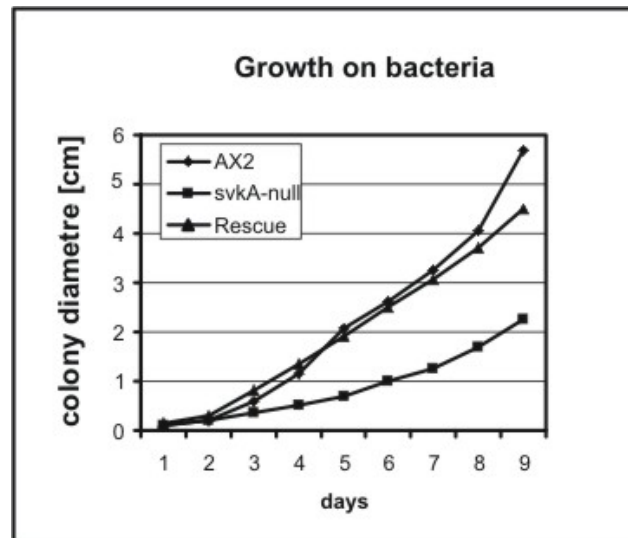


Figure 29: Growth of svkA-null mutant on bacteria

Growth of svkA-null mutants on a lawn of *K. aerogenes* under normal conditions was significantly hampered compared to AX2 wild-type cells. Under these conditions, growth of this mutant was rescued by the expression of N-GFP Svka

3.3.9 svkA-null mutants show a defect in phagocytosis

The inability of the severin kinase null mutants to grow on bacterial lawns like wild type suggested a possible defect in phagocytosis. Therefore uptake of yeast particles in suspension was tested (Maniak et al., 1995). For the uptake, cells were fed with heat-killed TRITC-labelled yeast cells. The lack of severin kinase resulted in a marked decrease in the uptake of yeast cells (Figure 30).

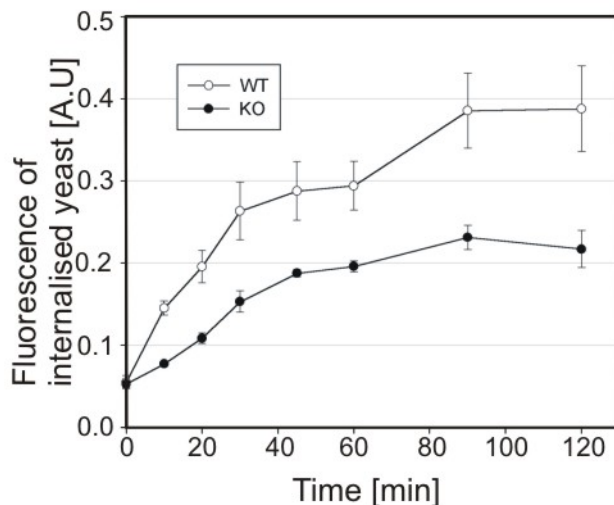


Figure 30: Phagocytosis of fluorescently labeled yeast

svkA-null mutants in shaking cultures were incubated with fluorescently labeled (TRITC) yeast particles and the uptake is monitored in a fluorimeter at different time points indicated. Their ability to phagocytose yeast was compared with the wild type AX2 cells.

3.3.10 *svkA*-null cells are defective in cytokinesis

Investigation of the null mutants under a phase contrast microscope showed obvious differences in cell shape and size. *svkA*-null mutant cells were very large when grown on plastic petri dishes, suggesting the cells have a cytokinesis defect (Figure 31A). Nuclear staining with 4,6-diamidino-2-phenylindole (DAPI) (Figure 31B) indicated that these giant null cells could have as many as 60 nuclei/cell (Figure 31C). Approximately 95% of the cells of the wild type strain AX2 have one or two nuclei compared with 38% for *svkA*-null cells. Furthermore, >60% of *svkA*-null cells have at least four or more nuclei per cell. A similar percentage of cells was multinucleated in shaking cultures as well compared to those on plastic surface. This feature distinguishes them from the myosin II null mutant (Fukui and Inoue, 1991) and the F-actin binding protein coronin both required for proper cytokinesis. While myosin II null mutants divide well on a solid substrate by traction-mediated cytofission, but remain multicellular in suspension, a coronin null mutant cells exhibit a stronger cytokinesis when grown on Petri dishes (de Hostos et al., 1993). Overexpression of *SvkA* as a N-GFP fusion under the actin 15 promoter in the null cells restored normal cytokinesis (Figure 31B).

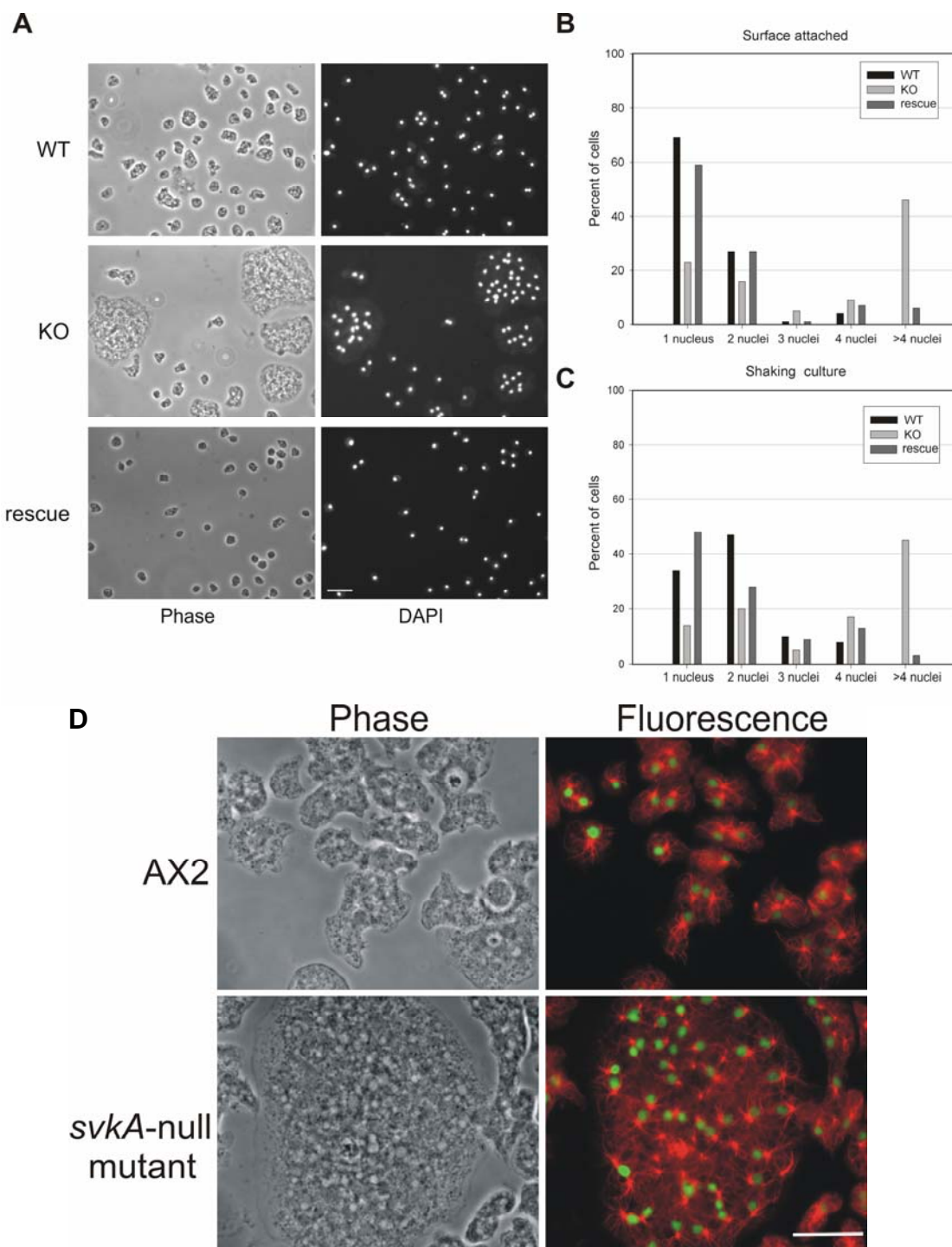


Figure 31: Cytokinesis defect of *svkA*-null cells

(A) Quantitative analysis of the cytokinesis defect Cells from suspension culture (B) and from shaking cultures (C) were fixed on glass coverslips with methanol and the nuclei were stained with DAPI. The nuclei of as many as 300 cells were counted for each strain. (D) An illustration of a large multinucleated cell in comparison to a wild type strain. Cell were fixed with cold methanol and stained of tubulin (red) and nuclei (green). Scale bar represents 10 μm .

3.3.11 *svkA*-null cells exhibit developmental defects

SvkA is expressed uniformly throughout the developmental cycle (Figure 32A). Figure 32B illustrates the development of *svkA*-null cells, null cells expressing N-GFP SvkA, and parental AX2 cells. When plated at a density of 1×10^8 cells/plate, null cells formed much smaller mounds and fruiting bodies than AX2 cells, which formed nearly normal-sized mounds when plated at the same density. The developmental timing was affected and mutant cells could not complete the entire development in 24 h. After 48 h small, abnormal fruiting body-like structures were formed which had an irregular sorus. The spores were elliptic similar to the wild type spores. Expression of N-GFP SvkA restored the normal development.

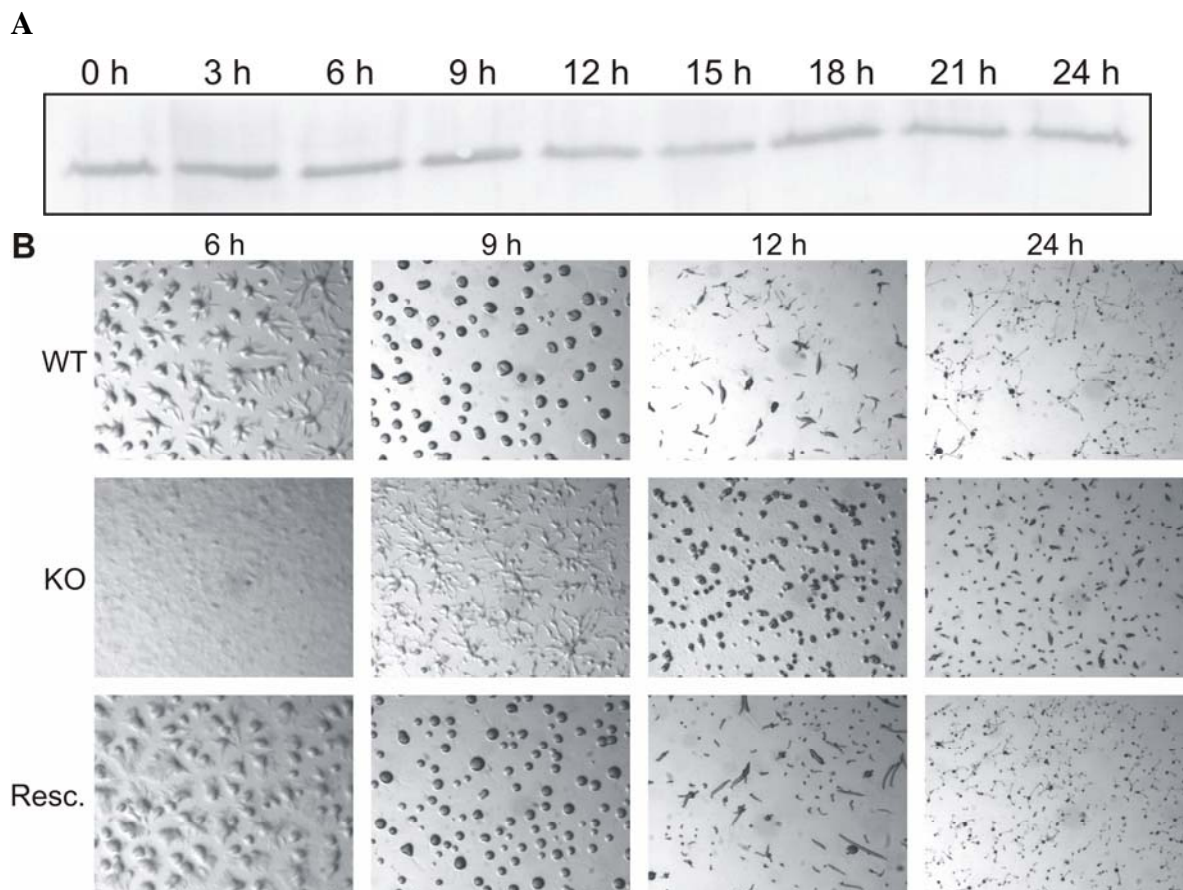


Figure 32: Development of *svkA*-null cells

(A) Expression profile of SvkA during development in wild type cells Wild type AX2 cells from nutrient medium were washed and starved on phosphate agar plates to induce development. Cells were harvested at every three hour interval and were lysed in SDS-lysis buffer. Equal amounts of cells were loaded and the expression of SvkA was checked in an immunoblot with anti-*svkA* antisera. SvkA is uniformly expressed throughout the development. (B) Developmental phenotype of *svkA*-null cells. Wild type AX2 cells, *svkA*-null cells and *svkA*-null cells expressing GFP-SvkA were washed in phosphate buffer and were plated on phosphate agar plates. Development of these cells at 21°C at different time

points was recorded at the same magnification. *svkA*-null cells show a significant delay in development.

3.3.12 *svkA*-null cells do not exhibit any motility defects

The aggregation and morphogenesis defects suggest that *svkA*-null cells may exhibit aberrant motility and chemotaxis defects as well. Random motility in nutrient medium and in phosphate buffer was measured by recording the motility of the cells by video microscopy as described in materials and methods. Speed, persistence and direction change were analyzed using the DIAS software only for cells that were in size similar to wild type cells. Large multinucleated cells were avoided as they show independent of the strain strongly reduced motility. Chemotaxis was examined by assaying the ability of aggregation-competent cells to migrate towards a micropipette emitting the chemoattractant cAMP. *svkA*-null cells were less polarized as compared to AX2 cells and these cells tended to adhere more strongly to glass surfaces as seen in the poor detachment at the rare ends which led frequently to rupturing of the cells. AX2 cells moved at a speed of 5.81 ± 0.49 $\mu\text{m}/\text{min}$ whereas the mutant cells moved at a speed of 4.52 ± 0.51 $\mu\text{m}/\text{min}$. These data indicate that SvkA does not have a drastic effect on the speed of random or directed motility.

3.3.13 SvkA is necessary for correct phototaxis

Upon starvation, individual amoebae aggregate and form multicellular slugs that exhibit positive photo- and thermotaxis. Changes in phototaxis seem to frequent in cytoskeletal and signalling mutants (Fisher et al., 1997; Stocker et al., 1999; Wilkins et al., 2000). Since mutant cells lacking severin kinase show significant developmental defects, the migratory behaviour of the mutant slugs was studied in a phototaxis assay. Severin kinase null mutants show defects in migration and do not move as far as the wild type cells over the same period of time (Figure 33). However, few slugs that migrate towards light show no defect in light sensing. Expression of GFP-severin kinase restores the normal movement of the slugs.

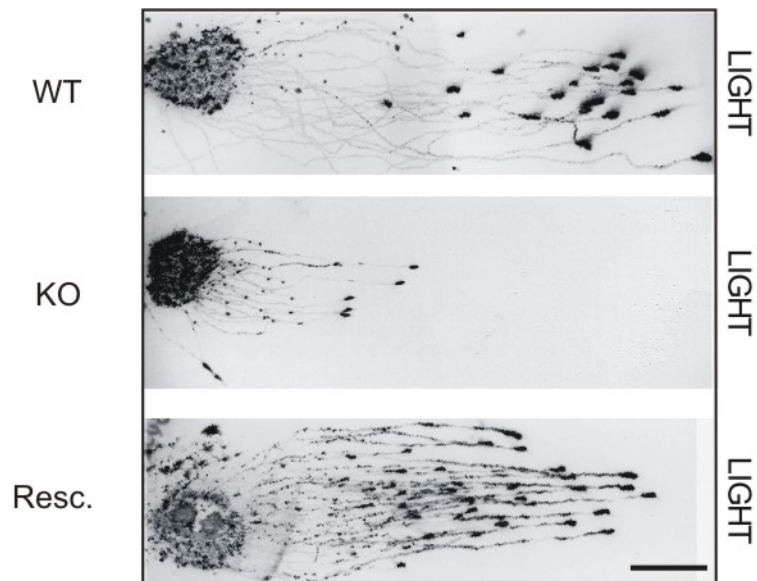


Figure 33: Phototaxis of wild type and mutant slugs

The migration of Severin kinase-deficient slugs towards light is drastically reduced compared to the wild type AX2 cells. The slugs were transferred onto nitrocellulose and stained with actin antibody. Expression of GFP-Severin kinase rescued the migration defects of the null mutants. The bar represents 1 cm

4 Discussion

The major goal of the thesis was the investigation of regulatory mechanisms in the actin cytoskeleton. This involved studies (i) on the molecular interaction of *D. discoideum* VASP (DdVASP) with formins and profilins, especially the yet unpublished profilin III (pIII), and (ii) on two kinases from the Ste20-like family which are most likely members of signalling cascades towards the microfilamentous system.

4.1 DdVASP

Based on the previous *in vivo* experiments by Hug et al (Hug et al., 1995) and *in vitro* studies by Vignjevic et al (Vignjevic et al., 2006; Vignjevic et al., 2003) it is now widely accepted that the activity of the barbed end capping protein (CP) regulates the transition between short highly branched actin networks to unbranched long actin filament bundles. A dendritic branching model for filopodia formation was recently proposed (Mejillano et al., 2004). According to this model, Ena/VASP proteins that are present on the tips of filopodia and lamellipodia play an important role in inhibiting the binding of CP to the barbed end of the filaments, thereby promoting barbed end elongation and formation of unbranched filopodia. This model was challenged by two recent findings: first the requirement of formins in the formation of filopodia (Peng et al., 2003; Schirenbeck et al., 2005) and, secondly formation of filopodia independent of the requirement of the Arp2/3 complex (Steffen et al., 2006). In the present study we re-evaluated the role of VASP in the filopodia formation. Using biochemical and cell biological approaches we proposed that VASP cannot bind to the barbed ends of the filaments, cannot antagonise the binding of CP to the barbed end, but is required for the bundling of the nascent actin filaments that are generated by the formin dDia2.

The following observations support our model:

(i) The *in vivo* nucleating activity of VASP is widely debated. VASP dependent nucleation of actin varies significantly and is dependent on the concentration of the actin and the actin bound metal ion whereupon Mg^{2+} -actin is preferred over Ca^{2+} -actin (Lambrechts et al., 2000). It was also shown that the nucleation of actin monomers by VASP is based on electrostatic interactions, is dependent on ionic strength (Laurent et al., 1999) and also on the pH of the buffer used. VASP nucleates at lower concentration in the presence of up to 50mM KCl (Skoble et al., 2001), whereas at physiological ionic strength nucleation is essentially non-existent (Bear et al., 2002; Samarin et al., 2003).

(ii) It was previously shown that VASP acts by competing with the capping protein for free barbed ends. Our data from the uncapping experiments do not support this notion and are consistent with the finding from Samarín et al (Samarín et al., 2003), who showed with a simplified biometric assay that the motility and the branching of the filaments remain unaffected in the presence of capping protein. In a recent study Barzik and coworkers (Barzik et al., 2005) investigated how mammalian VASP influenced actin polymerization in the presence of capping proteins. They proposed that VASP associated 'at or near' the barbed ends of actin filaments and thus could restrict access of barbed end CP. For reasons that we cannot explain, our data are different from the one obtained by Barzik et al. DdVASP and also HsVASP do not affect the behavior of barbed ends during dilution-induced depolymerization of filaments in the absence or presence of either CapG or Cap32/34. A direct interaction of VASP with the plus ends of filaments leading to competition with CP should, however, alter the depolymerization kinetics. Furthermore, VASP as an *in vitro* bundling protein must bind along the length of the entire actin filament and not only 'near' to the barbed end. Possible explanations for the contradictory results could be slightly different experimental setups. Whereas Barzik et al. mixed F-actin, VASP and capping protein, and then diluted the mixture to induce depolymerization, we tried to avoid the presence of VASP in the undiluted F-actin. We realized that the addition of VASP to F-actin before dilution caused immediate bundling, and thus a slower depolymerization occurred thereafter, presumably due to sterical hindrance or inhibition of monomer dissociation as soon as a crosslinking bridge in the bundle was reached. We therefore pre-capped the actin filaments and subsequently induced depolymerization by addition of buffer and VASP at the same time.

(iii) In addition to Ena/VASP, another group of proteins that antagonize capping and are also necessary for filopodia formation identified recently, are formins. *In vitro*, formins nucleate actin filaments and remain associated with their growing barbed ends (Evangelista et al., 2003; Pruyne et al., 2002) protecting them from capping (Evangelista et al., 2003). A combinational approach using VASP and formins showed that VASP cannot uncapse the capped filaments but formins do. Our data demonstrated that the FH1FH2 region of the formin dDia2 interacts with DdVASP during filopodia formation and that this interaction is crucial for the efficient elongation of actin filaments at the tips of protruding filopodia. Notably, *in vivo* VASP remains confined to the tips of protruding filopodia despite its F-actin binding and bundling activities.

From this results we conclude that the entire complex moves on with the filopodium tip, as has been already shown for dDia2 (Schirenbeck et al., 2005). In this scenario, filament bundling by VASP applies only to nascent filopodial filaments in the vicinity of the filopodial tip complex before other actin-bundling proteins like fascin, stabilize the emerging bundles in the filopodial shaft.

The involvement of formins in filopodia formation was reported recently not only for *Dictyostelium* (Schirenbeck et al., 2005), but also for vertebrate cells. An mDia2-mediated but Cdc42-independent pathway leading to the formation of filopodia has been described for the Rho GTPase Rif (Pellegrin and Mellor, 2005). Interestingly, elimination of mDia1 in mice resulted in an up-regulation of mDia2 and revealed its potential role as an effector of Cdc42, which in turn is involved in filopodia formation (Peng et al., 2003). Furthermore, overexpression of an EGFP-tagged constitutively active (i.e., truncated) mDia1 in fibroblasts led to a massive formation of actin fibers as well as to a large number of filopodia-like structures that were labelled at their tips with the EGFP fusion protein (Higashida et al., 2004). Finally, mDia1 was previously shown to coimmunoprecipitate with VASP (Grosse et al., 2003). In the light of the finding that *Dictyostelium* and vertebrate VASP behave virtually identical, it is tempting to speculate that the disclosed formin/VASP pathway of this study provides a conserved mechanism of filopodia formation.

4.2 Profilin III

In this study a third profilin isoform, profilin III, expressed in *D. discoideum* was characterized in detail. Profilins have been postulated to modulate actin polymerization, thus playing a role in cytoskeletal rearrangements. Profilin null mutants in a variety of species including *D. discoideum* strongly support the notion that profilin is absolutely important for cell shape, locomotion, cytokinesis, cell polarity and development (Balasubramanian et al., 1994; Haugwitz et al., 1994; Verheyen and Cooley, 1994). *D. discoideum* profilin III was identified by searching the completed *D. discoideum* genome project (Eichinger et al., 2005) and shares 56% and 61% identity with profilin I and profilin II, respectively. The difficulties to detect profilin III in profilin double minus cells (pI/II-) by poly-L-proline pull down assays and recent reports (Qian et al., 2005) about small adapter proteins that share profilin fold but no functional similarities led to the initial concern that the putative profilin III may be a non-functional profilin as well. To address these questions, recombinant protein was purified from *E. coli* and its biochemical

properties were tested. The data clearly showed that this isoforms behaved like a normal profilin: it bound to poly-L-proline, it inhibited the actin polymerization, and interacted with phospholipids.

The role of profilins in cytokinesis was well documented in protozoans (Edamatsu et al., 1992), fungi (Balasubramanian et al., 1994; Haugwitz et al., 1994) and animal cells (Witke et al., 2001b). Gene disruption of profilin I and II in *Dictyostelium* resulted in cells with impaired cell division. These cells provided a tool to investigate the role of profilin III *in vivo*. Overexpression of profilin III in these cells rescued the cytokinesis defect. These results showed that profilin III can fulfill normal profilin activities also *in vivo*.

The quantification of profilin III expression in wild type cells showed that this protein is expressed at very low levels (200nM), compared to the other two abundant isoforms profilin I (19 μ M) and profilin II (28 μ M) (Haugwitz et al., 1994). One can conclude from these data that profilin III behaves biochemically like a normal profilin and that it can rescue the aberrant phenotype of pI/II-minus cells as long as it is overexpressed. The low abundance in wild type cells however suggests that profilin III is a distinct and unique member of the *Dictyostelium* profilin gene family and has an yet unknown regulatory function.

Possible different biological functions may involve interactions with specific ligands. Proteins such as VASP (Reinhard et al., 1995), MENA (Gertler et al., 1996), p140mDia (Watanabe et al., 1997) or the Arp2/3 complex (Machesky et al., 1994a; Welch et al., 1997) have been shown to interact with profilin. Preferential binding of proteins with profilin isoforms was reported previously (Schirenbeck et al., 2005; Witke et al., 1998). We tested a potential interaction between DdVASP and profilin isoforms in a yeast two hybrid assay. Only profilin III specifically interacted with DdVASP. Deletions in DdVASP suggested the interaction through the proline rich domain. Although attempts were made to show this interaction through immunoprecipitation, GST-pull down assays and gel filtration, these experiments were unsuccessful, and we can not exclude that the interaction is too transient, too weak, that the turnover of the complex much too fast for the assays used (Harbeck et al., 2000). Certainly it is of high priority to confirm the interaction of DdVASP with profilin III in the yeast two hybrid system also biochemically.

The crystal structure of profilin in complex with poly-L-proline peptides was recently reported (Mahoney et al., 1997). Homology modelling of all three profilins probably will give insights into the critical amino acids that confer the specificity of this interaction and possible mutations with *in vivo* effects. The interaction between profilin and VASP was

previously shown to be necessary for funnelling the actin monomers to the sites of actin polymerization. Experiments with mutant VASP proteins lacking the proline rich domain (Geese et al., 2002; Marchand et al., 1995) or with cell extracts depleted of profilins, showed that e.g. the motility of *Listeria* was greatly reduced. The recruitment of profilin to the surface of *Listeria* was completely abolished when VASP was displaced from the surface of the bacteria, resulting in reduced motility (Geese et al., 2002; Geese et al., 2000; Smith et al., 1996).

Localisation studies showed that *D. discoideum* profilin III was distributed throughout the cell with enrichment along the filopodia and (similar to DdVASP) at the filopodial tips in pIII overexpressing cells. DdVASP null mutants have defects in cell motility during chemotaxis (Han et al., 2002). Because deletion of the profilin III led to defects in cell motility as well, it is a tempting working hypothesis that the interaction between DdVASP and profilin III is important for cytoskeletal dynamics and directed cellular movement.

4.3 Dictyostelium Ste20-like kinases

In search for kinases that phosphorylate and regulate actin binding proteins we previously reported the isolation of the severin kinase, a member of the Germinal Centre Kinase class in *D. discoideum* (Eichinger et al., 1998). The completion of the *D. discoideum* genome project made it feasible to identify more kinases of this emerging class. Unlike p21-activated kinases (PAK), the function and regulation of GCKs are less well characterized. The GCK members harbour a non-catalytic region of great structural diversity that enables the kinases to interact with various signaling molecules and regulatory proteins of the cytoskeleton. Many of these kinases are necessary for apoptosis, morphogenesis, cytoskeletal rearrangements and cell migration. (Dan et al., 2001). In this study, we describe the biochemical and cellular functions of Krs1 as well as characterization of a severin kinase null mutant, members of Group III and II of this kinase family, respectively.

4.3.1 Krs1

Sequence comparison and calculation of multiple alignments of the catalytic domain of Krs1 along with other members of this protein group shed some light onto the relationship among these kinases. Krs1 is a close homolog to MST2, MST1 and Hippo (Creasy and Chernoff, 1995a; Creasy and Chernoff, 1995b; Wu et al., 2003). *Dictyostelium* Krs2 which contains four calpain domain III homologies in the regulatory domain, is the closest

D. discoideum homolog. Krs1 shares two distinct regulatory motifs with its mammalian and insect homologs: (i) the recently described novel protein interaction motif SARAH, and (ii) an inhibitory domain that negatively regulates kinase activity. The SARAH domain in Krs1 spans approximately 50 amino acids and is thought to form short coiled-coil motifs necessary for protein-protein interactions.

The name SARAH (Sav-Rassf5-Hippo) was deduced from sequence similarities in the WW domain of the scaffolding protein Salvador (Sav), the tumor suppressor and regulator of apoptosis Rassf5/Nore1 and the Ste20 kinase Hippo. Members of these protein families seem to form multimers via the SARAH domain during apoptosis (O'Neill and Kolch, 2005; Scheel and Hofmann, 2003). This is especially highlighted in *Drosophila* where the Ste20 like kinase Hippo together with Sav and the downstream effector Warts plays a crucial role in coordination of cell proliferation and cell death needed during eye development (Pantalacci et al., 2003; Ryoo and Steller, 2003). The SARAH domain is versatile in the sense that it was shown to mediate heterotypic interaction in the case of Sav and Hippo (Harvey et al., 2003; Wu et al., 2003) as well as homotypic interactions as was shown for MST1 (Creasy et al., 1996). We assume that the large Krs1-containing complexes which we could detect in gel filtration chromatography are formed through the same motif, however it is not clear whether this is a homotypic or a heterotypic interaction with yet unknown binding proteins.

Previous characterization of the kinase activity of Krs1 showed that the *bona fide* catalytic domain (aa 1-287) as defined through the 12 subdomains (Hanks and Hunter, 1995) is inactive and needs a seven additional amino acids for the autophosphorylation activity. These previous findings were re-evaluated based on the crystal structure of TAO2 (Figure 34). The region corresponding to aa 288-308 of Krs1 is highly conserved among other members of this family of kinases and for TAO2 it was shown that these residues form two α -helices (α J and α K) which fold back towards the kinase domain (Zhou et al., 2004). Truncations of *D. melanogaster* Hippo at position Gln315 (corresponds to Glu296 in Krs1) showed all the characteristic phenotypes of reduced Hippo activity (Harvey et al., 2003), also indicating an important function for the region between the catalytic and the regulatory domain. We have to conclude that these highly conserved residues are necessary for the proper folding and kinase activity and an autophosphorylation site lies somewhere in the catalytic domain of Krs1. That would be in agreement with data from MST1 and MST2 where Thr183 (MST1) or Thr180 (MST2) in the activation loop are being phosphorylated (Deng et al., 2003; Glantschnig et al., 2002). The corresponding

residue in Krs1 is Thr173. The second autophosphorylation site in the regulatory domain is conserved as well. It was shown for MST1 that the highly conserved Ser327 (Ser321 in Krs1. Krs1 also contains two putative caspase cleavage sites DEQD (aa 287-290) and DSED (aa 317-320) between the catalytic and the regulatory domains. *D. discoideum* cells do undergo caspase-independent programmed cell death by differentiating into vacuolated stalk and spore cells (Golstein et al., 2003). Though programmed cell death in *Dictyostelium* differs from that in higher organisms, the molecular mechanisms (e.g. highly specific proteolysis) leading to cell death might remain conserved. Especially our biochemical data of the inhibitory C-terminal half of Krs1 suggests a putative activity switch in this domain. Whether this is facilitated by a possibly very specific protease that cleaves at the caspase consensus sequences is unclear.

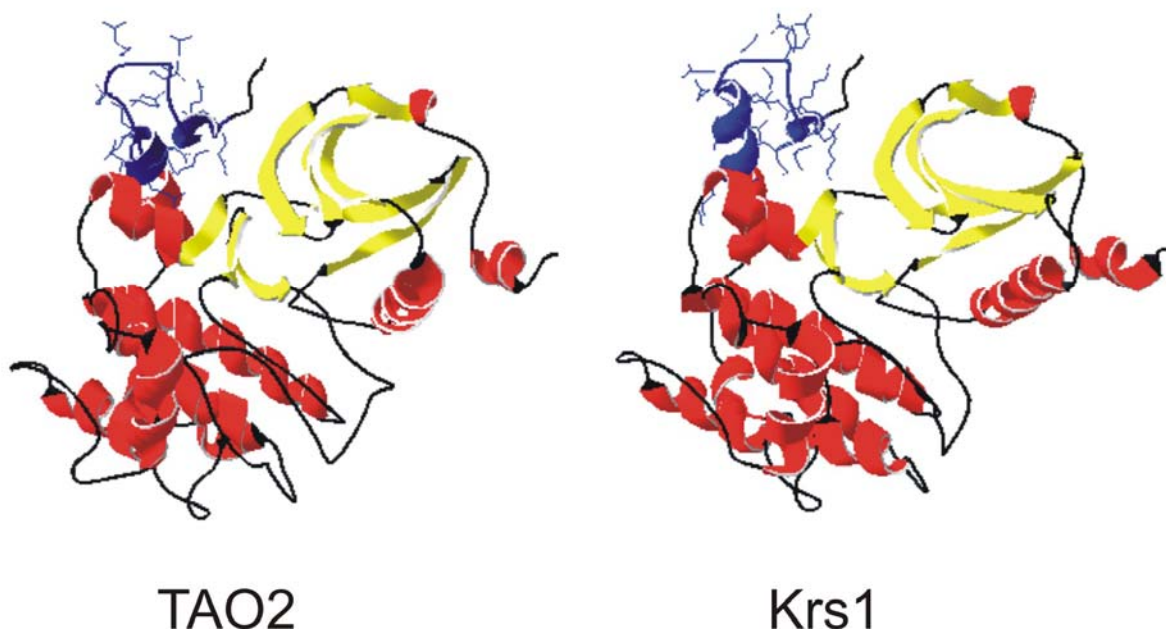


Figure 34: Comparative modeling of Krs1 catalytic domain based on the crystal structure of TAO2 kinase. The conserved residues that lie in the border between the catalytic and the regulatory domain (shown in blue) form a helix that is well conserved and is necessary for the activity.

As we did not see any cleaved fragments of Krs1 using GFP-Krs1 overexpressing cells, we would favor an alternate explanation where phosphorylation at the conserved Ser321 (adjacent to the caspase cleavage site in MST1 and MST2) regulates kinase dimerization and/or interaction with additional activators. This might also direct Krs1 towards the membrane as was observed in GFP-Krs1 overexpressing cells.

Unfortunately, there are only a few reports about putative *in vivo* substrates of the Ste20-like kinases from the GCK subfamily. Phosphorylation assays with different substrates showed that *in vitro* Krs1 phosphorylates the myelin basic protein as a general substrate and the gelsolin-like F-actin fragmenting protein severin and its construct DS211C (domains 2+3). Human MST2/Krs1 and MST1/Krs2 were previously shown to be activated upon subjecting the cells to various stress conditions (Taylor et al., 1996). Since Krs1 is a kinase responsive to stress 1-like kinase it is tempting to speculate that Krs1 is also activated under stress, resulting in the phosphorylation of severin. Regulation of severin phosphorylation by Krs1 seems to differ from severin kinase activity based on its cofactor requirements (Mn^{2+}/Mg^{2+}) and its Ca^{2+} independent activity. Analysis of severin phosphorylation in severin kinase null and Krs1 null should provide insights into putative differences of severin activity.

At present we are still at the beginning of characterizing Ste20 like kinases in *D. discoideum*. Their conservation in evolution is remarkable but we can not assume that the regulatory cascades are conserved as well. Thanks to the genome data we can exclude the major hypothesis for mammalian MSTs: there are no *bona fide* caspases in *D. discoideum*. On the other hand, the conserved caspase cleavage consensus in Krs1 might play an important role as well but due to the lack of caspases by a different regulatory reaction. To address these questions one needs a more significant change in the phenotype which could be achieved by generating multiple knockout mutants followed by a stepwise rescue approach.

4.3.2 Severin kinase

The *D. discoideum* severin kinase is highly homologous to the human proteins SOK1 (Tamari et al., 1999), MST3 (Lee et al., 2004b) and MST4/MASK (Dan et al., 2002). Though the role of these proteins in MAP-kinase pathways is not well documented, they are implicated in maintaining cell polarity during directed cell migration and cell proliferation (Dan et al., 2001). To understand the *in vivo* function of this kinase, a null mutant and null mutants expressing GFP-tagged active kinase were isolated. Observation of the null mutants suggested a failure in the completion of cytokinesis in these cells. Cytokinesis is a final step in cell division and its onset is tightly regulated both temporally and spatially to ensure that it occurs immediately after mitosis. Failure to do so results in multi-nucleated cells. Cytokinesis in *Dictyostelium* cells and mammalian cells occur via the formation and constriction of a actin/myosin II rich contractile ring in the cleavage

furrow, by traction-mediated cytofission on a surface or by a combination of both mechanisms. The cytokinesis defect in the *svk* knockout mutant could be due to altered actin rearrangements or to the failure to regulate a key component necessary to coordinate the mitosis and cytokinesis. So far only the closest relatives of MST kinases in budding/fission yeast (Cdc15p/Sid1p and Kic1p/Nak1p, respectively), and components of the Mitotic Exit Network (MEN)/Septation Initiation Network (SIN) (Bardin and Amon, 2001) were shown to regulate cytokinesis (Bardin et al., 2000; Guertin et al., 2002a; Guertin et al., 2002b). However, little is known about cytokinetic details at the molecular level (initiation, progression and exit). The yeast kinases were suggested to function as upstream kinases of NDR family members, also components of these two networks MEN/SIN. Only Cdc15p has been documented as an authentic upstream kinase *in vivo* (Mah et al., 2001). Cdc15p positively regulates the onset of cytokinesis by phosphorylating a NDR kinase family member Dbf2 in the Dbf2-Mob1 complex. Phosphorylation relocates the complex to the spindle pole body (SPB) and to the bud neck (cleavage site) during late mitosis. Though the changes in Svka kinase activity were not investigated yet, the requirement of an active kinase to complement the phenotype of the null mutant suggests a similar role of Svka in wild type cells. A closer look at the localisation of the GFP-severin kinase in cells undergoing cytokinesis should reveal if similar changes occur in these cells. In addition, the genome project identified at least four NDR kinases necessary for cytokinesis, and expression of a constitutively active NDR-B, the closest homolog of Dbf-2, could tell us whether this signalling network is active in *D. discoideum* as well.

5 References

- Ahern-Djamali, S.M., Bachmann, C., Hua, P., Reddy, S.K., Kastenmeier, A.S., Walter, U. and Hoffmann, F.M. (1999) Identification of profilin and src homology 3 domains as binding partners for Drosophila enabled. *Proc Natl Acad Sci U S A*, **96**, 4977-4982.
- Ahern-Djamali, S.M., Comer, A.R., Bachmann, C., Kastenmeier, A.S., Reddy, S.K., Beckerle, M.C., Walter, U. and Hoffmann, F.M. (1998) Mutations in Drosophila enabled and rescue by human vasodilator-stimulated phosphoprotein (VASP) indicate important functional roles for Ena/VASP homology domain 1 (EVH1) and EVH2 domains. *Mol Biol Cell*, **9**, 2157-2171.
- Amann, K.J. and Pollard, T.D. (2001) The Arp2/3 complex nucleates actin filament branches from the sides of pre-existing filaments. *Nat Cell Biol*, **3**, 306-310.
- Aszodi, A., Pfeifer, A., Ahmad, M., Glauner, M., Zhou, X.H., Ny, L., Andersson, K.E., Kehrel, B., Offermanns, S. and Fassler, R. (1999) The vasodilator-stimulated phosphoprotein (VASP) is involved in cGMP- and cAMP-mediated inhibition of agonist-induced platelet aggregation, but is dispensable for smooth muscle function. *Embo J*, **18**, 37-48.
- Bachmann, C., Fischer, L., Walter, U. and Reinhard, M. (1999) The EVH2 domain of the vasodilator-stimulated phosphoprotein mediates tetramerization, F-actin binding, and actin bundle formation. *J Biol Chem*, **274**, 23549-23557.
- Balasubramanian, M.K., Hirani, B.R., Burke, J.D. and Gould, K.L. (1994) The Schizosaccharomyces pombe cdc3+ gene encodes a profilin essential for cytokinesis. *J Cell Biol*, **125**, 1289-1301.
- Ball, L.J., Kuhne, R., Hoffmann, B., Hafner, A., Schmieder, P., Volkmer-Engert, R., Hof, M., Wahl, M., Schneider-Mergener, J., Walter, U., Oschkinat, H. and Jarchau, T. (2000) Dual epitope recognition by the VASP EVH1 domain modulates polyproline ligand specificity and binding affinity. *Embo J*, **19**, 4903-4914.
- Bardin, A.J. and Amon, A. (2001) Men and sin: what's the difference? *Nat Rev Mol Cell Biol*, **2**, 815-826.
- Bardin, A.J., Visintin, R. and Amon, A. (2000) A mechanism for coupling exit from mitosis to partitioning of the nucleus. *Cell*, **102**, 21-31.
- Barzik, M., Kotova, T.I., Higgs, H.N., Hazelwood, L., Hanein, D., Gertler, F.B. and Schafer, D.A. (2005) Ena/VASP proteins enhance actin polymerization in the presence of barbed end capping proteins. *J Biol Chem*, **280**, 28653-28662.
- Bear, J.E., Krause, M. and Gertler, F.B. (2001) Regulating cellular actin assembly. *Curr Opin Cell Biol*, **13**, 158-166.

- Bear, J.E., Loureiro, J.J., Libova, I., Fassler, R., Wehland, J. and Gertler, F.B. (2000) Negative regulation of fibroblast motility by Ena/VASP proteins. *Cell*, **101**, 717-728.
- Bear, J.E., Svitkina, T.M., Krause, M., Schafer, D.A., Loureiro, J.J., Strasser, G.A., Maly, I.V., Chaga, O.Y., Cooper, J.A., Borisy, G.G. and Gertler, F.B. (2002) Antagonism between Ena/VASP proteins and actin filament capping regulates fibroblast motility. *Cell*, **109**, 509-521.
- Beneken, J., Tu, J.C., Xiao, B., Nuriya, M., Yuan, J.P., Worley, P.F. and Leahy, D.J. (2000) Structure of the Homer EVH1 domain-peptide complex reveals a new twist in polyproline recognition. *Neuron*, **26**, 143-154.
- Blanchoin, L., Amann, K.J., Higgs, H.N., Marchand, J.B., Kaiser, D.A. and Pollard, T.D. (2000) Direct observation of dendritic actin filament networks nucleated by Arp2/3 complex and WASP/Scar proteins. *Nature*, **404**, 1007-1011.
- Boujemaa-Paterski, R., Gouin, E., Hansen, G., Samarin, S., Le Clainche, C., Didry, D., Dehoux, P., Cossart, P., Kocks, C., Carlier, M.F. and Pantaloni, D. (2001) Listeria protein ActA mimics WASp family proteins: it activates filament barbed end branching by Arp2/3 complex. *Biochemistry*, **40**, 11390-11404.
- Bradford, M.M. (1976) A rapid and sensitive method for the quantitation of microgram quantities of protein utilizing the principle of protein-dye binding. *Anal Biochem*, **72**, 248-254.
- Braun, A., Aszodi, A., Hellebrand, H., Berna, A., Fassler, R. and Brandau, O. (2002) Genomic organization of profilin-III and evidence for a transcript expressed exclusively in testis. *Gene*, **283**, 219-225.
- Bryan, J. and Kurth, M.C. (1984) Actin-gelsolin interactions. Evidence for two actin-binding sites. *J Biol Chem*, **259**, 7480-7487.
- Carlier, M.F., Pantaloni, D. and Korn, E.D. (1986) The effects of Mg²⁺ at the high-affinity and low-affinity sites on the polymerization of actin and associated ATP hydrolysis. *J Biol Chem*, **261**, 10785-10792.
- Carlsson, L., Nystrom, L.E., Sundkvist, I., Markey, F. and Lindberg, U. (1977) Actin polymerizability is influenced by profilin, a low molecular weight protein in non-muscle cells. *J Mol Biol*, **115**, 465-483.
- Chakraborty, T., Ebel, F., Domann, E., Niebuhr, K., Gerstel, B., Pistor, S., Temm-Grove, C.J., Jockusch, B.M., Reinhard, M., Walter, U. and et al. (1995) A focal adhesion factor directly linking intracellularly motile *Listeria monocytogenes* and *Listeria ivanovii* to the actin-based cytoskeleton of mammalian cells. *Embo J*, **14**, 1314-1321.
- Chang, F., Drubin, D. and Nurse, P. (1997) cdc12p, a protein required for cytokinesis in fission yeast, is a component of the cell division ring and interacts with profilin. *J Cell Biol*, **137**, 169-182.

- Chenna, R., Sugawara, H., Koike, T., Lopez, R., Gibson, T.J., Higgins, D.G. and Thompson, J.D. (2003) Multiple sequence alignment with the Clustal series of programs. *Nucleic Acids Res*, **31**, 3497-3500.
- Cheung, W.L., Ajiro, K., Samejima, K., Kloc, M., Cheung, P., Mizzen, C.A., Beeser, A., Etkin, L.D., Chernoff, J., Earnshaw, W.C. and Allis, C.D. (2003) Apoptotic phosphorylation of histone H2B is mediated by mammalian sterile twenty kinase. *Cell*, **113**, 507-517.
- Chisholm, R.L. and Firtel, R.A. (2004) Insights into morphogenesis from a simple developmental system. *Nat Rev Mol Cell Biol*, **5**, 531-541.
- Christensen, H.E., Ramachandran, S., Tan, C.T., Surana, U., Dong, C.H. and Chua, N.H. (1996) Arabidopsis profilins are functionally similar to yeast profilins: identification of a vascular bundle-specific profilin and a pollen-specific profilin. *Plant J*, **10**, 269-279.
- Chung, C.Y. and Firtel, R.A. (1999) PAKa, a putative PAK family member, is required for cytokinesis and the regulation of the cytoskeleton in Dictyostelium discoideum cells during chemotaxis. *J Cell Biol*, **147**, 559-576.
- Comer, A.R., Ahern-Djamali, S.M., Juang, J.L., Jackson, P.D. and Hoffmann, F.M. (1998) Phosphorylation of Enabled by the Drosophila Abelson tyrosine kinase regulates the in vivo function and protein-protein interactions of Enabled. *Mol Cell Biol*, **18**, 152-160.
- Coppolino, M.G., Krause, M., Hagendorff, P., Monner, D.A., Trimble, W., Grinstein, S., Wehland, J. and Sechi, A.S. (2001) Evidence for a molecular complex consisting of Fyb/SLAP, SLP-76, Nck, VASP and WASP that links the actin cytoskeleton to Fcgamma receptor signalling during phagocytosis. *J Cell Sci*, **114**, 4307-4318.
- Corpet, F. (1988) Multiple sequence alignment with hierarchical clustering. *Nucleic Acids Res*, **16**, 10881-10890.
- Creasy, C.L., Ambrose, D.M. and Chernoff, J. (1996) The Ste20-like protein kinase, Mst1, dimerizes and contains an inhibitory domain. *J Biol Chem*, **271**, 21049-21053.
- Creasy, C.L. and Chernoff, J. (1995a) Cloning and characterization of a human protein kinase with homology to Ste20. *J Biol Chem*, **270**, 21695-21700.
- Creasy, C.L. and Chernoff, J. (1995b) Cloning and characterization of a member of the MST subfamily of Ste20-like kinases. *Gene*, **167**, 303-306.
- Dan, I., Ong, S.E., Watanabe, N.M., Blagoev, B., Nielsen, M.M., Kajikawa, E., Kristiansen, T.Z., Mann, M. and Pandey, A. (2002) Cloning of MASK, a novel member of the mammalian germinal center kinase III subfamily, with apoptosis-inducing properties. *J Biol Chem*, **277**, 5929-5939.
- Dan, I., Watanabe, N.M. and Kusumi, A. (2001) The Ste20 group kinases as regulators of MAP kinase cascades. *Trends Cell Biol*, **11**, 220-230.

- Darcy, P.K., Wilczynska, Z. and Fisher, P.R. (1994) The role of cGMP in photosensory and thermosensory transduction in *Dictyostelium discoideum*. *Microbiology*, **140** (Pt 7), 1619-1632.
- de Hostos, E.L., Rehfuess, C., Bradtke, B., Waddell, D.R., Albrecht, R., Murphy, J. and Gerisch, G. (1993) *Dictyostelium* mutants lacking the cytoskeletal protein coronin are defective in cytokinesis and cell motility. *J Cell Biol*, **120**, 163-173.
- Deng, Y., Pang, A. and Wang, J.H. (2003) Regulation of mammalian STE20-like kinase 2 (MST2) by protein phosphorylation/dephosphorylation and proteolysis. *J Biol Chem*, **278**, 11760-11767.
- Dong, J., Radau, B., Otto, A., Muller, E., Lindschau, C. and Westermann, P. (2000) Profilin I attached to the Golgi is required for the formation of constitutive transport vesicles at the trans-Golgi network. *Biochim Biophys Acta*, **1497**, 253-260.
- dos Remedios, C.G., Chhabra, D., Kekic, M., Dedova, I.V., Tsubakihara, M., Berry, D.A. and Nosworthy, N.J. (2003) Actin binding proteins: regulation of cytoskeletal microfilaments. *Physiol Rev*, **83**, 433-473.
- Drogen, F., O'Rourke, S.M., Stucke, V.M., Jaquenoud, M., Neiman, A.M. and Peter, M. (2000) Phosphorylation of the MEKK Ste11p by the PAK-like kinase Ste20p is required for MAP kinase signaling in vivo. *Curr Biol*, **10**, 630-639.
- Dumontier, M., Hocht, P., Mintert, U. and Faix, J. (2000) Rac1 GTPases control filopodia formation, cell motility, endocytosis, cytokinesis and development in *Dictyostelium*. *J Cell Sci*, **113** (Pt 12), 2253-2265.
- Edamatsu, M., Hirono, M. and Watanabe, Y. (1992) Tetrahymena profilin is localized in the division furrow. *J Biochem (Tokyo)*, **112**, 637-642.
- Edgar, B.A. (2006) From cell structure to transcription: hippo forges a new path. *Cell*, **124**, 267-273.
- Edmunds, J.W. and Mahadevan, L.C. (2004) MAP kinases as structural adaptors and enzymatic activators in transcription complexes. *J Cell Sci*, **117**, 3715-3723.
- Eichinger, L., Bahler, M., Dietz, M., Eckerskorn, C. and Schleicher, M. (1998) Characterization and cloning of a *Dictyostelium* Ste20-like protein kinase that phosphorylates the actin-binding protein severin. *J Biol Chem*, **273**, 12952-12959.
- Eichinger, L., Noegel, A.A. and Schleicher, M. (1991) Domain structure in actin-binding proteins: expression and functional characterization of truncated severin. *J Cell Biol*, **112**, 665-676.
- Eichinger, L., Pachebat, J.A., Glockner, G., Rajandream, M.A., Sugang, R., Berriman, M., Song, J., Olsen, R., Szafranski, K., Xu, Q., Tunggal, B., Kummerfeld, S., Madera, M., Konfortov, B.A., Rivero, F., Bankier, A.T., Lehmann, R., Hamlin, N., Davies, R., Gaudet, P., Fey, P., Pilcher, K., Chen, G., Saunders, D., Sodergren, E.,

- Davis, P., Kerhornou, A., Nie, X., Hall, N., Anjard, C., Hemphill, L., Bason, N., Farbrother, P., Desany, B., Just, E., Morio, T., Rost, R., Churcher, C., Cooper, J., Haydock, S., van Driessche, N., Cronin, A., Goodhead, I., Muzny, D., Mourier, T., Pain, A., Lu, M., Harper, D., Lindsay, R., Hauser, H., James, K., Quiles, M., Madan Babu, M., Saito, T., Buchrieser, C., Wardroper, A., Felder, M., Thangavelu, M., Johnson, D., Knights, A., Loulseged, H., Mungall, K., Oliver, K., Price, C., Quail, M.A., Urushihara, H., Hernandez, J., Rabbinowitsch, E., Steffen, D., Sanders, M., Ma, J., Kohara, Y., Sharp, S., Simmonds, M., Spiegler, S., Tivey, A., Sugano, S., White, B., Walker, D., Woodward, J., Winckler, T., Tanaka, Y., Shaulsky, G., Schleicher, M., Weinstock, G., Rosenthal, A., Cox, E.C., Chisholm, R.L., Gibbs, R., Loomis, W.F., Platzer, M., Kay, R.R., Williams, J., Dear, P.H., Noegel, A.A., Barrell, B. and Kuspa, A. (2005) The genome of the social amoeba *Dictyostelium discoideum*. *Nature*, **435**, 43-57.
- Engqvist-Goldstein, A.E. and Drubin, D.G. (2003) Actin assembly and endocytosis: from yeast to mammals. *Annu Rev Cell Dev Biol*, **19**, 287-332.
- Evangelista, M., Pruyne, D., Amberg, D.C., Boone, C. and Bretscher, A. (2002) Formins direct Arp2/3-independent actin filament assembly to polarize cell growth in yeast. *Nat Cell Biol*, **4**, 260-269.
- Evangelista, M., Zigmond, S. and Boone, C. (2003) Formins: signaling effectors for assembly and polarization of actin filaments. *J Cell Sci*, **116**, 2603-2611.
- Faix, J., Gerisch, G. and Noegel, A.A. (1992) Overexpression of the csA cell adhesion molecule under its own cAMP-regulated promoter impairs morphogenesis in *Dictyostelium*. *J Cell Sci*, **102 (Pt 2)**, 203-214.
- Faix, J., Kreppel, L., Shaulsky, G., Schleicher, M. and Kimmel, A.R. (2004) A rapid and efficient method to generate multiple gene disruptions in *Dictyostelium discoideum* using a single selectable marker and the Cre-loxP system. *Nucleic Acids Res*, **32**, e143.
- Faix, J., Steinmetz, M., Boves, H., Kammerer, R.A., Lottspeich, F., Mintert, U., Murphy, J., Stock, A., Aebi, U. and Gerisch, G. (1996) Cortexillins, major determinants of cell shape and size, are actin-bundling proteins with a parallel coiled-coil tail. *Cell*, **86**, 631-642.
- Fedorov, A.A., Fedorov, E., Gertler, F. and Almo, S.C. (1999) Structure of EVH1, a novel proline-rich ligand-binding module involved in cytoskeletal dynamics and neural function. *Nat Struct Biol*, **6**, 661-665.
- Fedorov, A.A., Magnus, K.A., Graupe, M.H., Lattman, E.E., Pollard, T.D. and Almo, S.C. (1994) X-ray structures of isoforms of the actin-binding protein profilin that differ in their affinity for phosphatidylinositol phosphates. *Proc Natl Acad Sci U S A*, **91**, 8636-8640.
- Finger, F.P. and Novick, P. (1997) Sec3p is involved in secretion and morphogenesis in *Saccharomyces cerevisiae*. *Mol Biol Cell*, **8**, 647-662.

- Fisher, P.R., Noegel, A.A., Fechheimer, M., Rivero, F., Prassler, J. and Gerisch, G. (1997) Photosensory and thermosensory responses in Dictyostelium slugs are specifically impaired by absence of the F-actin cross-linking gelation factor (ABP-120). *Curr Biol*, **7**, 889-892.
- Fukui, Y. and Inoue, S. (1991) Cell division in Dictyostelium with special emphasis on actomyosin organization in cytokinesis. *Cell Motil Cytoskeleton*, **18**, 41-54.
- Fukuoka, M., Suetsugu, S., Miki, H., Fukami, K., Endo, T. and Takenawa, T. (2001) A novel neural Wiskott-Aldrich syndrome protein (N-WASP) binding protein, WISH, induces Arp2/3 complex activation independent of Cdc42. *J Cell Biol*, **152**, 471-482.
- Gareus, R., Di Nardo, A., Rybin, V. and Witke, W. (2006) Mouse profilin 2 regulates endocytosis and competes with SH3 ligand binding to dynamin 1. *J Biol Chem*, **281**, 2803-2811.
- Geese, M., Loureiro, J.J., Bear, J.E., Wehland, J., Gertler, F.B. and Sechi, A.S. (2002) Contribution of Ena/VASP proteins to intracellular motility of listeria requires phosphorylation and proline-rich core but not F-actin binding or multimerization. *Mol Biol Cell*, **13**, 2383-2396.
- Geese, M., Schluter, K., Rothkegel, M., Jockusch, B.M., Wehland, J. and Sechi, A.S. (2000) Accumulation of profilin II at the surface of Listeria is concomitant with the onset of motility and correlates with bacterial speed. *J Cell Sci*, **113 (Pt 8)**, 1415-1426.
- Gerisch, G. (1987) Cyclic AMP and other signals controlling cell development and differentiation in Dictyostelium. *Annu Rev Biochem*, **56**, 853-879.
- Gerisch, G. and Keller, H.U. (1981) Chemotactic reorientation of granulocytes stimulated with micropipettes containing fMet-Leu-Phe. *J Cell Sci*, **52**, 1-10.
- Gertler, F.B., Comer, A.R., Juang, J.L., Ahern, S.M., Clark, M.J., Liebl, E.C. and Hoffmann, F.M. (1995) enabled, a dosage-sensitive suppressor of mutations in the Drosophila Abl tyrosine kinase, encodes an Abl substrate with SH3 domain-binding properties. *Genes Dev*, **9**, 521-533.
- Gertler, F.B., Doctor, J.S. and Hoffmann, F.M. (1990) Genetic suppression of mutations in the Drosophila abl proto-oncogene homolog. *Science*, **248**, 857-860.
- Gertler, F.B., Niebuhr, K., Reinhard, M., Wehland, J. and Soriano, P. (1996) Mena, a relative of VASP and Drosophila Enabled, is implicated in the control of microfilament dynamics. *Cell*, **87**, 227-239.
- Gibbon, B.C., Ren, H. and Staiger, C.J. (1997) Characterization of maize (*Zea mays*) pollen profilin function in vitro and in live cells. *Biochem J*, **327 (Pt 3)**, 909-915.

- Glantschnig, H., Rodan, G.A. and Reszka, A.A. (2002) Mapping of MST1 kinase sites of phosphorylation. Activation and autophosphorylation. *J Biol Chem*, **277**, 42987-42996.
- Goldberg, J.M., Manning, G., Liu, A., Fey, P., Pilcher, K.E., Xu, Y. and Smith, J.L. (2006) The dictyostelium kinome--analysis of the protein kinases from a simple model organism. *PLoS Genet*, **2**, e38.
- Golstein, P., Aubry, L. and Levraud, J.P. (2003) Cell-death alternative model organisms: why and which? *Nat Rev Mol Cell Biol*, **4**, 798-807.
- Grosse, R., Copeland, J.W., Newsome, T.P., Way, M. and Treisman, R. (2003) A role for VASP in RhoA-Diaphanous signalling to actin dynamics and SRF activity. *Embo J*, **22**, 3050-3061.
- Guertin, D.A., Trautmann, S. and McCollum, D. (2002a) Cytokinesis in eukaryotes. *Microbiol Mol Biol Rev*, **66**, 155-178.
- Guertin, D.A., Venkatram, S., Gould, K.L. and McCollum, D. (2002b) Dma1 prevents mitotic exit and cytokinesis by inhibiting the septation initiation network (SIN). *Dev Cell*, **3**, 779-790.
- Halliburton, W.D. (1887) On muscle plasma. *J. Physiol*, **8**.
- Han, Y.H., Chung, C.Y., Wessels, D., Stephens, S., Titus, M.A., Soll, D.R. and Firtel, R.A. (2002) Requirement of a vasodilator-stimulated phosphoprotein family member for cell adhesion, the formation of filopodia, and chemotaxis in dictyostelium. *J Biol Chem*, **277**, 49877-49887.
- Hanks, S.K. and Hunter, T. (1995) Protein kinases 6. The eukaryotic protein kinase superfamily: kinase (catalytic) domain structure and classification. *Faseb J*, **9**, 576-596.
- Harbeck, B., Huttelmaier, S., Schluter, K., Jockusch, B.M. and Illenberger, S. (2000) Phosphorylation of the vasodilator-stimulated phosphoprotein regulates its interaction with actin. *J Biol Chem*, **275**, 30817-30825.
- Hartmann, H., Noegel, A.A., Eckerskorn, C., Rapp, S. and Schleicher, M. (1989) Ca²⁺-independent F-actin capping proteins. Cap 32/34, a capping protein from Dictyostelium discoideum, does not share sequence homologies with known actin-binding proteins. *J Biol Chem*, **264**, 12639-12647.
- Harvey, K.F., Pflieger, C.M. and Hariharan, I.K. (2003) The Drosophila Mst ortholog, hippo, restricts growth and cell proliferation and promotes apoptosis. *Cell*, **114**, 457-467.
- Haugwitz, M., Noegel, A.A., Karakesisoglou, J. and Schleicher, M. (1994) Dictyostelium amoebae that lack G-actin-sequestering profilins show defects in F-actin content, cytokinesis, and development. *Cell*, **79**, 303-314.

- Haugwitz, M., Noegel, A.A., Rieger, D., Lottspeich, F. and Schleicher, M. (1991) Dictyostelium discoideum contains two profilin isoforms that differ in structure and function. *J Cell Sci*, **100 (Pt 3)**, 481-489.
- Hay, B.A. and Guo, M. (2003) Coupling cell growth, proliferation, and death. Hippo weighs in. *Dev Cell*, **5**, 361-363.
- Higashida, C., Miyoshi, T., Fujita, A., Ocegüera-Yanez, F., Monypenny, J., Andou, Y., Narumiya, S. and Watanabe, N. (2004) Actin polymerization-driven molecular movement of mDia1 in living cells. *Science*, **303**, 2007-2010.
- Higgs, H.N. (2005) Formin proteins: a domain-based approach. *Trends Biochem Sci*, **30**, 342-353.
- Hofmann, C., Shepelev, M. and Chernoff, J. (2004) The genetics of Pak. *J Cell Sci*, **117**, 4343-4354.
- Holmes, D.S. and Quigley, M. (1981) A rapid boiling method for the preparation of bacterial plasmids. *Anal Biochem*, **114**, 193-197.
- Holt, M.R., Critchley, D.R. and Brindle, N.P. (1998) The focal adhesion phosphoprotein, VASP. *Int J Biochem Cell Biol*, **30**, 307-311.
- Hug, C., Jay, P.Y., Reddy, I., McNally, J.G., Bridgman, P.C., Elson, E.L. and Cooper, J.A. (1995) Capping protein levels influence actin assembly and cell motility in dictyostelium. *Cell*, **81**, 591-600.
- Huttelmaier, S., Harbeck, B., Steffens, O., Messerschmidt, T., Illenberger, S. and Jockusch, B.M. (1999) Characterization of the actin binding properties of the vasodilator-stimulated phosphoprotein VASP. *FEBS Lett*, **451**, 68-74.
- Janmey, P.A., Chaponnier, C., Lind, S.E., Zaner, K.S., Stossel, T.P. and Yin, H.L. (1985) Interactions of gelsolin and gelsolin-actin complexes with actin. Effects of calcium on actin nucleation, filament severing, and end blocking. *Biochemistry*, **24**, 3714-3723.
- Kaiser, D.A., Vinson, V.K., Murphy, D.B. and Pollard, T.D. (1999) Profilin is predominantly associated with monomeric actin in Acanthamoeba. *J Cell Sci*, **112 (Pt 21)**, 3779-3790.
- Kandasamy, M.K., McKinney, E.C. and Meagher, R.B. (2002) Plant profilin isovariants are distinctly regulated in vegetative and reproductive tissues. *Cell Motil Cytoskeleton*, **52**, 22-32.
- Karakesisoglou, I., Janssen, K.P., Eichinger, L., Noegel, A.A. and Schleicher, M. (1999) Identification of a suppressor of the Dictyostelium profilin-minus phenotype as a CD36/LIMP-II homologue. *J Cell Biol*, **145**, 167-181.

- Karakesisoglou, I., Schleicher, M., Gibbon, B.C. and Staiger, C.J. (1996) Plant profilins rescue the aberrant phenotype of profilin-deficient *Dictyostelium* cells. *Cell Motil Cytoskeleton*, **34**, 36-47.
- Kobielak, A., Pasolli, H.A. and Fuchs, E. (2004) Mammalian formin-1 participates in adherens junctions and polymerization of linear actin cables. *Nat Cell Biol*, **6**, 21-30.
- Kosta, A., Roisin-Bouffay, C., Luciani, M.F., Otto, G.P., Kessin, R.H. and Golstein, P. (2004) Autophagy gene disruption reveals a non-vacuolar cell death pathway in *Dictyostelium*. *J Biol Chem*, **279**, 48404-48409.
- Kouyama, T. and Mihashi, K. (1981) Fluorimetry study of N-(1-pyrenyl)iodoacetamide-labelled F-actin. Local structural change of actin protomer both on polymerization and on binding of heavy meromyosin. *Eur J Biochem*, **114**, 33-38.
- Kovar, D.R. (2006) Molecular details of formin-mediated actin assembly. *Curr Opin Cell Biol*, **18**, 11-17.
- Kovar, D.R., Harris, E.S., Mahaffy, R., Higgs, H.N. and Pollard, T.D. (2006) Control of the assembly of ATP- and ADP-actin by formins and profilin. *Cell*, **124**, 423-435.
- Krause, M., Sechi, A.S., Konradt, M., Monner, D., Gertler, F.B. and Wehland, J. (2000) Fyn-binding protein (Fyb)/SLP-76-associated protein (SLAP), Ena/vasodilator-stimulated phosphoprotein (VASP) proteins and the Arp2/3 complex link T cell receptor (TCR) signaling to the actin cytoskeleton. *J Cell Biol*, **149**, 181-194.
- Kwiatkowski, A.V., Gertler, F.B. and Loureiro, J.J. (2003) Function and regulation of Ena/VASP proteins. *Trends Cell Biol*, **13**, 386-392.
- Kyriakis, J.M. (1999) Signaling by the germinal center kinase family of protein kinases. *J Biol Chem*, **274**, 5259-5262.
- Laemmli, U.K. (1970) Cleavage of structural proteins during the assembly of the head of bacteriophage T4. *Nature*, **227**, 680-685.
- Lambrechts, A., Kwiatkowski, A.V., Lanier, L.M., Bear, J.E., Vandekerckhove, J., Ampe, C. and Gertler, F.B. (2000) cAMP-dependent protein kinase phosphorylation of EVL, a Mena/VASP relative, regulates its interaction with actin and SH3 domains. *J Biol Chem*, **275**, 36143-36151.
- Lanier, L.M., Gates, M.A., Witke, W., Menzies, A.S., Wehman, A.M., Macklis, J.D., Kwiatkowski, D., Soriano, P. and Gertler, F.B. (1999) Mena is required for neurulation and commissure formation. *Neuron*, **22**, 313-325.
- Laurent, V., Loisel, T.P., Harbeck, B., Wehman, A., Grobe, L., Jockusch, B.M., Wehland, J., Gertler, F.B. and Carlier, M.F. (1999) Role of proteins of the Ena/VASP family in actin-based motility of *Listeria monocytogenes*. *J Cell Biol*, **144**, 1245-1258.

- Lee, S., Rivero, F., Park, K.C., Huang, E., Funamoto, S. and Firtel, R.A. (2004a) Dictyostelium PAKc is required for proper chemotaxis. *Mol Biol Cell*, **15**, 5456-5469.
- Lee, W.S., Hsu, C.Y., Wang, P.L., Huang, C.Y., Chang, C.H. and Yuan, C.J. (2004b) Identification and characterization of the nuclear import and export signals of the mammalian Ste20-like protein kinase 3. *FEBS Lett*, **572**, 41-45.
- Loomis, W.F. (1996) Genetic networks that regulate development in Dictyostelium cells. *Microbiol Rev*, **60**, 135-150.
- Lu, J. and Pollard, T.D. (2001) Profilin binding to poly-L-proline and actin monomers along with ability to catalyze actin nucleotide exchange is required for viability of fission yeast. *Mol Biol Cell*, **12**, 1161-1175.
- Machesky, L.M., Atkinson, S.J., Ampe, C., Vandekerckhove, J. and Pollard, T.D. (1994a) Purification of a cortical complex containing two unconventional actins from *Acanthamoeba* by affinity chromatography on profilin-agarose. *J Cell Biol*, **127**, 107-115.
- Machesky, L.M., Cole, N.B., Moss, B. and Pollard, T.D. (1994b) Vaccinia virus expresses a novel profilin with a higher affinity for polyphosphoinositides than actin. *Biochemistry*, **33**, 10815-10824.
- Mah, A.S., Jang, J. and Deshaies, R.J. (2001) Protein kinase Cdc15 activates the Dbf2-Mob1 kinase complex. *Proc Natl Acad Sci U S A*, **98**, 7325-7330.
- Mahoney, N.M., Janmey, P.A. and Almo, S.C. (1997) Structure of the profilin-poly-L-proline complex involved in morphogenesis and cytoskeletal regulation. *Nat Struct Biol*, **4**, 953-960.
- Maniak, M., Rauchenberger, R., Albrecht, R., Murphy, J. and Gerisch, G. (1995) Coronin involved in phagocytosis: dynamics of particle-induced relocalization visualized by a green fluorescent protein Tag. *Cell*, **83**, 915-924.
- Marchand, J.B., Moreau, P., Paoletti, A., Cossart, P., Carlier, M.F. and Pantaloni, D. (1995) Actin-based movement of *Listeria monocytogenes*: actin assembly results from the local maintenance of uncapped filament barbed ends at the bacterium surface. *J Cell Biol*, **130**, 331-343.
- Mejillano, M.R., Kojima, S., Applewhite, D.A., Gertler, F.B., Svitkina, T.M. and Borisy, G.G. (2004) Lamellipodial versus filopodial mode of the actin nanomachinery: pivotal role of the filament barbed end. *Cell*, **118**, 363-373.
- Metzler, W.J., Farmer, B.T., 2nd, Constantine, K.L., Friedrichs, M.S., Lavoie, T. and Mueller, L. (1995) Refined solution structure of human profilin I. *Protein Sci*, **4**, 450-459.

- Muller-Taubenberger, A., Bretschneider, T., Faix, J., Konzok, A., Simmeth, E. and Weber, I. (2002) Differential localization of the Dictyostelium kinase DPAKa during cytokinesis and cell migration. *J Muscle Res Cell Motil*, **23**, 751-763.
- Mykkanen, O.M., Gronholm, M., Ronty, M., Lalowski, M., Salmikangas, P., Suila, H. and Carpen, O. (2001) Characterization of human palladin, a microfilament-associated protein. *Mol Biol Cell*, **12**, 3060-3073.
- Nachmias, V.T. (1993) Small actin-binding proteins: the beta-thymosin family. *Curr Opin Cell Biol*, **5**, 56-62.
- Nezami, A.G., Poy, F. and Eck, M.J. (2006) Structure of the autoinhibitory switch in formin mDia1. *Structure*, **14**, 257-263.
- Niebuhr, K., Ebel, F., Frank, R., Reinhard, M., Domann, E., Carl, U.D., Walter, U., Gertler, F.B., Wehland, J. and Chakraborty, T. (1997) A novel proline-rich motif present in ActA of *Listeria monocytogenes* and cytoskeletal proteins is the ligand for the EVH1 domain, a protein module present in the Ena/VASP family. *Embo J*, **16**, 5433-5444.
- Nishida, E., Maekawa, S., Muneyuki, E. and Sakai, H. (1984) Action of a 19K protein from porcine brain on actin polymerization: a new functional class of actin-binding proteins. *J Biochem (Tokyo)*, **95**, 387-398.
- Nodelman, I.M., Bowman, G.D., Lindberg, U. and Schutt, C.E. (1999) X-ray structure determination of human profilin II: A comparative structural analysis of human profilins. *J Mol Biol*, **294**, 1271-1285.
- Noegel, A.A. and Schleicher, M. (2000) The actin cytoskeleton of Dictyostelium: a story told by mutants. *J Cell Sci*, **113 (Pt 5)**, 759-766.
- O'Neill, E. and Kolch, W. (2005) Taming the Hippo: Raf-1 controls apoptosis by suppressing MST2/Hippo. *Cell Cycle*, **4**, 365-367.
- O'Neill, E., Rushworth, L., Baccarini, M. and Kolch, W. (2004) Role of the kinase MST2 in suppression of apoptosis by the proto-oncogene product Raf-1. *Science*, **306**, 2267-2270.
- O'Neill, E.E., Matallanas, D. and Kolch, W. (2005) Mammalian sterile 20-like kinases in tumor suppression: an emerging pathway. *Cancer Res*, **65**, 5485-5487.
- Otomo, T., Tomchick, D.R., Otomo, C., Panchal, S.C., Machius, M. and Rosen, M.K. (2005) Structural basis of actin filament nucleation and processive capping by a formin homology 2 domain. *Nature*, **433**, 488-494.
- Pantalacci, S., Tapon, N. and Leopold, P. (2003) The Salvador partner Hippo promotes apoptosis and cell-cycle exit in *Drosophila*. *Nat Cell Biol*, **5**, 921-927.
- Parast, M.M. and Otey, C.A. (2000) Characterization of palladin, a novel protein localized to stress fibers and cell adhesions. *J Cell Biol*, **150**, 643-656.

- Pardee, J.D. and Spudich, J.A. (1982) Purification of muscle actin. *Methods Cell Biol*, **24**, 271-289.
- Pellegrin, S. and Mellor, H. (2005) The Rho family GTPase Rif induces filopodia through mDia2. *Curr Biol*, **15**, 129-133.
- Peng, J., Wallar, B.J., Flanders, A., Swiatek, P.J. and Alberts, A.S. (2003) Disruption of the Diaphanous-related formin Drf1 gene encoding mDia1 reveals a role for Drf3 as an effector for Cdc42. *Curr Biol*, **13**, 534-545.
- Pollard, T.D. and Borisy, G.G. (2003) Cellular motility driven by assembly and disassembly of actin filaments. *Cell*, **112**, 453-465.
- Pollard, T.D. and Cooper, J.A. (1986) Actin and actin-binding proteins. A critical evaluation of mechanisms and functions. *Annu Rev Biochem*, **55**, 987-1035.
- Popowicz, G.M., Schleicher, M., Noegel, A.A. and Holak, T.A. (2006) Filamins: promiscuous organizers of the cytoskeleton. *Trends Biochem Sci*, **31**, 411-419.
- Prassler, J., Stocker, S., Marriott, G., Heidecker, M., Kellermann, J. and Gerisch, G. (1997) Interaction of a Dictyostelium member of the plastin/fimbrin family with actin filaments and actin-myosin complexes. *Mol Biol Cell*, **8**, 83-95.
- Prehoda, K.E., Lee, D.J. and Lim, W.A. (1999) Structure of the enabled/VASP homology 1 domain-peptide complex: a key component in the spatial control of actin assembly. *Cell*, **97**, 471-480.
- Pruyne, D., Evangelista, M., Yang, C., Bi, E., Zigmond, S., Bretscher, A. and Boone, C. (2002) Role of formins in actin assembly: nucleation and barbed-end association. *Science*, **297**, 612-615.
- Qian, C., Zhang, Q., Wang, X., Zeng, L., Farooq, A. and Zhou, M.M. (2005) Structure of the adaptor protein p14 reveals a profilin-like fold with distinct function. *J Mol Biol*, **347**, 309-321.
- Reinhard, M., Giehl, K., Abel, K., Haffner, C., Jarchau, T., Hoppe, V., Jockusch, B.M. and Walter, U. (1995) The proline-rich focal adhesion and microfilament protein VASP is a ligand for profilins. *Embo J*, **14**, 1583-1589.
- Reinhard, M., Halbrugge, M., Scheer, U., Wiegand, C., Jockusch, B.M. and Walter, U. (1992) The 46/50 kDa phosphoprotein VASP purified from human platelets is a novel protein associated with actin filaments and focal contacts. *Embo J*, **11**, 2063-2070.
- Reinhard, M., Jarchau, T. and Walter, U. (2001) Actin-based motility: stop and go with Ena/VASP proteins. *Trends Biochem Sci*, **26**, 243-249.
- Renfranz, P.J. and Beckerle, M.C. (2002) Doing (F/L)PPPPs: EVH1 domains and their proline-rich partners in cell polarity and migration. *Curr Opin Cell Biol*, **14**, 88-103.

- Rothkegel, M., Mayboroda, O., Rohde, M., Wucherpennig, C., Valenta, R. and Jockusch, B.M. (1996) Plant and animal profilins are functionally equivalent and stabilize microfilaments in living animal cells. *J Cell Sci*, **109** (Pt 1), 83-90.
- Rottner, K., Behrendt, B., Small, J.V. and Wehland, J. (1999) VASP dynamics during lamellipodia protrusion. *Nat Cell Biol*, **1**, 321-322.
- Ryoo, H.D. and Steller, H. (2003) Hippo and its mission for growth control. *Nat Cell Biol*, **5**, 853-855.
- Samarin, S., Romero, S., Kocks, C., Didry, D., Pantaloni, D. and Carlier, M.F. (2003) How VASP enhances actin-based motility. *J Cell Biol*, **163**, 131-142.
- Sambrook, J. and Russell, D.W. (2001) *Molecular Cloning*. Cold Spring Harbor Laboratory Press.
- Sawin, K.E. (2002) Cell polarity: following formin function. *Curr Biol*, **12**, R6-8.
- Scheel, H. and Hofmann, K. (2003) A novel interaction motif, SARAH, connects three classes of tumor suppressor. *Curr Biol*, **13**, R899-900.
- Schirenbeck, A., Arasada, R., Bretschneider, T., Stradal, T.E., Schleicher, M. and Faix, J. (2006) The bundling activity of vasodilator-stimulated phosphoprotein is required for filopodium formation. *Proc Natl Acad Sci U S A*, **103**, 7694-7699.
- Schirenbeck, A., Bretschneider, T., Arasada, R., Schleicher, M. and Faix, J. (2005) The Diaphanous-related formin dDia2 is required for the formation and maintenance of filopodia. *Nat Cell Biol*, **7**, 619-625.
- Schleicher, M., Andre, B., Andreoli, C., Eichinger, L., Haugwitz, M., Hofmann, A., Karakesisoglou, J., Stockelhuber, M. and Noegel, A.A. (1995) Structure/function studies on cytoskeletal proteins in Dictyostelium amoebae as a paradigm. *FEBS Lett*, **369**, 38-42.
- Schleicher, M., Gerisch, G. and Isenberg, G. (1984) New actin-binding proteins from Dictyostelium discoideum. *Embo J*, **3**, 2095-2100.
- Schutt, C.E., Myslik, J.C., Rozycki, M.D., Goonesekere, N.C. and Lindberg, U. (1993) The structure of crystalline profilin-beta-actin. *Nature*, **365**, 810-816.
- Skoble, J., Auerbuch, V., Goley, E.D., Welch, M.D. and Portnoy, D.A. (2001) Pivotal role of VASP in Arp2/3 complex-mediated actin nucleation, actin branch-formation, and Listeria monocytogenes motility. *J Cell Biol*, **155**, 89-100.
- Skriwan, C., Fajardo, M., Hagele, S., Horn, M., Wagner, M., Michel, R., Krohne, G., Schleicher, M., Hacker, J. and Steinert, M. (2002) Various bacterial pathogens and symbionts infect the amoeba Dictyostelium discoideum. *Int J Med Microbiol*, **291**, 615-624.

- Smith, G.A., Theriot, J.A. and Portnoy, D.A. (1996) The tandem repeat domain in the *Listeria monocytogenes* ActA protein controls the rate of actin-based motility, the percentage of moving bacteria, and the localization of vasodilator-stimulated phosphoprotein and profilin. *J Cell Biol*, **135**, 647-660.
- Son, H.-J. (2003) Cloning and characterisation of a Dictyostelium STE20-like protein kinase DST2. *Cell Biology*. Ludwig Maximilians University, Munich, Vol. Ph. D.
- Spudich, J.A. and Watt, S. (1971) The regulation of rabbit skeletal muscle contraction. I. Biochemical studies of the interaction of the tropomyosin-troponin complex with actin and the proteolytic fragments of myosin. *J Biol Chem*, **246**, 4866-4871.
- Steffen, A., Faix, J., Resch, G.P., Linkner, J., Wehland, J., Small, J.V., Rottner, K. and Stradal, T.E. (2006) Filopodia formation in the absence of functional WAVE- and Arp2/3-complexes. *Mol Biol Cell*, **17**, 2581-2591.
- Stocker, S., Hiery, M. and Marriott, G. (1999) Phototactic migration of Dictyostelium cells is linked to a new type of gelsolin-related protein. *Mol Biol Cell*, **10**, 161-178.
- Stossel, T.P., Chaponnier, C., Ezzell, R.M., Hartwig, J.H., Janmey, P.A., Kwiatkowski, D.J., Lind, S.E., Smith, D.B., Southwick, F.S., Yin, H.L. and et al. (1985) Nonmuscle actin-binding proteins. *Annu Rev Cell Biol*, **1**, 353-402.
- Stossel, T.P., Condeelis, J., Cooley, L., Hartwig, J.H., Noegel, A., Schleicher, M. and Shapiro, S.S. (2001) Filamins as integrators of cell mechanics and signalling. *Nat Rev Mol Cell Biol*, **2**, 138-145.
- Suggs, S.V., Wallace, R.B., Hirose, T., Kawashima, E.H. and Itakura, K. (1981) Use of synthetic oligonucleotides as hybridization probes: isolation of cloned cDNA sequences for human beta 2-microglobulin. *Proc Natl Acad Sci U S A*, **78**, 6613-6617.
- Szent-Gyorgyi, A. (1945) Studies on muscle. *Acta Physiol Scandinav*, **9 (suppl. 25)**.
- Tamari, M., Daigo, Y. and Nakamura, Y. (1999) Isolation and characterization of a novel serine threonine kinase gene on chromosome 3p22-21.3. *J Hum Genet*, **44**, 116-120.
- Taylor, L.K., Wang, H.C. and Erikson, R.L. (1996) Newly identified stress-responsive protein kinases, Krs-1 and Krs-2. *Proc Natl Acad Sci U S A*, **93**, 10099-10104.
- Temesvari, L., Zhang, L., Fodera, B., Janssen, K.P., Schleicher, M. and Cardelli, J.A. (2000) Inactivation of ImpA, encoding a LIMPII-related endosomal protein, suppresses the internalization and endosomal trafficking defects in profilin-null mutants. *Mol Biol Cell*, **11**, 2019-2031.
- Thery, C., Boussac, M., Veron, P., Ricciardi-Castagnoli, P., Raposo, G., Garin, J. and Amigorena, S. (2001) Proteomic analysis of dendritic cell-derived exosomes: a secreted subcellular compartment distinct from apoptotic vesicles. *J Immunol*, **166**, 7309-7318.

- Towbin, H., Staehelin, T. and Gordon, J. (1979) Electrophoretic transfer of proteins from polyacrylamide gels to nitrocellulose sheets: procedure and some applications. *Proc Natl Acad Sci U S A*, **76**, 4350-4354.
- Ura, S., Masuyama, N., Graves, J.D. and Gotoh, Y. (2001) Caspase cleavage of MST1 promotes nuclear translocation and chromatin condensation. *Proc Natl Acad Sci U S A*, **98**, 10148-10153.
- Uren, A.G., O'Rourke, K., Aravind, L.A., Pisabarro, M.T., Seshagiri, S., Koonin, E.V. and Dixit, V.M. (2000) Identification of paracaspases and metacaspases: two ancient families of caspase-like proteins, one of which plays a key role in MALT lymphoma. *Mol Cell*, **6**, 961-967.
- Valenta, R., Ferreira, F., Grote, M., Swoboda, I., Vrtala, S., Duchene, M., Deviller, P., Meagher, R.B., McKinney, E., Heberle-Bors, E. and et al. (1993) Identification of profilin as an actin-binding protein in higher plants. *J Biol Chem*, **268**, 22777-22781.
- Vandekerckhove, J.S., Kaiser, D.A. and Pollard, T.D. (1989) Acanthamoeba actin and profilin can be cross-linked between glutamic acid 364 of actin and lysine 115 of profilin. *J Cell Biol*, **109**, 619-626.
- Vasioukhin, V. and Fuchs, E. (2001) Actin dynamics and cell-cell adhesion in epithelia. *Curr Opin Cell Biol*, **13**, 76-84.
- Vavylonis, D., Kovar, D.R., O'Shaughnessy, B. and Pollard, T.D. (2006) Model of formin-associated actin filament elongation. *Mol Cell*, **21**, 455-466.
- Verheyen, E.M. and Cooley, L. (1994) Profilin mutations disrupt multiple actin-dependent processes during Drosophila development. *Development*, **120**, 717-728.
- Vignjevic, D., Peloquin, J. and Borisy, G.G. (2006) In vitro assembly of filopodia-like bundles. *Methods Enzymol*, **406**, 727-739.
- Vignjevic, D., Yarar, D., Welch, M.D., Peloquin, J., Svitkina, T. and Borisy, G.G. (2003) Formation of filopodia-like bundles in vitro from a dendritic network. *J Cell Biol*, **160**, 951-962.
- Vinson, V.K., Archer, S.J., Lattman, E.E., Pollard, T.D. and Torchia, D.A. (1993) Three-dimensional solution structure of Acanthamoeba profilin-I. *J Cell Biol*, **122**, 1277-1283.
- Vinson, V.K., De La Cruz, E.M., Higgs, H.N. and Pollard, T.D. (1998) Interactions of Acanthamoeba profilin with actin and nucleotides bound to actin. *Biochemistry*, **37**, 10871-10880.
- Walders-Harbeck, B., Khaitlina, S.Y., Hinssen, H., Jockusch, B.M. and Illenberger, S. (2002) The vasodilator-stimulated phosphoprotein promotes actin polymerisation through direct binding to monomeric actin. *FEBS Lett*, **529**, 275-280.

- Waldmann, R., Nieberding, M. and Walter, U. (1987) Vasodilator-stimulated protein phosphorylation in platelets is mediated by cAMP- and cGMP-dependent protein kinases. *Eur J Biochem*, **167**, 441-448.
- Watabe, M., Kakeya, H., Onose, R. and Osada, H. (2000) Activation of MST/Krs and c-Jun N-terminal kinases by different signaling pathways during cytotrienin A-induced apoptosis. *J Biol Chem*, **275**, 8766-8771.
- Watanabe, N., Madaule, P., Reid, T., Ishizaki, T., Watanabe, G., Kakizuka, A., Saito, Y., Nakao, K., Jockusch, B.M. and Narumiya, S. (1997) p140mDia, a mammalian homolog of *Drosophila* diaphanous, is a target protein for Rho small GTPase and is a ligand for profilin. *Embo J*, **16**, 3044-3056.
- Welch, M.D., Iwamatsu, A. and Mitchison, T.J. (1997) Actin polymerization is induced by Arp2/3 protein complex at the surface of *Listeria monocytogenes*. *Nature*, **385**, 265-269.
- Wilkins, A., Khosla, M., Fraser, D.J., Spiegelman, G.B., Fisher, P.R., Weeks, G. and Insall, R.H. (2000) Dictyostelium RasD is required for normal phototaxis, but not differentiation. *Genes Dev*, **14**, 1407-1413.
- Williams, C., und Newell, G. (1976) A genetic study of aggregation in the cellular slime mold *Dictyostelium discoideum* using complementation analysis. *Genetics*, **82**, 287-307.
- Winter, D., Podtelejnikov, A.V., Mann, M. and Li, R. (1997) The complex containing actin-related proteins Arp2 and Arp3 is required for the motility and integrity of yeast actin patches. *Curr Biol*, **7**, 519-529.
- Witke, W., Li, W., Kwiatkowski, D.J. and Southwick, F.S. (2001a) Comparisons of CapG and gelsolin-null macrophages: demonstration of a unique role for CapG in receptor-mediated ruffling, phagocytosis, and vesicle rocketing. *J Cell Biol*, **154**, 775-784.
- Witke, W., Podtelejnikov, A.V., Di Nardo, A., Sutherland, J.D., Gurniak, C.B., Dotti, C. and Mann, M. (1998) In mouse brain profilin I and profilin II associate with regulators of the endocytic pathway and actin assembly. *Embo J*, **17**, 967-976.
- Witke, W., Schleicher, M., Lottspeich, F. and Noegel, A. (1986) Studies on the transcription, translation, and structure of alpha-actinin in *Dictyostelium discoideum*. *J Cell Biol*, **103**, 969-975.
- Witke, W., Sutherland, J.D., Sharpe, A., Arai, M. and Kwiatkowski, D.J. (2001b) Profilin I is essential for cell survival and cell division in early mouse development. *Proc Natl Acad Sci U S A*, **98**, 3832-3836.
- Wu, C., Whiteway, M., Thomas, D.Y. and Leberer, E. (1995) Molecular characterization of Ste20p, a potential mitogen-activated protein or extracellular signal-regulated kinase kinase (MEK) kinase kinase from *Saccharomyces cerevisiae*. *J Biol Chem*, **270**, 15984-15992.

- Wu, S., Huang, J., Dong, J. and Pan, D. (2003) hippo encodes a Ste-20 family protein kinase that restricts cell proliferation and promotes apoptosis in conjunction with salvador and warts. *Cell*, **114**, 445-456.
- Xu, W. (2006) A lock on formins. *Structure*, **14**, 168-169.
- Xu, Y., Moseley, J.B., Sagot, I., Poy, F., Pellman, D., Goode, B.L. and Eck, M.J. (2004) Crystal structures of a Formin Homology-2 domain reveal a tethered dimer architecture. *Cell*, **116**, 711-723.
- Yanisch-Perron, C., Vieira, J. and Messing, J. (1985) Improved M13 phage cloning vectors and host strains: nucleotide sequences of the M13mp18 and pUC19 vectors. *Gene*, **33**, 103-119.
- Zallar, A. and Szabo, T. (1989) Habent sua fata libelli: the adventurous story of Albert Szent-Gyorgyi's book entitled Studies on Muscle (1945). *Acta Physiol Scand*, **135**, 423-424.
- Zhou, T., Raman, M., Gao, Y., Earnest, S., Chen, Z., Machius, M., Cobb, M.H. and Goldsmith, E.J. (2004) Crystal structure of the TAO2 kinase domain: activation and specificity of a Ste20p MAP3K. *Structure*, **12**, 1891-1900.
- Zimmerle, C.T. and Frieden, C. (1988) Effect of pH on the mechanism of actin polymerization. *Biochemistry*, **27**, 7766-7772.

6 Abbreviations

ATP	adenosine 5'-triphosphate
bp	base pair(s)
BSA	bovine serum albumin
CLSM	confocal laser scanning microscopy
Cy3	carboxymethyl-indole-cyanine
DMSO	dimethyl sulfoxide
DNA	deoxyribonucleic acid
DNase	deoxyribonuclease
dNTPs	deoxyribonucleotide triphosphate
DTT	1,4-dithiothreitol
EDTA	ethylenediaminetetraacetic acid
EGTA	ethylene glycol-bis (2-aminoethyl ether)- ,N,N',N'-tetraacetic acid
F-actin	filamentous (polymerized) actin
g	ground acceleration; gram(s)
G-actin	globular actin (monomer)
GFP	green fluorescent protein
h	hour(s)
HEPES	N-2-hydroxyethylpiperazine-N'-2 - ethanesulfonic acid
IgG	immunoglobulin G
IPTG	isopropyl- β -thiogalactopyranoside
kb	kilobase(s)
kDa	kilodalton
l	litre(s)
LMW	low molecular weight
μ	micro
M	molar
mAb	monoclonal antibody
MES	2-(N-morpholino)ethanesulfonic acid
min	minute(s)
ml	millilitres
μ m	micrometer
mM	millimolar
MOPS	3-(N-morpholino)propanesulfonic acid
mS	milli-Siemens
nm	nanometer
NP40	nonylphenyl polyethyleneglycol
OD	optical density
PAGE	polyacrylamide gel electrophoresis
PBS	phosphate buffered saline
PCR	polymerase chain reaction
PMSF	phenylmethylsulfonyl fluoride
psi	pounds per square inch, 1 psi = 6897 Pa
RNA	ribonucleic acid
RNase	ribonuclease
rpm	revolutions per minute

RT	room temperature
s	second(s)
SDS	sodium dodecyl sulfate
TEMED	N,N,N',N'-tetramethylethylenediamine
Tris	Tris-(hydroxymethyl)-aminomethane
TRITC	tetramethylrhodamine isothiocyanate
Triton X-100	octylphenolpoly(ethyleneglycolether) _n
Tween 20	polyoxyethylene-sorbitanmonolaurate
U	unit(s)
V	volt
v/v	volume per volume
vol.	volume(s)
w/v	weight per volume

Curriculum Vitae

Rajesh Arasada

Dept. of Molecular, Cellular and Developmental Biology
Yale University
New Haven
06511 CT

Email rajesh.arasada@yale.edu

Born: March 22nd 1978

Nationality: Indian

Marital status: Married

EDUCATION:

- 1995-1998 Andhra University, Visakhapatnam, India
B.Sc., Botany, Biochemistry, Biotechnology
- 1998-2000 Madurai Kamaraj University, Madurai, India
M.Sc., Microbial Gene Technology
- 2000-2001 Jawaharlal Nehru Centre for Advanced Scientific Research,
Bangalore, India
Junior Research Fellow
- 2001-2007 Ludwig-Maximilians-University, Muenchen, Germany
Ph.D., Cell Biology

Acknowledgments

Many people have been a part of my graduate education, as friends, teachers, and colleagues.

Prof. Dr. Michael Schleicher, first and foremost, has been all of these. The best advisor and teacher I could have wished for. His trust and scientific excitement inspired me in the most important moments of making the right decisions, and I am glad I had the opportunity to work with him.

I would like to express my gratitude to *Prof. Dr. Angelika Noegel* and *Prof. Dr. Manfred Schliwa* for their advice and generosity in sharing lab space and equipment.

Many heartfelt thanks to *Dr. Jan Faix*, from the Department of Biophysical Chemistry in Hannover, Germany, with whom I had many exciting scientific discussions during his stay in Munich. Thanks for his patience and his impressive professionalism at the bench. I am also indebted to *Dr. Meino Rohlf*s for his valuable advice and his incredibly unselfish support in our collaborative projects. I am very grateful to *Drs. Ralph Gräf and Annette Müller-Taubenberger*, especially for their useful tips and help in confocal microscopy.

A million thanks to *Daniela Rieger* for patiently teaching me how to handle *Dictyostelium* cells from the very basics, and to *Dr. Meino Rohlf*s, *Annette Vogel*, *Petros Batsios* for their computer expertise and tireless offer of computer assistance.

I would also like to thank some people from the early days. *Drs. Hyun-Ju Son, René Rost, Lars Israel, Jibi Jacob, and Annika Gloss* who were among those who kept me going at the beginning.

In addition, I was lucky enough to have the support of many good friends. Life would not have been the same without *Annette 'Google'* who has been a constant source of information, without *Nagendran Ramalingam, Petros Batsios, Antje Schirenbeck, Peter Kastner, Tina Müller, Marlis Fürbringer and Maria Beer*.

Most of all, I would like to thank my parents and my wife *Deepa*, for their absolute confidence in me.